

UNIVERSITY OF TRENTO

Department of Mathematics



PhD in Mathematics

XXVIII CYCLE

From data to mathematical analysis and
simulation in models in epidemiology and ecology

Advisor:

Prof. Andrea Pugliese

PhD student:

Valentina Clamer

Year 2016

Committee members for defense of Ph.D dissertation:

Prof. Gianpaolo Scalia Tomba (Second University of Rome, Italy)
Prof. Marino Gatto (Politecnico Milano, Italy)
Prof. Stefano Bonaccorsi (University of Trento, Italy)

Defense of Ph.D dissertation:

Department of Mathematics, University of Trento
April 29, 2016

If I know what love is, it is because of you.

— Herman Hesse

To the loves of my life.

Contents

Introduction	xvii
I Estimating transmission probability in schools for the 2009 H1N1 influenza pandemic in Italy	1
1 Introduction	3
2 Background on mathematical models	5
2.1 Deterministic models	6
2.2 Stochastic models	7
2.2.1 Background on stochastic systems	7
2.2.2 A chain binomial model	8
2.2.3 Methods	8
2.3 Introduction to Monte Carlo Markov Chain	9
2.3.1 The Metropolis-Hastings algorithm	9
3 Methods	11
3.1 Data	11
3.2 Epidemic model	13
4 Parameters estimation	15
4.1 Basic reproduction number	15
4.2 Tests on simulated data	16
4.2.1 Test with missing data	20
4.2.2 Test with missing data and errors	21
4.3 Model variants	21
4.4 Estimates of transmission probabilities	23
4.5 Model validation	24

5 Discussion	27
A The algorithm used	33
A.1 Parameters updating	34
II Dynamics of Host-Parasitoid Interactions and Co- existence of Different Hosts	37
1 Introduction	39
2 Background on population models	41
2.1 Classical models	41
2.2 Delay differential equations	42
2.2.1 Age structure models	42
3 Model	45
4 Invasibility conditions	49
4.1 Single host equilibria	49
4.2 Invasibility under periodic conditions	54
4.3 Approximation of dominant eigenvalue	60
4.4 Application to host-parasitoid model	63
5 Discussion	65
A The characteristic equation	69
A.1 Density-dependence two hosts present	72
III Simulations of biological control through parasitoids of <i>Drosophila suzukii</i>	73
1 Introduction	75
1.1 Biological background	75
1.2 Experiments	77
2 Methods	79
2.1 Two hosts-two parasitoids model	79
2.1.1 Equilibria Coexistence	80

<i>CONTENTS</i>	vii
2.2 One host-one parasitoid model	82
2.2.1 Equilibrium with no parasitoids	83
2.3 Parameters extrapolation	83
3 Preliminary results	87
3.1 Simulations	87
3.1.1 Laboratory conditions	87
3.1.2 Increased death rates	93
4 Discussion	95
Bibliography	99

List of Figures

3.1	Daily number of new cases in school A (panel a) and in school B (panel b), as derived from the collected data.	12
4.1	Linear regression on cumulative infection data in school A (panel a) and in school B (panel b). Black points were used in the linear regression procedure for estimating the epidemic growth rate. . . .	16
4.2	Estimates of γ (panels a and c) and of q_c (panels b and d) in 9 sets of simulations performed by varying γ and q_c while keeping $R_0 \approx 1.48$ (in Table 4.1). Panels a) and b) have $n = 25$, c) and d) have $n = 250$. The reference values used in the simulations are represented as white dots, while the means of the posterior distribution are represented as black dots, with the bars representing 95%-credible intervals.	18
4.3	(a) Ten sets of 50 simulations starting from reference values represented as white dots (in Table 4.2) and $\varepsilon = 10^{-3}$. The estimated values are represented as black dots with the 95%-credible intervals (b) Fraction of simulations for which the 95%-credible intervals for the different parameters do not intersect.	20
4.4	Fifty simulations (panels a and c) starting from reference values represented by white dots (in Table 4.2) and $\varepsilon = 10^{-3}$ by assuming that a 20% of the data of each class is not reported. The estimated values are represented as black dots with the 95%-credible intervals. Fraction of simulations in which the 95%-credible intervals for the different parameters do not intersect in panels b) and d). In panels a) and b) 20% of the data are considered to be missing. In panels c) and d) 20% of the data of each class are not regarded and only the 70% of the data are correct, the 20% of them correspond to a ± 1 and the remaining 10% to a ± 2	22

4.5 Estimated values of the transmission parameters for school A and B. White and black dots represent the mean of the posterior distribution for school A and school B respectively, bars represent 95%-credible intervals. (b) Estimated values of the basic reproduction number R_0 inside schools A and B. Thick line and bars represent means and 95%-credible intervals. 24

4.6 The plot of the total number of infectious individuals (panel a) and the duration of the epidemic (panel b) in 400 simulations. The black dot indicates the observed number of infectious individuals and the observed length of the epidemic in the two schools. Thick line and bars represent means and 95%-credible intervals. 25

4.1 Eigenvalues at Hopf bifurcation for $d_{A_1} = d_{HB_1} \approx 0.3089$ and $\rho_1 = 5$ (left) and periodic solutions for $d_{A_1} = 0.35$ and $\rho_1 = 5$ (right) of Host 1 for the parameters values in Table 4.2. 56

4.2 The thick line represents the boundary that divides the (d_{A_2}, ρ_2) -plane into stable and unstable regions by having fixed $\rho_1 = 5$, $d_{A_1} = 0.35$. The straight dashed line represent instead the value $\rho_1 e^{-\frac{\nu_L d_P T_L}{\alpha s_P}}$ that comes from (4.7). 57

4.3 For $\rho_1 = 5$, and $d_{A_1} = d_{A_2} = var$, when $d_A > d_{HB}$, host 2 can invade for $\rho_2 > \bar{\rho}(d_A)$, a decreasing function of d_A , and host 1 can invade for $\rho_1 < \hat{\rho}(d_A)$, an increasing function of d_A 58

4.4 The thick curve represents the condition for invasibility of the host 2 periodic solution with $\rho_1 = 5$, $d_{A_1} = 0.3$ and $\nu_{L_1} = \nu_{L_2} = 0$. The solid thick curve represents instead the boundary that divides the (d_{A_2}, ρ_2) -plane into stable and unstable regions, below which coexistence is not possible. The dotted thin curve is the bifurcation curve of the equilibrium $Eq2$: the right curve part is the locus of the Hopf bifurcations leading to periodic solutions; the bottom segment is the locus of trans critical bifurcation with the trivial equilibrium. 60

3.1 Under laboratory conditions simulations. Panel (a), (b), (c) and (d) represent the case with an initial adult parasitoid value equal to 10% of adult hosts, in 500 days with attack rates $\frac{\alpha}{10}, \frac{\alpha}{4}, \frac{\alpha}{2}, \alpha$ respectively. 89

3.2 Under laboratory conditions simulations when no parasitoids are introduced and we start with only five adult hosts. 90

3.3	Under laboratory conditions simulations with an initial adult parasitoid value equal to 10% of adult hosts introduced at time $x = 20$, in 500 days with attack rates $\frac{\alpha}{10}$	91
3.4	Under laboratory conditions simulations. Panel (a), (b), (c) and (d) represent the case with an initial adult parasitoid constant value equal to 0.5, in 500 days introduced when host population is at equilibrium with attack rates $\frac{\alpha}{10}, \frac{\alpha}{4}, \frac{\alpha}{2}, \alpha$ respectively.	92
3.5	Increased death rates. Panel (a) and (b) represent the case with fixed $\alpha = 0.036$ and an initial adult parasitoid value equal to 10%, in 500 days introduced when host population is at equilibrium. Laboratory death rates in panel a), and increased death rates in panel b)	94

List of Tables

3.1	Collected data. Summary of the main features emerging from the questionnaires collected in schools A and B in Trento, Italy in 2009.	12
3.2	Model parameters and variables. Description of the notation used.	14
4.1	Parameter values for the probability of remaining infective for two days γ , and the class infection probability q_c used in the 9 sets of simulations as to have $R_0 \approx 1.48$ with a class of $n = 25$ students and the fictional case of a class of $n = 250$ students.	17
4.2	Parameter values of the class infection probability q_c , the grade infection probability q_g and the school infection probability q_s used in the 10 sets of simulations.	19
4.3	DIC values of the different models considered. Model CGS has three different transmission rates inside the school (q_c , q_g and q_s). Model S has a homogeneous infection rate inside the school (q_c). Model CS has a transmission rate for the class (q_c) and a different transmission rate in the remaining part of the school (q_g). Model CGSvar is the same as CGS but with with a non-constant ε .	23
4.4	Mean and 95%-credible intervals of the estimates for the infection probabilities in schools A and B, when considering model CGS.	23
3.1	Model parameters present in the 2 host-parasitoid model. All parameters are kept constant and density-independent except the larval death rate $d_{L_i}(L_i(t)) = \mu_{L_i} + \nu_{L_i}L_i(t)$ that depends on a constant background mortality, μ_{L_i} , and on the quantity for which the pro capita mortality changes by adding a new individual, ν_{L_i} .	47
4.1	Parameter values used in the computation. We analyse the case when two hosts are identical except for the adult host mortality d_A and the fecundity ρ .	55

4.2	Parameter values used to compute a distinct periodic solution for $d_{A_1} = 0.35$	57
2.1	Model parameters present in the two hosts-two parasitoids model. All parameters are kept constant and density-independent except of the larval death rate that depends on larvae density.	81
2.2	Model parameters present in the one host-one parasitoid model. All parameters are kept constant and density-independent except of the larval death rate that depends on larvae density.	84
2.3	Parameter extrapolated from [110, 144] used to see parasitoids impact on a host population at equilibrium.	86
3.1	Time needed by parasitoids to halve host pupae under different combinations of attack rate and percentage of introduced parasitoids.	88
3.2	Parameters obtained by considering that probably in nature death rates both of hosts and of parasitoids can be higher than the rates obtained under laboratory conditions.	93
3.3	Time needed by parasitoids to obtain 50 host pupae under different combinations of attack rate and percentage of introduced parasitoids when the attack rate is at its maximum value 0.036. .	94

Abstract

This dissertation is divided into three different parts.

In the first part we analyse collected data on the occurrence of influenza-like illness (ILI) symptoms regarding the 2009 influenza A/H1N1 virus pandemic in two primary schools of Trento, Italy. These data were used to calibrate a discrete-time SIR model, which was designed to estimate the probabilities of influenza transmission within the classes, grades and schools using Markov Chain Monte Carlo (MCMC) methods. We found that the virus was mainly transmitted within class, with lower levels of transmission between students in the same grade and even lower, though not significantly so, among different grades within the schools. We estimated median values of R_0 from the epidemic curves in the two schools of 1.16 and 1.40; on the other hand, we estimated the average number of students infected by the first school case to be 0.85 and 1.09 in the two schools. This discrepancy suggests that household and community transmission played an important role in sustaining the school epidemics. The high probability of infection between students in the same class confirms that targeting within-class transmission is key to controlling the spread of influenza in school settings and, as a consequence, in the general population.

In the second part, by starting from a basic host-parasitoid model, we study the dynamics of a 2 hosts-1 parasitoid model assuming, for the sake of simplicity, that larval stages have a fixed duration. If each host is subjected to density-dependent mortality in its larval stage, we obtain explicit conditions for coexistence of both hosts, as long as each 1 host-parasitoid system would tend to an equilibrium point. Otherwise, if mortality is density-independent, under the same conditions host coexistence is impossible. On the other hand, if at least one of the 1 host-parasitoid systems has an oscillatory dynamics (which happens under some parameter values), we found, through numerical bifurcation, that coexistence is favoured. It is also possible that coexistence between the two hosts

occurs even in the case without density-dependence. Analysis of this case has been based on methods of approximation of the dominant characteristic multipliers of the monodromy operator using a recent method introduced by Breda *et al.* Models of this type may be relevant for modelling control strategies for *Drosophila suzukii*, a recently introduced fruit fly that caused severe production losses, based on native parasitoids of indigenous fruit flies.

In the third part, we present a starting point to analyse raw data collected by Stacconi *et al.* in the province of Trento, Italy. We present an extensions of the model presented in Part II where we have two hosts and two parasitoids. Since its analysis is complicated, we begin with a simpler one host-one parasitoid model to better understand the possible impact of parasitoids on a host population. We start by considering that the host population is at an equilibrium without parasitoids, which are then introduced as different percentages of initial adult hosts. We compare the times needed by parasitoids to halve host pupae and we found that the best percentage choice is 10%. Thus we decide to fix this percentage of parasitoid introduction and analyse what happens if parasitoids are introduced when the host population is not at equilibrium both by introducing always the same percentage or the same amount of parasitoids. In this case, even if the attack rate is at $\frac{1}{10}$ of its maximum value, parasitoids would have a strong effect on host population, shifting it to an oscillatory regime. However we found that this effect would require more than 100 days but we also found that it can faster if parasitoids are introduced before the host population has reached the equilibrium without parasitoids. Thus there could be possible releases when host population is low. Last we investigate also what happens if in nature mortality rates of these species increase and we found that there is not such a big difference respect to the results obtained using laboratory data.

*The essence of mathematics is not to make simple things complicated, but to
make complicated things simple.*

— S. Gudder

Acknowledgements

I would like to thank my advisor, Prof. Andrea Pugliese, for his teaching and support and all the people with whom I had useful discussions about this work.

I thank the headmasters of the primary schools of Povo and Villazzano, Trento (Italy) for permitting us to run the survey and the students' parents and carers for their participation. I am grateful to Prof. Mimmo Iannelli and Antonella Lunelli for their collaboration in the design and distribution of the questionnaire and digitalization of the data, to Caterina Rizzo for her help in designing the questionnaire and for providing the InluNet data.

I thank Valerio Rossi Stacconi for providing the data on *Drosophila suzukii* and its parasitoids and Prof. Dimitri Breda and Davide Liessi for their collaboration in finding numerically coexistence conditions with periodic solutions. I am grateful to the Lexem Project that financially supported part of this thesis.

Last but not least, I would also like to thank my family, the loves of my life and all my friends for their support, patience and smiles during the last three years of my life, even when I was mostly stressed. You make me happy.

V. C.

Introduction

This Ph.D dissertation summarizes the results of two different works. The research of the first topic during my Ph.D program originates from a result first presented in my Master thesis and presented here in a developed version, the analysis of collected data on the 2009 influenza A/H1N1 virus pandemic in two primary schools of Trento, Italy, using Markov Chain Monte Carlo (MCMC) methods.

The choice of the second topic is due to an offer that was made to me less than two years ago that has intrigued me. This offer consisted in a collaboration with the Edmund Mach Foundation to the Lexem Project that aims at producing new strategic knowledge and innovative tools useful for supporting decision-making for what concerns the crop pest *Drosophila suzukii*. In fact, since its first detection in 2008, *D. suzukii* has provoked serious damages to orchards causing significant economic losses and this has revived the interest in understanding multi-hosts multi-parasitoids interactions.

Even if the two parts that constitute this thesis are very different one from the other, we can find a leitmotiv that links their topics, mathematical modelling. Mathematical models are in fact a useful tool to simulate epidemic spread scenarios or dynamics that result from the interactions of different species, and can be a significant help for public health policies decisions. Formulation of a model depends indeed on the aspects chosen by the modeller, and, for this reason, it can easily be used to analyse different real-life situations and can be applied to different fields of study such as biology, epidemiology, demography, finance . . .

Part I focusses on the study of a discrete-time SIR model.

This part has been inspired by a real outbreak that occurred in two primary schools in the province of Trento, Italy, in 2009. Parameters estimation

in such a situation is a key part of the modelling process and Bayesian inference has been performed in this thesis.

The modelling framework presented here constitutes a novel approach that can be applied to different infections detected in many countries.

In this Part we present a brief overview of mathematical models used in epidemiology and on Markov Chain Monte Carlo methods. Then we analyse data collected in two primary schools in the province of Trento, Italy, with an epidemic discrete-time SIR model, where the transmission parameters are estimated via Markov chain Monte Carlo methods. Last, we apply different parameters estimations. We start with a basic concept that characterize epidemiology, the basic reproduction number, and then we apply a developed model that is based on three different kinds of interactions: within class, grade and school. The first test on simulated data that we have performed refers to a simple case of a single class with different class sizes, aiming at the estimate of the probabilities to remain infectious for two days and to be infected from someone inside the class. Then we test the model and the estimation algorithm under different parametrizations. We compare three variants of the model using an adapted version of the deviance information criterion. Finally, we validate the presented model and estimate model parameters in the two selected primary schools.

Part II of this dissertation looks at the dynamics that result from the interactions of different species.

In particular we take into account a recently introduced fruit fly, *Drosophila suzukii*, whose main characteristic that differentiate this species from most other species of Drosophilidae is its ability to lay eggs in healthy, ripening fruits that may become unmarketable causing significant economic losses.

To reduce *D. suzukii* populations several approaches have been attempted: chemical control, trap control or natural enemies control. The control method that is taken into account in this thesis is the use of natural enemies as possible biocontrol agents against *D. suzukii*. These natural enemies are generally parasitoids that induce a high rate of mortality in their host populations due to high natural average rate of parasitism.

We establish conditions for species coexistence and for competitive exclusion by considering a 2 host- parasitoid model. It begins with a brief overview

on biological motivations for our study and on classical population models that provide the model prototype of host-parasitoid models. Then we introduce a 2 host-parasitoid model based on delay differential equation that is an extension of a model already presented in the literature. In this model we consider that adult parasitoids can attack only host larvae (adult hosts are invulnerable to parasitism) whose mortality can depend or not on their density at time t . We give coexistence condition of the presented model that are found by linearising the system around the equilibria with only one host species present. We show that, when no density-dependence is present, the two hosts cannot coexist but, once density-dependence is introduced, we can find some conditions for hosts coexistence. Last, we discuss also what happens if we are in periodic conditions using numerical approximations and we give a mathematical proof of what we have found through the analysis.

Part III summarizes the first results of a topic that we started working on recently, application of the model to raw data.

In particular, we present the experiments conducted by Tochen *et al.* and Stacconi *et al.* that can be considered useful to apply the presented model to raw data. However, we have to keep in mind that field and semi field experiments were performed late in the season and thus the obtained value are not reliable and are not use in these preliminary simulations.

To apply data extrapolated from the studies of Tochen *et al.* and Stacconi *et al.*, we first introduce an extended version of the model presented in Part II in which we add a new class in host life stages and a different parasitoid. In this way, we obtain a model that can describe more realistically what happens in the fields of the province of Trento, Italy. However, since the analysis and the application of this model are very complicated and require a lot of unknown parameters, we start with a simpler situation to try to understand parasitoids impact on host populations. In this Part we consider different situations in which parasitoids are introduced at different time and under different conditions regarding their amount respect to the host population. In particular, we start from laboratory data and we suppose that there is a fixed amount of pupae at equilibrium and then we study what happens if the actual attack rate is smaller or if the mortality rates are greater than the one obtained under laboratory conditions.

Part I

Estimating transmission probability in schools for the 2009 H1N1 influenza pandemic in Italy

Chapter 1

Introduction

In this chapter we give an introduction to epidemic models. These models are in fact being extensively used to understand the main pathways of spread of infectious diseases, and thus to assess control methods. In particular, we present a brief overview of what has been done and used in this work.

Generally, epidemic models are fitted to rather aggregated datasets reporting number of new cases (possibly stratified by age or other variables of interest) in each time interval (often a week, although sometimes daily reports are available, especially at the initial outbreak of an infection). In some cases, data on all individuals of a small community have been available [1], and this has allowed to obtain a better understanding of the person-to-person spread. Still, the question rises of whether small isolated communities are representative of disease spread in more usual contexts.

The attention that was given to the A/H1N1 2009 flu pandemic has made it possible to collect detailed data on the epidemic spread in more typical contexts. Schools are well known to represent hot spots for epidemic spread, as can be seen in [2–13]. Contact rates within schools are generally higher than outside, as was also noticed in [3, 14, 15]. Using detailed data on an outbreak of 2009 pandemic influenza in a school, Cauchemez *et al.* [16] estimated the different infection probabilities within each class, or grade, and in the whole school, as well as quantified the spread through other household members, and were also able to assess the role of heterogeneities in contact rates.

In this work we provide estimates for transmission rates of 2009 A/H1N1 pandemic influenza at the three levels of class, grade and school by analysing

data on the occurrence of influenza-like illness (ILI) symptoms among pupils of two primary schools in Trento (Italy). The data were collected retrospectively in December 2009, a few weeks after the epidemic peak, through a questionnaire delivered to the parents of the pupils attending the two primary schools. As far as we know, this is the first case in Italy, and one of the first in Europe, in which influenza transmission is estimated in a school. The estimates appear consistent between the two schools and with the general understanding of influenza transmission.

We developed a discrete-time SIR model to analyse the collected data, where the transmission parameters were then estimated via Markov chain Monte Carlo methods, appropriate to make parameter inference in presence of missing data [17, 18].

In order to understand the power of the method, we applied the algorithm also to synthetic data, generated to reproduce a school structure, under several hypotheses on the transmission dynamics. This work on synthetic data made us, on the one hand, get a better interpretation of the results obtained, showing for instance to which degree parameters are identifiable; on the other hand, assess the loss in accuracy resulting from missing data and other sources of error.

A background on stochastic systems, on some methods for parameters estimation and on MCMC methods are presented in Chapter 2. In Chapter 3 we introduce the data and the model to analyse them, while results, model comparison and validation are presented in Chapter 4 and discussed in Chapter 5. Last, we give details on the algorithm used and on parameters updating in Appendix A.

Chapter 2

Background on mathematical models

This chapter summarizes some preliminaries on mathematical models generally used in epidemiology and on Markov Chain Monte Carlo methods that would be useful for the analysis of the transmission probabilities in schools for the 2009 H1N1 influenza pandemic in Italy. This is in fact one of the main characteristic of epidemiology that wants to understand the complex mechanisms behind an observed outbreak to try to control it using mathematical models [19–21].

When we consider epidemics within a population, traditionally we focus on the dynamics among individuals of the population and not on the process that occurs within a single component of the community at a pathogen level. In fact, since we are interested in the number of infected individuals and in the infection spread, we can disregard the mechanisms inside an individual that make him sick. Hence, when we describe an epidemic at the population level, we can distinguish three main categories in which to divide the population: susceptibles (healthy and infectable individuals), infectives (infected and infectious individuals) and removed (usually immune individuals after recovery). The first mathematical models appeared at the beginning of the 20th century [22–28]. In particular, Kermack and McKendrick in [26–28] laid the foundations of one of the most relevant mathematical frameworks for epidemic description in this field, the SIR model. In their paper that differs in the interpretation from the one present in this dissertation, Kermack and McKendrick includes into the removed not only immune individual but also dead or quarantined individuals because of the

infection.

By following the description of the epidemic given in these papers, the state of the population can be identified by three basic variables: $S(t)$, the number of susceptibles at time t , $I(t)$, the number of infectives at time t and $R(t)$, the number of removed at time t . As we have said previously, these are only the foundations to describe an epidemic. In fact, actually, there may be other characterizing classes, for instance exposed (infected individual that are not infectious) or differently infectious infectives. However a general understanding of the problem can be obtained by considering only the three main class introduced above.

After the division of the population into epidemiological classes, both deterministic or stochastic models can be used. The choice between them follows from the size of the population taken into account. In fact, one of the main assumption in deterministic population models is that the population has to be very large, otherwise epidemic models fail to catch the random nature of transmission events. In the following Section we present and discuss briefly similarities and differences between these two different models. However, generally, when an epidemic is described, we have to distinguish if the disease taken into account impart lifelong immunity or not. In the first case we have the so called SIR models, in the latter SIS or SIRS (according to the presence of a transitory immunity or not).

2.1 Deterministic models

A deterministic model is characterized by the fact that, once initial conditions and parameter values are fixed, its evolution is uniquely determined. This kind of models has been used to understand a huge variety of situations such as parameters estimation and surveillance data fitting [29–31], control measures impact assessment [32], antibiotic use investigation [33] or transmission dynamics analysis [34–37].

Even if deterministic models are easy to simulate and analyse, when low levels of infections or small populations are present or when the whole epidemic outbreak is not observed, this kind of model fails to catch the random nature of transmission events.

Thus, since we analyse a pandemic in two primary schools that represent small communities, it is easy to understand that a deterministic model is not really useful. Instead a stochastic model can be used.

2.2 Stochastic models

Differently from deterministic models, stochastic models are based on probabilities on the occurrence of a certain event. Thus, the study of temporal evolution of such a model is more complex than the study of a deterministic model and, for this reason, computer simulations are very useful.

2.2.1 Background on stochastic systems

In this dissertation we analyse a pandemic that occurred in two primary schools of Trento, Italy. Analysing data from infectious diseases is a non-standard problem and the inference problems are complicated because these data are highly dependent, incomplete data that come from only partially observable real-life situations. However it is possible to develop a simple stochastic model that has to be a close approximation of the real system considered. The model that we take into account and that can be used as a starting point for inference tries to imitate the behaviour of this system by studying the interactions among the pupils of a primary school. These interactions can be divided into internal relationships that connect pupils within the school, and external relationships that connect pupils with the world outside the school.

The importance of a model to study a system has been discussed by Rosenbluth and Wiener [38], who wrote:

No substantial part of the universe is so simple that it can be grasped and controlled without abstraction. Abstraction consists in replacing the part of the universe under consideration by a model of similar but simpler structure. Models . . . are thus a central necessity of scientific procedure.

After model formulation it is usual to perform a lot of simulations that can be regarded as statistical experiments, to keep track of parameters of interest and, at the end, to ensure that there is enough confidence in the results. Naylor et al. [39] wrote that:

The fundamental rationale for using simulation is man's unceasing quest for knowledge about the future. This search for knowledge and the desire to predict the future are so old as the history of mankind. But prior to the seventeenth century the pursuit of predictive power was limited almost entirely to the purely deductive methods of such philosophers as Plato, Aristotele, Euclid, and others.

A model that can describe the epidemic process in a real-life situation is the chain binomial model.

2.2.2 A chain binomial model

By following the previous assumptions on population division into epidemiological classes, we assume that the probability that a susceptible escapes infection when exposed to the i infectives of a generation is q_i , $i = 1, 2, \dots$. For the sake of simplicity, assume that there are no sub clinical infections (all infectives can be recognized) and that after the infection each individual acquires immunity. These assumptions led us to deduce that the number of individuals that remain susceptible is $S_{t+1} = S_t - I_{t+1}$, by knowing the initial values $I_0 = i_0$ and $S_0 = s_0$. Thus, the probability of having x infectives at time $t + 1$, by knowing that at time t there are s susceptibles and i infectives, is

$$P(I_{t+1} = x | S_t = s, I_t = i) = \frac{s!}{x!(s-x)!} p_i^x q_i^{s-x} \quad (2.1)$$

where $p_i = 1 - q_i$.

Reed-Frost (related to [40]) and Greenwood [41] formulated two particular cases of the chain binomial model by making different assumptions on the way in which q_i depends on i .

In 1928 in a biostatistic lecture, Reed and Frost assumed that, when the disease transmission occurs through close person-to-person contacts, $q_i = q_1^i$ that means that the probability of escaping infection when exposed to i infectives of one generation is equivalent to escaping infection when exposed to a single infective in each of i separate generations.

On the other side, in 1931 Greenwood assumed that, when the probability of infection depends more on the behaviour of one individual than on the environment, $q_i = q$, $i = 1, 2, \dots$ and $q_0 = 1$. Thus the chance of infection is the same when exposed to one infective as when more than one infective is present.

2.2.3 Methods

Parameters of these models can be estimated both via likelihood maximization that maximize the probability to observe what has been noticed in the dataset, and Bayesian inference that tries to summarize the posterior distribution of parameters given observations [42, 43]. In the latter methods, model parameters are regarded as random variables. Thus, the posterior density, which contains

all the informations about the parameters, is defined via Bayes' Theorem as the normalized product of the prior density and the likelihood.

To summarize briefly this method, denote with D observed data and with ϑ model parameters and missing data.

Formal inference requires a joint probability distribution $P(D, \vartheta)$ given by

$$P(D, \vartheta) = P(D|\vartheta)P(\vartheta). \quad (2.2)$$

Thus, through Bayes theorem, by having observed D , the posterior distribution is

$$P(\vartheta|D) = \frac{P(\vartheta)P(D|\vartheta)}{P(D)} = \frac{P(\vartheta)P(D|\vartheta)}{\int P(\vartheta)P(D|\vartheta)d\vartheta}. \quad (2.3)$$

Since the integral at denominator can be regarded as a normalising constant to ensure that $P(\vartheta|D)$ is a proper density, (2.3) can be written as

$$P(\vartheta|D) \propto P(D|\vartheta)P(\vartheta). \quad (2.4)$$

2.3 Introduction to Monte Carlo Markov Chain

One of the most important methodology to analyse real-life situations is the methodology of Monte Carlo Markov Chain (MCMC). Its name comes from the generation of a Markov chain using the previous sample value to randomly generate the next one. It was first described by Metropolis *et al.* [44] and later refined by other people including Hastings [45], Geman and Geman [46], Gelfand and Smith [47], Gelman and Rubin [48, 49], and Green [50].

MCMC methods try to solve the problem in obtaining samplers from some complex probability distribution that we can face with the integration. This would seem to provide the solution to our problem, but first we need to discover how to construct a Markov chain such that its stationary distribution $\pi(\cdot)$ is our distribution of interest. Constructing such a Markov chain is surprisingly easy.

2.3.1 The Metropolis-Hastings algorithm

The form due to Hastings in 1970 is a generalization of the method of Metropolis *et al.* using an arbitrary transition probability function $q(Y|X) = P(X \rightarrow Y)$.

At each time t , the next state X_{t+1} is chosen sampling Y from a proposal distribution $q(\cdot|X_t)$ and the acceptance probability is given by

$$\alpha(X, Y) = \min \left(1, \frac{\pi(Y)q(X|Y)}{\pi(X)q(Y|X)} \right) \quad (2.5)$$

If Y is accepted, the next state will be $X_{t+1} = Y$, if it is rejected $X_{t+1} = X_t$.

To implement successfully this algorithm, we have to keep in mind that initial simulations, the so called burn-in period, have to be discarded since it would be unlikely that they come from the stationary distribution of interest. After that we have to decide if the chain is a well mixing chain by considering an acceptance probability A that will say us if the chain mixes well or not. This is defined as the number of iterations where new values are accepted out of a batch of iterations. By following [16, 51], the acceptance probability value for a good mixing is between 10% and 40%. However, it should be borne in mind that an optimal A does not necessary imply convergence to a stationary distribution, although poor A could be due to a lack of mixing and convergence. It is also possible to have high acceptance and very low convergence [52].

Another problem when analysing epidemic outbreaks is the missingness of some data that can cause a distorted or inefficient analysis. To overcome this difficulty we can simply impute missing data by substituting them with alternative plausible values obtained from the data [16]. Thus, in a Bayesian approach, missing data become simply extra parameters to be evaluated.

Chapter 3

Methods

This chapter presents the collected data of two primary schools in the province of Trento, Italy, and the epidemic discrete-time SIR model used to analyse these data, where the transmission parameters were then estimated via Markov chain Monte Carlo methods.

3.1 Data

In December 2009 we delivered a questionnaire to the parents of the pupils of two primary schools in Povo (A) and Villazzano (B) in the province of Trento (Italy). School A consisted of 307 students divided into 14 classes of 5 different grades, while school B consisted of 214 students divided into 10 classes of 5 different grades. The questionnaire reported a description of ILI symptoms, asked the parents to report whether any member of the family had experienced ILI symptoms in the preceding months and, if that was the case, to report the date of symptoms onset (or an estimate of it) for each member of the family, similarly to what was done in [3, 4, 53]. Table 3.1 and Figure 3.1 summarize the data collected concerning the students of the two primary schools. The information provided on all the other members of the families were scarce and for this reason they were excluded from our study.

	School A	School B
School size	307	214
Number of classes	14	10
Number of responses	260	168
Number of ILI cases	121	103
Response rate	85%	79%
Reported Attack rate	46%	61%

Table 3.1: *Collected data. Summary of the main features emerging from the questionnaires collected in schools A and B in Trento, Italy in 2009.*

The overall response rate to the questionnaire was 82% (428/521) and the reported ILI cases were 224 (52%) (Table 3.1). In school A, the first two cases were reported on 16 October 2009 and the last case was reported 56 days later. In school B, the first case was reported on 10 October 2009 and the last case occurred 64 days later.

Figure 3.1 represents the number of new cases in the two schools and shows that most cases occurred within the central 30 days in school A, and even 20 days in school B.

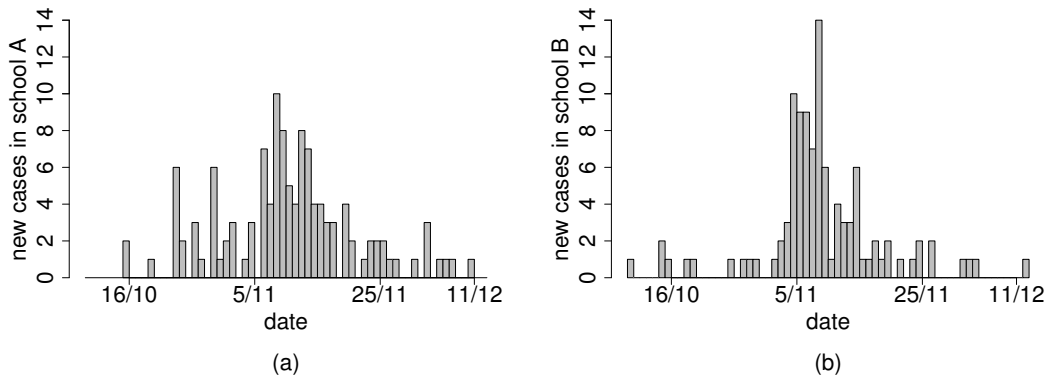


Figure 3.1: *Daily number of new cases in school A (panel a) and in school B (panel b), as derived from the collected data.*

3.2 Epidemic model

The epidemic process is described using a discrete-time SIR model, with a time step of 1 day. Following [54], we assume that the incubation period (time from infection to symptom occurrence) is on average 2 days and varies between 1 and 3 days, and that the infectiousness profile is as described in [55]. This led us to do the following assumptions: if a child is infected at school on day t , he/she will be at school and infectious on day $t + 1$; on day $t + 2$ he/she will be infectious and either kept at home, or still at school with probability γ : from Figures 1b) and 1d) of [54] we estimate $\gamma = 0.1$. Hence, we assume that the school population can be divided into: susceptible individuals S , infectious individuals I (infected children who can transmit the disease, divided into two sub-compartments I_1 and I_2 depending on them being in the first or second day of infectiousness, respectively) and recovered subjects R (including both recovered children and children kept at home after symptoms onset).

The model is a Markov chain where the individual transitions are given by

$$S \rightarrow I_1, \quad I_1 \xrightarrow{\gamma} I_2 \quad I_1 \xrightarrow{1-\gamma} R \quad I_2 \xrightarrow{1} R.$$

The transition $S \rightarrow I_1$ depends on the infectious population. For the sake of simplicity, we assume that I_1 and I_2 individuals are equally infectious. Furthermore, by following [16], we assume different probabilities of infection: within-class (q_c), in the same grade but in a different class (q_g), in the same school but in a different grade (q_s) and in households or in the general community (ϵ). We define

- $I_t^{j,h}$ the number of infectious students (either in their first or second day of infectiousness) in grade j , class h at time t ;
- $I_t'^{j,h} = \sum_{k \neq h} I_t^{j,k}$ the number of infectious students in the classes of grade j other than h at time t
 $= I_t^j$ (number of infectious students in all classes of grade j) $- I_t^{j,h}$;
- $I_t''^j = \sum_{i \neq j, h} I_t^{i,h}$ the number of infectious students in grades other than j at time t
 $= I_t$ (number of infectious in all classes of the school) $- I_t^j$,

The probability for a susceptible student in grade j , class h to remain susceptible is

$$p_t^{j,h} = (1 - q_c)^{I_t^{j,h}} (1 - q_g)^{I_t'^{j,h}} (1 - q_s)^{I_t''^j} (1 - \epsilon) \quad (3.1)$$

and $1 - p_t^{j,h}$ is the probability of becoming I_1 at time $t + 1$. Then the probability of having $S_{t+1}^{j,h}$ susceptibles at time $t + 1$, by considering the school at time t , can be obtained as

$$P(S_{t+1}^{j,h} | S_t^{j,h}, I_t^{j,h}, I_t^j, I_t) = \binom{S_t^{j,h}}{S_{t+1}^{j,h}} (p_t^{j,h})^{S_{t+1}^{j,h}} (1 - p_t^{j,h})^{(S_t^{j,h} - S_{t+1}^{j,h})} \quad (3.2)$$

The full list of variables and parameters of the model is reported in Table 3.2. Model parameters have been estimated using MCMC methods, as described in [17, 56]. The estimated parameters are the infection probabilities within-class q_c , within the same grade q_g , among different grades of the schools q_s and from outside the schools ϵ and the augmented data are all unobserved events such as the infection dates and the infection state of the children whose questionnaires were not filled (see Appendix A for further details).

Symbol	Description
q_c	within-class infection probability
q_g	same grade infection probability
q_s	within-school infection probability
ϵ	outside-school infection probability
γ	probability to remain infective for two days
I_t	number of infective subjects at time t in the whole school
I_t^j	number of infective subjects at time t in grade j
$I_t^{j,h}$	number of infective subjects at time t in grade j and class h
$S_t^{j,h}$	number of susceptible individuals at time t of grade j and class h
n_j	number of classes of grade j

Table 3.2: *Model parameters and variables. Description of the notation used.*

Chapter 4

Parameters estimation

We summarize in this part of the dissertation some different parameters estimations. We start with a basic concept that characterizes epidemiology, the basic reproduction number and then we apply the model presented in Section 3.2, CGS (Class-Grade-School) model, to simulated data. The first test on simulated data in this chapter refers to a simple case of a single class with different class sizes, aiming at the estimate of the probabilities to remain infectious for two days and to be infected from someone inside the class. Then we test the model and the estimation algorithm under different parametrizations. We compare three variants of the model using an adapted version of the deviance information criterion and, finally, we estimate model parameters in schools A and B and we validate it.

4.1 Basic reproduction number

A typical summary indicator of an epidemic is its basic reproduction number R_0 , which represents the expected number of secondary cases generated by a single typical infection in a completely naive population. The reproduction number estimated in this work is school-specific. R_0 can be estimated through the rate of initial epidemic growth r using the formula $R_0 = 1 + rT_I$ [57], where T_I represents the mean generation time; r has been estimated through the fit of a linear model either to the incidence data (grouped by 3 days) or to the cumulative number of cases (see [58] for a statistical analysis of the consequences of either choice) in the log-scale (Figure 4.1 shows the fit to the curve of cumulative cases over a specific time window).

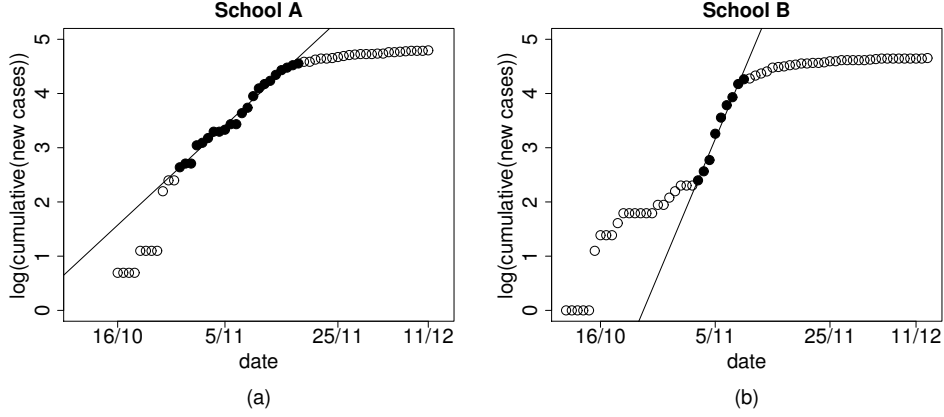


Figure 4.1: *Linear regression on cumulative infection data in school A (panel a) and in school B (panel b). Black points were used in the linear regression procedure for estimating the epidemic growth rate.*

We estimated the initial growth rate r both from the (grouped) incidence curve and from the cumulative curve (Figure 4.1), selecting those time windows in the growing part of the epidemic for which R^2 was sufficiently high (> 0.95 for the cumulative curve, > 0.7 for the incidence curve); assuming that the infectious period at school T_I is 1.1 day, we obtained a median R_0 of 1.16 for school A and 1.40 for school B; the overall range of confidence intervals (obtained from the different time windows) is 0.93-1.43 for school A; 1.08-1.76 for school B using the fit from incidence curves. The intervals obtained from cumulative curve are much narrower, but may be deceptively so [58].

The classical definition of R_0 in a finite population stochastic model is generally based on the limit as the population grows to infinity (see, for instance, [59]). Instead of doing this, we rely on a simple operational definition, namely we define R_0 as the average number of students infected by the first infected student in the school. By assuming to have n_s grades (5 in Italian primary schools), each with n_g classes with n students, then we obtain

$$R_0 = (q_c(n-1) + q_g n(n_g-1) + q_s n n_g (n_s-1))(1+\gamma). \quad (4.1)$$

4.2 Tests on simulated data

We tested the model and the estimation algorithm on simulated data obtained using model CGS under different parametrizations.

We started with the simple case of a single class, aiming at the estimate of the probabilities to remain infectious for two days, γ , and to be infected from someone inside the same class, q_c . We performed a series of simulations varying γ from 0.1 (the probability to remain infective for two days is very low) to $\gamma = 0.9$ (the probability to become an I_2 is very high) with a step of 0.1; correspondingly, q_c is changed in such a way that R_0 (in this case $nq_c(1 + \gamma)$) remains constant. In Table 4.1 the parameters values from which we started are shown, both for a class of $n = 25$ children and for a (fictional) case of a class of 250 children. Figure 4.2 shows the results obtained in the case of a class of $n = 25$ children or in the (fictional) case of a class of 250 children.

Simulation set	$n = 25$		$n = 250$
	γ	q_c	q_c
1	0.1	0.054	0.0054
2	0.2	0.049	0.0049
3	0.3	0.046	0.0046
4	0.4	0.042	0.0042
5	0.5	0.039	0.0039
6	0.6	0.037	0.0037
7	0.7	0.035	0.0035
8	0.8	0.033	0.0033
9	0.9	0.031	0.0031

Table 4.1: *Parameter values for the probability of remaining infective for two days γ , and the class infection probability q_c used in the 9 sets of simulations as to have $R_0 \approx 1.48$ with a class of $n = 25$ students and the fictional case of a class of $n = 250$ students.*

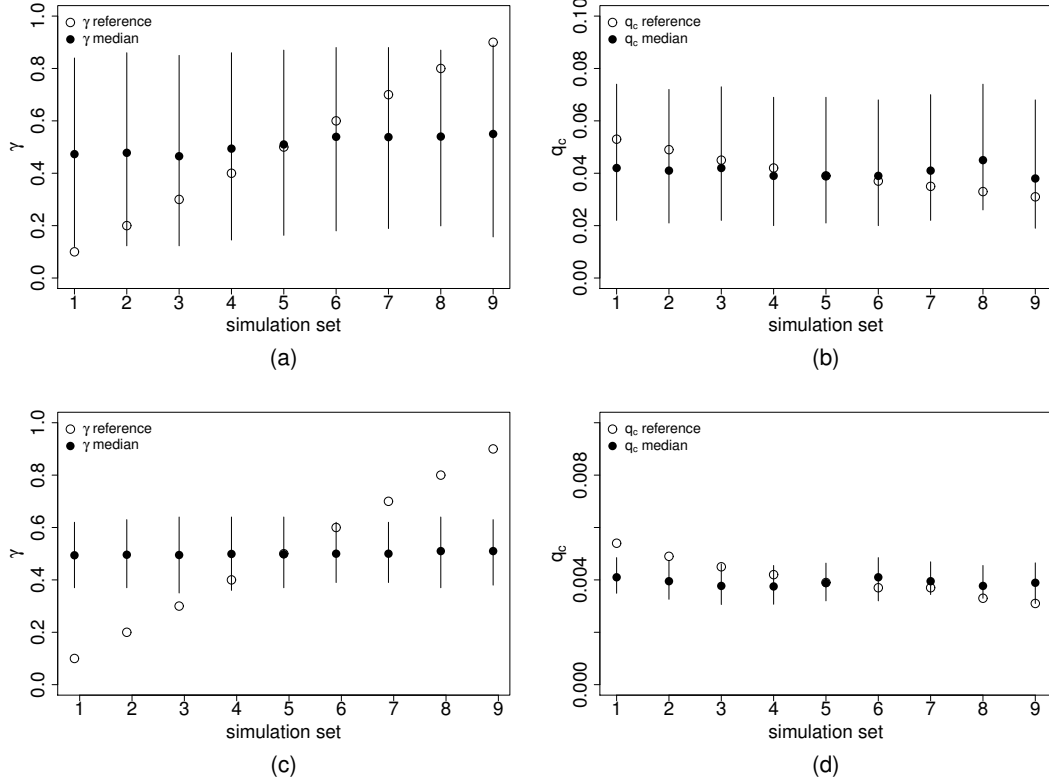


Figure 4.2: Estimates of γ (panels a and c) and of q_c (panels b and d) in 9 sets of simulations performed by varying γ and q_c while keeping $R_0 \approx 1.48$ (in Table 4.1). Panels a) and b) have $n = 25$, c) and d) have $n = 250$. The reference values used in the simulations are represented as white dots, while the means of the posterior distribution are represented as black dots, with the bars representing 95%-credible intervals.

It may be noticed that the mean value of estimated γ is always close to 0.5, independently of the value of γ used in simulations. Increasing n reduces the width of credible intervals, but does not remove the bias. Also the mean estimated value of q_c is almost constant, independently of the value used in the simulations, at the value that would be correct for $\gamma = 0.5$.

Because of this problem, in all the following simulations we set γ equal to 0.1 without estimating it. The following simulations are based on the same school structure, similar to the one of school A: a total of 15 classes, 3 for each of the 5 different grades, and each class composed of 25 children (according to the Italian primary schools structure).

We generated data under different parameter values, ranging from the case where q_c , q_g and q_s are approximately equal (transmission homogeneous among all students in a school) to another one where $q_c = 10q_s$ and q_g is intermediate (transmission is higher to students in the same class, then to those in the same grade, and lowest to all other students of the school). The parameter values have been chosen so as to have (using formula (4.1) of the main text) $R_0 \approx 1.48$ [54, 60–62].

Precisely, we performed 10 sets (labelled 1 to 10) of 50 simulations with the parameter values shown in Table 4.2, and for each simulation we ran the MCMC algorithm to obtain *a posteriori* distribution of the parameters q_c , q_g , q_s and ε . The results are shown in Figure 4.3 (panel a)).

It can be seen that the estimates are reasonably correct, with the mean of the posterior distributions around the reference values. It may be noticed, however, that, when the three parameters q_c , q_g and q_s are close to each other, the algorithm tends to overestimate q_c , the transmission rate in the same class.

Simulation set	q_c	q_g	q_s
1	0.0037	0.0029	0.0037
2	0.0066	0.0037	0.0033
3	0.009	0.0042	0.003
4	0.011	0.0044	0.0028
5	0.013	0.0046	0.0026
6	0.015	0.0047	0.0024
7	0.016	0.0048	0.0023
8	0.018	0.0049	0.0022
9	0.019	0.00497	0.0021
10	0.02	0.005	0.002

Table 4.2: *Parameter values of the class infection probability q_c , the grade infection probability q_g and the school infection probability q_s used in the 10 sets of simulations.*

An interesting question is whether the 95%-credible intervals for the three parameters intersect each other. The answers are shown in Figure 4.3 (panel b)). It can be seen that, when the parameters are indeed equal, around 5% of the times one obtains non-intersecting 95%-credible intervals, something close to expectations.

On the other hand, a difference is picked up almost always between q_c and q_s from set 4 onwards (i. e. when the ratio $q_c/q_s \approx 3.8$) and between q_c and q_g from set 8 onwards (i. e. when the ratio $q_c/q_g \approx 3.7$), while the ratio q_g/q_s never reaches such values, and thus a difference between q_g and q_s is seen only occasionally in the simulations. We found that the infection probabilities q_c , q_g ,

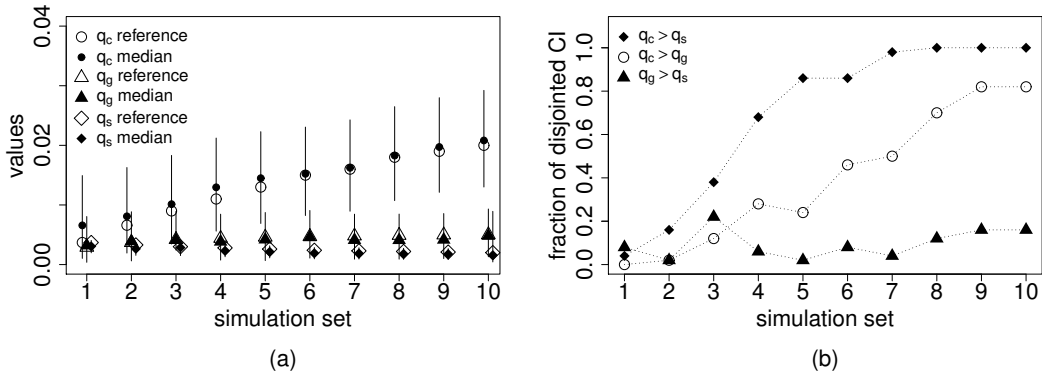


Figure 4.3: (a) Ten sets of 50 simulations starting from reference values represented as white dots (in Table 4.2) and $\varepsilon = 10^{-3}$. The estimated values are represented as black dots with the 95%-credible intervals (b) Fraction of simulations for which the 95%-credible intervals for the different parameters do not intersect.

q_s and ε were successfully identified .

4.2.1 Test with missing data

To test the behaviour of the algorithm when dealing with missing data, as in the case of actual data, we looked again at previous simulations, but we assumed that a random 20% of the data of each class is not reported and thus cannot be used in the estimation procedure. The results obtained are shown in Figure 4.4 (panels a) and b)). The results can be considered almost as satisfactory as in the case without missing data. As expected, the credible intervals are somewhat

wider than in the case without missing data, and thus they intersect somewhat more often. It can also be remarked that, with missing data, the transmission rate inside the class q_c is on average overestimated in all simulation sets.

4.2.2 Test with missing data and errors

To see if the algorithm works also in the most general case in which some reported data are wrong, we consider that 20% of the data of each class are not regarded and that only the 70% of the data that we have are correct, the 20% of them correspond to a ± 1 and the remaining 10% to a ± 2 and we report the results in Figure 4.4 (panels c) and d)). Also in this case the estimation of the data is reasonably correct and this indicates that we have obtained a robust result, although the absolute value of q_c is somewhat overestimated when the parameters are close to each other.

4.3 Model variants

We considered the following two simplifications of the CGS model presented in Section 3.2: model CS (Class-School) where we differentiate between within-class transmission and within-school transmission only, without considering a separate probability of transmission within the same grades and model S (School only), where we assume that the probability of transmission is the same for all students in the school. We explore a further variant of model CGS (CGS-var), where the probability of infection from outside the school, instead of being constant over time, is assumed to be proportional (through a constant ε) to the ILI incidence at the corresponding week in the province of Trento, as reported by the surveillance system InInNet of the Italian Institute of Health [63].

We compare the model variants using an adapted version of the deviance information criterion (DIC) described in [64, 65]. Specifically, distinguishing between actual model parameters (ϑ) and unobserved events (Y), we computed a marginalized DIC as

$$\text{DIC} = -4\mathbb{E}_{(\vartheta, Y)} \log(L(X, Y|\vartheta)) + 2\mathbb{E}_Y \log(L(X, Y|\bar{\vartheta}))$$

where X are observed data, while $L(\cdot|\vartheta)$ is the likelihood of the complete data under the Markov chain with parameters ϑ . DIC values for the four different models considered in this study (see Section 4.3) are presented in Table 4.3. In school A, CGS model clearly is preferred to the others because its DIC value is

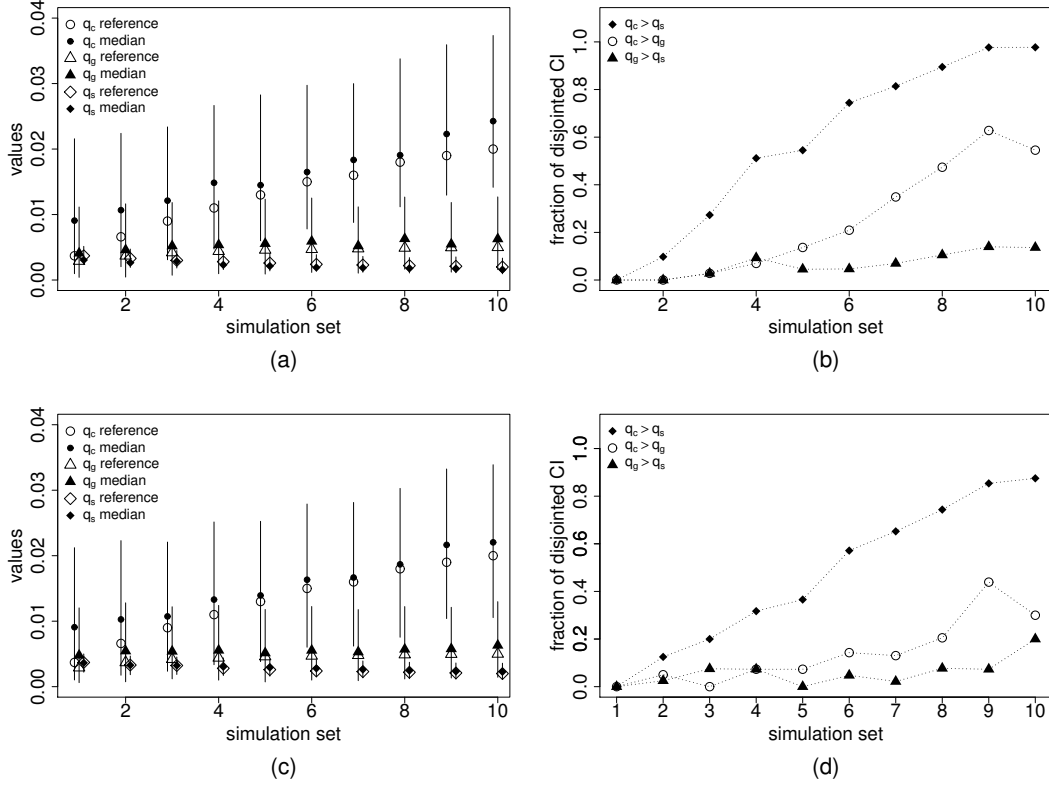


Figure 4.4: Fifty simulations (panels a and c) starting from reference values represented by white dots (in Table 4.2) and $\varepsilon = 10^{-3}$ by assuming that a 20% of the data of each class is not reported. The estimated values are represented as black dots with the 95%-credible intervals. Fraction of simulations in which the 95%-credible intervals for the different parameters do not intersect in panels b) and d). In panels a) and b) 20% of the data are considered to be missing. In panels c) and d) 20% of the data of each class are not regarded and only the 70% of the data are correct, the 20% of them correspond to a ± 1 and the remaining 10% to a ± 2 .

much lower. In School B CGS with constant ε is, according to DIC value, only slightly better than CG model, and both are definitely preferred to S; on the other hand, the model with varying probability of infection from outside is much better than all others.

Model	School A	School B
CGS ($q_c, q_g, q_s, \varepsilon$)	702.8314	757.9087
S ($q_c = q_g = q_s, \varepsilon$)	799.9111	779.3803
CS ($q_c, q_g = q_s, \varepsilon$)	774.9074	761.1634
CGSvar ($q_c, q_g, q_s, \varepsilon_{var}$)	751.2	426.21

Table 4.3: *DIC values of the different models considered. Model CGS has three different transmission rates inside the school (q_c , q_g and q_s) . Model S has a homogeneous infection rate inside the school (q_c). Model CS has a transmission rate for the class (q_c) and a different transmission rate in the remaining part of the school (q_g). Model CGSvar is the same as CGS but with with a non-constant ε .*

4.4 Estimates of transmission probabilities

Table 4.4 summarizes the estimated infection probabilities within-class q_c , in the same grade q_g , in different grades, within the schools q_s and from outside the schools for schools A and B, and Figure 4.5a presents a comparison of the estimates obtained for the two schools.

Parameters	School A	School B
mean of q_c [95% CI]	1.39×10^{-2} [$8.1 \times 10^{-3} - 2.03 \times 10^{-2}$]	1.96×10^{-2} [$1.11 - 2.89 \times 10^{-2}$]
mean of q_g [95% CI]	4.36×10^{-3} [$9.61 \times 10^{-4} - 8.34 \times 10^{-3}$]	4.61×10^{-3} [$2.98 \times 10^{-4} - 1.15 \times 10^{-2}$]
mean of q_s [95% CI]	9.52×10^{-4} [$2.87 \times 10^{-4} - 1.82 \times 10^{-3}$]	2.96×10^{-3} [$1.64 - 4.45 \times 10^{-3}$]
mean of ε [95% CI]	3.70×10^{-3} [$1.95 - 5.69 \times 10^{-3}$]	2.65×10^{-3} [$1.37 - 4.2 \times 10^{-3}$]

Table 4.4: *Mean and 95%-credible intervals of the estimates for the infection probabilities in schools A and B, when considering model CGS.*

The most evident feature of these results is that, for both schools, the

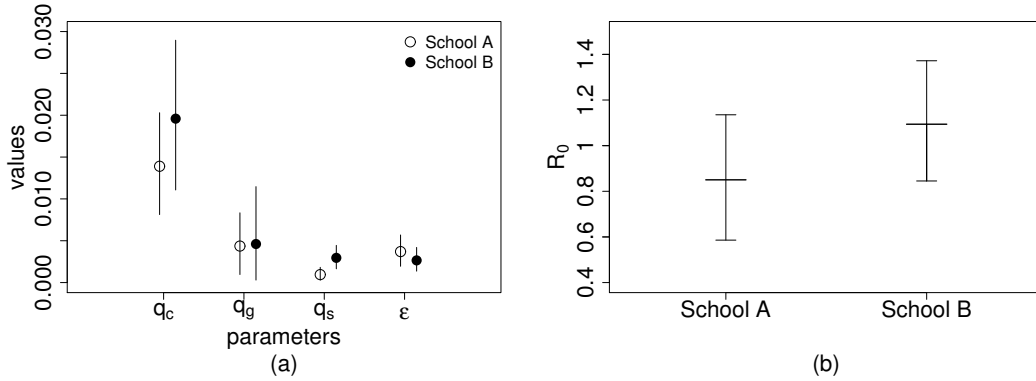


Figure 4.5: *Estimated values of the transmission parameters for school A and B. White and black dots represent the mean of the posterior distribution for school A and school B respectively, bars represent 95%-credible intervals. (b) Estimated values of the basic reproduction number R_0 inside schools A and B. Thick line and bars represent means and 95%-credible intervals.*

estimated class infection transmission probability is the highest of all settings. Grade transmission probability is estimated in both schools to be higher than school transmission; however the respective 95%-credible intervals overlap (just barely in school A, largely in school B).

As for comparisons between schools, estimates of class and grade transmission probability are similar, as is the probability of transmission from outside the school. On the other hand, estimates of school transmission probability differ between the two schools (95%-credible intervals barely overlap).

Using these estimates for transmission probabilities, we obtain from (4.1) the values of R_0 shown in Figure 4.5b, with an average of 0.8503 in school A and 1.094 in school B. Note that (4.1) is based only on within-school transmission and does not include transmissions to household members or acquaintances; on the other hand, the estimates based on Figure 4.1 depend on all infected students, whatever their source of infection.

4.5 Model validation

In order to assess whether the CGS model is compatible with the data, we performed 400 simulations (for each school) having randomly drawn the parameter values from the relative posterior distributions. The model was compared with

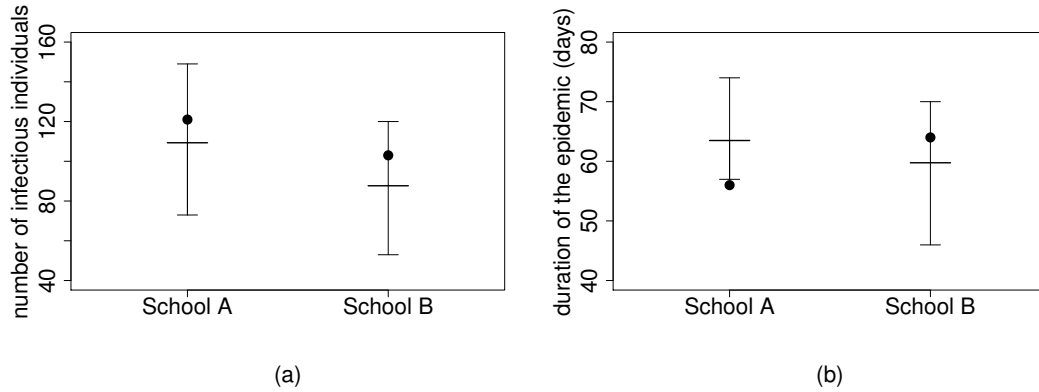


Figure 4.6: *The plot of the total number of infectious individuals (panel a) and the duration of the epidemic (panel b) in 400 simulations. The black dot indicates the observed number of infectious individuals and the observed length of the epidemic in the two schools. Thick line and bars represent means and 95%-credible intervals.*

the data (see Figure 4.6) through two different indicators: the total number of infected children and the total length of the epidemic.

Chapter 5

Discussion

In this chapter we summarize and discuss the main results obtained by analysing the epidemic model introduced in Section 3.2 and we show how our results can be compared with the ones obtained in other works. We stress the limitations and introduce some possible improvements for this particular model such as explicit household transmission, school closure during weekends or asymptomatic cases.

We estimated influenza transmission probabilities in a school setting, using the (incomplete) data collected through a retrospective survey conducted in December 2009 in two primary schools and we found that, in both schools, influenza was mainly transmitted within-class (Figure 4.5). Same- and different-grade transmission, as well as outside-school transmission, were all significantly lower than within-class transmission, with no significant differences between them (Figure 4.5).

We found that for both primary schools model CGS (that distinguishes within-class, same-grade and different-grade transmission) has the lowest DIC, i.e. is the favourite model overall. According to the DIC, models CGS and CS (that distinguishes within-class transmission from the general within-school transmission only) are equivalently good for school B, which reflects the similarity observed in the estimated same-grade and different-grade transmissions (Figure 4.5).

Similar results were obtained by Cauchemez *et al.* [16], where the transmission probability between students of the same class was five times greater than the transmission probability between students of the same grade and, in turn, this was five times higher than the transmission probability between students of different

grades. The estimates we obtained are similar, with factors of 3-4 instead of 5, except for the grade-school ratio in school B, which is just above 1. These results are also consistent with the studies presented in [66, 67], where children used wearable sensors: in these studies it was found that children spent on average three times more time with children of the same class than with children of other classes. The fact that within-class transmission is estimated to be higher than within-school transmission can have implications on the design of school closure policies aimed at mitigating the spread of influenza, especially on evaluating the effectiveness of gradual closures (where single classes close first, then grades and finally the entire school) [66, 68, 69].

Another interesting result emerges from the comparison between the two schools involved in the study: while the estimates for within-class q_c and within-grade q_g transmission probabilities are similar for the two schools, the estimate for school-wide transmission q_s is remarkably different, as 95%-credible intervals barely overlap. This result can bear on the issue on whether infection transmission should depend on the density or the frequency of infectious individuals [70, 71]. In the model, we have assumed that transmission probability per individual is a constant. Alternatively, we could have adhered to the more usual assumption that transmission probability is inversely proportional to the number of individuals in that setting [72]; in case of school transmission, we should have used $q_s(A) = c/n_s(A)$ and $q_s(B) = c/n_s(B)$. As $n_s(A) \approx 1.5n_s(B)$, this results into $q_s(B) \approx 1.5q_s(A)$. The mean estimated q_s for school B is about 3 times the estimated mean for school A, but 1.5 sits well inside the ratios of values in the 95%-credible intervals. Thus we can conclude that a frequency-dependent transmission probability is compatible with our findings, whereas density-dependent is not. It is remarkable that, while the estimates of transmission probabilities obtained in [16] are somewhat higher than ours, as for within-class and within-grade transmission, those of within-school transmission are similar to those of school A; this pattern appears to confirm that indeed larger school size (436 in the school studied in [16]) decreases per person transmission probability within school, although the social context may be very different, and there is no reason why contact patterns should be similar in Pennsylvania as in Italy. More studies comparing infection patterns in schools of different size but in a homogeneous social system, would be needed for such a conclusion.

One could have used frequency-dependent transmission probability also for within-class and within-grade transmission probabilities, but, as class size is approximately constant, results could not have changed remarkably. One could improve a model with frequency-dependent transmission by taking into account

the actual number of students in class each day; unfortunately such data was not available to us.

The estimates of the school R_0 [School A mean and 95% CI 0.8503 (0.5859-1.1353) and School B 1.094 (0.845-1.372)] lie in the low end of the spectrum of values estimated from influenza spread in schools [60]. In particular, our model provides estimates of R_0 lower than 1 for school A, which highlights the importance of outside transmission (with a likely strong role of households) in maintaining the school outbreak, consistently with the findings of [16].

As information on household cases was scarce, we had to rely on two simple models for outside transmission: either a constant probability ε or a probability proportional to influenza incidence in the population (variable ε). Concerning the latter, we could use only the weekly ILI incidence estimated through the surveillance system InluNet; we used it at the Trento province level, that, on the one hand, is probably much larger than the territory where students of the two schools live, and, on the other hand, is smaller than the recommended aggregation level of sentinel data that makes them statistically significant. Despite these limitations, we deem that it yields the best available alternative to a constant probability of outside infection. The results of the comparison between the two model variants are not unequivocal: in School A model CGS with varying ε yields a larger DIC than model CGS with a constant ε , while in School B the model with varying ε is much better than the model with constant ε .

An explanation for this contrasting result can be found in Figure 3.1. In School A, many scattered cases occur before infection takes off, while in School B almost no cases are recorded before the infection peak. Thus, to fit the pattern of infection observed in school A, the probability of infection from outside the school must have been non-negligible already from the second half of October, when overall ILI incidence was very low; if the probability of outside-school infection were proportional to ILI incidence, this would have forced it to become extremely large in November, which is hardly compatible with observed data. On the other hand, the infection trend school B is quite aligned with overall ILI incidence; thus, a model with outside-transmission proportional to overall incidence fits data very well. Clearly, this is an explanation for the statistical result, but does not clarify the reason (a localized epidemic in the community?) for the many scattered cases in School A before the epidemic start.

The robustness of the results obtained has been supported by the analysis of simulated data. Indeed, the tests show that very seldom 95%-credible intervals do not intersect without an actual difference in the transmission probabilities in the different contexts: precisely, when $q_c = q_s$ (simulation 1 of Figure 4.3) only 4

times out of 50, it is found that 95%-credible intervals do not intersect, although, when it occurs, q_c is always larger than q_s . On the other hand, when q_c is at least 3 times larger than q_s (simulations 3-10 of Figure 4.3) a difference is picked up in at least 85% of the cases. Furthermore, the algorithm produces correct estimates even in presence of missing data (we assumed 20% of those, similarly to actual data) and with errors in the reported dates (we assumed 30% of these), with the only visible effect of yielding somewhat wider credible intervals, relatively to the case of no missing data and no errors.

The choice of $\gamma = 0.1$ for the probability that the effective (at school) infectious period lasts 2 days has been extrapolated from limited data presented in [54]) may appear questionable, and one may ask whether γ could have been estimated as well from data. However, we show (Figure S1) that the algorithm we used is not capable on simulated data of estimating the probability γ of being infectious (at school) for 2 days, whatever is population size and the value of γ used for simulating data. Indeed, in most cases length of the infectious period and generation time are estimated from household studies or other cases where dates of infections can be independently established [70, 73]. As far as we know, the only exception is the study by White *et al.* [74], who were able to obtain an estimate of the serial interval from a detailed epidemiological curve. Our study shows that it is generally very difficult to do so.

Although the value of γ used in the study may be somewhat arbitrary, the main conclusions obtained on the differences between transmission probabilities in the different contexts and between two different schools do not depend on the exact value of γ ; changing its value simply results in changing the numerical estimates of q_c , q_g and q_s but not their relative features.

Similar identifiability problems led us to assume the simplified assumption that each student infected at school is infectious at school the following day, while it can be argued from the results in [54] that some will be infectious only in their second day after infection, and others will show symptoms before the first day and will be already kept home. Allowing for such possibilities would introduce other parameters that are difficult to estimate, without relevant effects on the main results.

There are several other aspects that we did not consider in our model, such as explicit household transmission, school closure during weekends or asymptomatic cases.

It has been estimated [75] that school closures during weekends contributes to decrease the effective reproduction number of about 8%. Since the generation

time in the school setting is short, weekends can break the transmission chain at school thus having an impact on the transmission pattern, as can be seen in [66, 67, 72, 75]. On the other hand, household and outside transmission is likely to increase during weekends, as often assumed in modelling studies [72, 76]. Again, for the sake of simplicity, we preferred to avoid the introduction of parameters that may not be easily estimated, but in principle the model could be extended to distinguish between weekdays and weekends.

Our model assumes that all infections are symptomatic and lead to the same level of infectiousness. Indeed, using raw data, the estimate of children showing influenza symptoms is 52%. This value is comparable to the estimate of 56.9% infection rate for 2009H1N1v in primary-school children in Italy, that was derived from serological data [77]; thus, it seems likely that only a small number of children in those schools got infected with influenza without showing symptoms. Indeed, it is possible that the fraction of children of the schools considered in our study that got infected was much higher than the national average of 56.9%. Alternatively, it is possible that some of the children that reported symptoms were not actually infected with influenza virus, while others were infected but did not show symptoms. The lack of serological data prevents from a choice between different alternatives. Accordingly, we decided to use the most parsimonious alternative, namely to neglect asymptomatic infections.

Despite these limitations, our analysis provides evidence of different influenza transmission in class and grade. We have shown that the MCMC algorithm used can yield plausible results even starting from incomplete and possibly inaccurate data (such as those derived from questionnaires); further and more detailed data (including also serology) would be useful to improve the model and the corresponding estimates.

Appendix A

Algorithm used to estimate transmission probability in schools for the 2009 H1N1 influenza pandemic in Italy

The available data are the knowledge on whether students have acquired infection or not, as well as the days of symptom onset (all this information will be named Z , where Z_i is the day of symptom onset for individuals i having acquired infection, while $Z_i = \infty$ for the others). For the moment, we neglect the problem of missing data.

We wish to obtain *a posteriori* distributions for the parameters q_s , q_A , q_B and γ (collectively named ϑ). As computing the likelihood of the data Z would be very complex, we include in the parameters to be estimated the dates Y of infection of the individuals that have become infected.

Then, through Bayes' formula

$$f_{post}(\vartheta, Y) \propto P(Z|\vartheta, Y)f_{prior}(\vartheta, Y) = \frac{P(Z, Y|\vartheta)}{P(Y|\vartheta)}P(Y|\vartheta)\pi(\vartheta) = P(Z, Y|\vartheta)\pi(\vartheta). \quad (\text{A.1})$$

where

$$P(Z, Y|\vartheta) = \prod_{j,h} \prod_{t=t_{min}}^{T_{max}-1} \gamma^{I_t^{j,h}} (1-\gamma)^{(I_t^{j,h}-I_{t+1}^{j,h})} P(S_{t+1}^{j,h}|S_t^{j,h}, I_t^{j,h}, I_t^j, I_t). \quad (\text{A.2})$$

$P(S_{t+1}^{j,h}|S_t^{j,h}, I_t^{j,h}, I_t^j, I_t)$ can be obtained from (3.2), and the quantities $S_t^{j,h}$, $I_t^{j,h}$, I_t^j , I_t can all be easily computed from Y and Z .

The transition probabilities $p_t^{j,h}$ used in (3.2) can be written in a computationally more efficient way, by introducing the quantities q_A and q_B as

$$\begin{aligned} 1 - q_A &= \frac{1 - q_c}{1 - q_g} \\ 1 - q_B &= \frac{1 - q_g}{1 - q_s} \end{aligned}$$

as

$$p_t^{j,h} = (1 - q_A)^{I_t^{j,h}} (1 - q_B)^{I_t^j} (1 - q_s)^{I_t} (1 - \varepsilon) \quad (\text{A.3})$$

using the quantities

$$\begin{aligned} I_t^j &= \sum_{l=1}^{n_j} I_t^{jl} \quad (\text{total number of infectious in grade } j) \\ I_t &= \sum_{m=1}^5 \sum_{l=1}^{n_m} I_t^{ml} \quad (\text{total number of infectious in the school}) \end{aligned}$$

Missing data can be handled very easily in this framework: it is enough including in the vector of added parameters Y the state (eventually infected or not) and, if so, the dates of infection and removal for all students whose information is missing.

The posterior distribution is estimated as the stationary distribution of the Markov chain resulting from Metropolis-Hastings algorithm [42, 56].

A.1 Parameters updating

To update the parameters we use a Single Component Metropolis-Hastings (see [56]) because, instead of updating all the parameters at once, it is often computationally convenient to do that in different steps.

If we consider one of the infection rates $q_c, q_g, q_s, \varepsilon$, the new state x is obtained in the following way

$$x = \frac{ye^{ra}}{1 - y + ye^{ra}} \rightarrow \begin{cases} 1 & r \rightarrow \infty \\ y & r = 0 \\ 0 & r \rightarrow -\infty \end{cases}$$

where a is from a multivariate normal and so, by changing r , we can find a chain with a good mixing and a good convergence.

So, by simple calculations, we obtain that,

$$q(y|x) = \frac{1}{y(1-y)\sqrt{2\pi r}} e^{-\frac{1}{2r^2}[\log(x)+\log(1-y)-\log(y)+\log(1-x)]^2}$$

$$q(x|y) = \frac{1}{x(1-x)\sqrt{2\pi r}} e^{-\frac{1}{2r^2}[\log(x)+\log(1-y)-\log(y)+\log(1-x)]^2}$$

and then $\frac{q(y|x)}{q(x|y)}$ is equal to

$$\frac{q(y|x)}{q(x|y)} = \frac{x(1-x)}{y(1-y)}.$$

To update the day of infection we use a different method. We choose randomly the grade and the class to be updated and, by considering that we can have only two choices for the infection days, we simply change $-1 \rightarrow -2$ or $-2 \rightarrow -1$ so to have a different day of infection.

Part II

Dynamics of Host-Parasitoid Interactions and Coexistence of Different Hosts

Chapter 1

Introduction

opulation models are being extensively used to describe the dynamics that result from the interactions between different species. In this part of the thesis we establish conditions for species coexistence and for competitive exclusion by considering a 2 host-parasitoid model that can be applied to relevant problems in agriculture.

Parasitoids are a widespread group of insects often employed as a tool for biological control, and thus have been subjected to many modelling efforts [78].

Many parasitoid species are generalist [79] that are capable of attacking different host species. Conversely, often host species are attacked by different parasitoids. Several modelling papers have addressed this latter phenomenon, which at first sight may appear in contrast with the competitive exclusion principle [80, 81]; indeed, Briggs [82] has been able to prove that two parasitoid species can coexist at equilibrium on a single host species, as long as they attack different host-stages, and the length of each stage is sufficiently variable.

On the other hand, very little attention has, to our knowledge, been paid to the interactions of one or more parasitoid species with multiple hosts species. It must be remarked that several models have been devoted to the evolution of host choice by parasitoids; however, in this approach host densities are simply taken as given without considering the dynamics of species interactions.

The recent invasion from Eastern Asia of *Drosophila suzukii*, spotted-wing fruit-fly [83], into Europe and North America has revived the interest in understanding multi-hosts multi-parasitoids interactions and the evolution of host choice. In fact, since its first detection in 2008 [84–89] it has provoked serious damages to orchards causing significant economic losses [90–94] and control

through insecticides is difficult and risks leaving significant residues in the fruit.

While the introduction into Europe and North America of native parasitoids would require careful studies and a long protocol for authorizations, it has been found out that *D. suzukii* is attacked by several indigenous parasitoids of other *Drosophila* spp. in particular a larval koinobiont and solitary endoparasitoid, *Leptopilina heterotoma* and a generalist pupal ectoparasitoid, *Pachycrepoideus vindemiae*.

In order to simplify the problem, we limit ourselves to consider the case of a single parasitoid species. We will develop a model based on the scheme proposed by [95] (earlier by [96] and generalized by [82,97]) where time is continuous and delays (fixed or distributed) occur between host stages.

To our knowledge, this model has never been extended to a two host species model. Thus, by starting from [82], we keep only the larval-stage parasitoid that can however attack two different host species. The developed 2 host-parasitoid model analyses the interactions between two different hosts and one parasitoid and determines whether the parasitoid has a preference not only for the life stage but also for the host species.

A background on historical population model is presented in Chapter 2. In Chapter 3 we describe the model studied and discuss the assumptions. In Chapter 4 we compute the equilibria and their stability, and find the conditions for equilibrium coexistence of the host species. We extend the analysis to the case where the one-host model exhibits attracting periodic solutions; the analysis of the stability with respect to the complete system of such periodic solutions requires the use of numerical methods recently developed to approximate the dominant multiplier(s) of linear delay-differential equations with periodic coefficients; it is also necessary to approximate the periodic solutions, and to use a continuation algorithm to track them when varying model parameters. It turns out that the periodicity induced by host-parasitoid interactions makes it easier for more host species to coexist, up to the point that species can coexist even when no density-dependence exists and their densities are controlled only by the parasitoids. Finally, in Chapter 5 we discuss the implications and the limitations of the results obtained, while longer computations are left to Appendix A.

Chapter 2

Background on population models

This chapter summarizes some preliminaries on population models useful for the analysis of the interactions between *D. suzukii* and its predators. The aim of these models is in fact to study population dynamics and to establish conditions for species coexistence or for competitive exclusion.

2.1 Classical models

When we consider dynamics between populations we usually refer to the classical Lotka-Volterra model that describes prey-predator interactions. This model was formulated about the same time both by Vito Volterra in 1926 [98] to explain the fluctuations in the Adriatic sea fish population that were of great concern to fishermen in times of low fish populations and by Alfred J. Lotka in 1925 [99]. This model is a simple and unrealistic model that is able to explain the essential mechanisms behind the interactions of two different populations. In fact, it considers two species in the same habitat of which one of these species is the main resource for the other. The main assumption of this model is that the survival of the predator depends on the abundance of the prey and the prey is uniquely controlled by the predator.

By following the description of the interactions between species, the state of the population can be identified by $H(t)$ and $P(t)$ that are the numbers of preys and predators at time t . This description provides a basic framework to explain periodic variations in nature and it may be varied by considering

Verhulst-logistic growth in absence of predators, the effect of harvesting on the ecosystem, the Gauss-type model or the Rosenzweig-MacArthur model [100].

Obviously in nature competition among species is not reserved only to two single population but it can involve also other populations that can share the same resource, $H(t)$, or have common predators, $P(t)$. Moreover prey and predators, in the absence of the other class in which the population is divided, can compete among them for the habitat. By following this principle, Volterra in 1926 provided the mathematical basis for the exclusion principle [101]:

two different species cannot indefinitely occupy the same ecological niche, but one of the two necessarily goes extinct, while the other saturates the niche.

This principle is a fundamental principle in Ecology but has also to be balanced by the fact that competition among species may have more complex outcomes than exclusion.

2.2 Delay differential equations

Classical models can be extended by taking into account that events, lost in the past, can still influence events in the present or future time. Thus a more realistic model should include some of the past history of the system and delay differential equations are an important key to describe real situation. In fact, when we describe the status of an ecosystem at a certain time, we should keep in mind that some past events may have influenced the status of the population at the time taken into account. The simplest example is represented by the reproduction of a species since the present birth rate depends on the population abundance in the past. Thus, by considering delay differential equations, we can include into the population model all the needed informations that can help us to better understand present and future dynamics.

By following this concept, we can introduce another concept of delays in population modelling, the age structure of the population.

2.2.1 Age structure models

The age structure of a population is what differentiate living organisms. In fact, generally, relevant parameters that characterize a population, such as fertility

and mortality, depends on age and change during individuals life. Thus, when we describe a population, we should consider not only the time but also the age distribution of the population at that time. According to that, all individuals of a population can be considered identical except for their age. This is in contrast with the classical models considered in the previous Section because in those cases all the individuals were considered interchangeable. Thus, more complex models that try to describe in a more realistic way a population add a structure that can depend on spatial location or age. As we have said, age is one of the most important parameter that distinguish individuals in a population because individuals of different ages can have different reproduction or mortality rates. The characteristic of the fecundity or of the mortality rate as a function of age is significant to the resulting dynamical growth and age distribution of the population.

The first age structured model was presented in 1910 by McKendrick [102] and it is the base for further models in this field. In this dissertation, we are interested in particular in maturation periods as a delay and instability causing mechanism. Delays in mortality rates are considered less important [103–109] and are equivalent to the assumption that the survivor ship is exponentially decreasing.

Chapter 3

Model

In this chapter we introduce a 2 host-parasitoid model based on delay differential equations that is an extension of the model presented in [95], and then extended in [82] and [97]. In particular, we consider here that adult parasitoids can attack only host larvae (adult hosts are invulnerable to parasitism) whose mortality can depend or not on their density at time t .

We introduce a 2 host-parasitoid model to study the interaction between different species as was done by Murdoch *et al.* [95] and by Briggs *et al.* [82, 97]. We assume that the life cycle of the host can be divided into three developmental stages: eggs E , larvae L (including also pupae, for *D. suzukii*) and adults A . We assume that the two hosts considered do not compete and that an interspecific competition is present at the larval stage so that, in absence of parasitoids, it leads the two host species to a carrying capacity.

According to the results obtained by [110], we assume that adult parasitoids P can attack only the larval stage of the host (adult hosts are invulnerable to parasitism) and that they can lay a single egg inside the host. Juvenile parasitoids develop then inside the larvae using them as food and emerge from them after a fixed host-dependent time T_{iP} , $i = 1, 2$ [95, 97, 110]. For the sake of simplicity, we assume that hosts can not survive to parasitoids attack by encapsulating them (see [110] for general details on encapsulation) and that parasitoids attack and death rates and host birth and death rates (except for the larval stage) and stages duration are kept constant and density-independent. In [97], Briggs *et al.* introduced into the model also other developmental delays by considering different weighting functions $w(x)$, where x is the time spent in a stage and the

mean delay would have been

$$T = \int_0^{\infty} w(x)xdx. \quad (3.1)$$

Furthermore, we suppose that

$$d_{L_i}(L_i(t)) = \mu_{L_i} + \nu_{L_i}L_i(t), \quad (3.2)$$

where μ_{L_i} is a constant background mortality and ν_{L_i} is the quantity for which the pro capita mortality changes by adding a new individual.

Thus, the 2 host-parasitoid model is given by

$$\begin{aligned} E'_i(t) &= R_{E_i}(t) - M_{E_i}(t) - d_{E_i}E_i(t) \\ L'_i(t) &= M_{E_i}(t) - M_{L_i}(t) - \alpha_i P(t)L_i(t) - d_{L_i}(L_i(t))L_i(t) \\ A'_i(t) &= M_{L_i}(t) - d_{A_i}A_i(t) \\ P'(t) &= \sum_{i=1}^2 \alpha_i P(t - T_{iP})L_i(t - T_{iP})s_{iP} - d_P P(t) \end{aligned} \quad (3.3)$$

where

$$\begin{aligned} R_{E_i}(t) &= \rho_i d_{A_i} A_i(t) \\ M_{E_i}(t) &= \rho_i d_{A_i} A_i(t - T_{E_i}) e^{-d_{E_i} T_{E_i}} \\ M_{L_i}(t) &= M_{E_i}(t - T_{L_i}) e^{-\int_{t-T_{L_i}}^t (\alpha_i P(y) + d_{L_i}(L_i(y))) dy} \end{aligned} \quad (3.4)$$

The host birth rate, $\beta_i = \rho_i d_{A_i}$, for simplicity in the analysis, is defined as the product between the mortality $d_{A_i} = 1/T_{A_i}$ that can be seen as the velocity of the species i (T_{A_i} is the average duration of the adult host stage) and a parameter ρ_i that represents the mean number of eggs produced per adult lifetime. The maturation rate from eggs to larvae, $M_{E_i}(t)$, is given by the sum of all the hosts recruited after a fixed time T_{E_i} and survived to mortality until the larval stage. Instead, the maturation rate from larvae to adults, $M_{L_i}(t)$, is given by the sum of all the hosts coming from the larval stage after a fixed time T_{L_i} and survived both to mortality and to the attack of the parasitoids.

All model parameters are described in Table 3.1.

Symbol	Description
ρ_i	Total lifetime host fecundity
d_{E_i}	Mortality of host eggs
$d_{L_i}(L_i(t))$	Mortality of host larvae
μ_{L_i}	Constant background mortality of host larvae
ν_{L_i}	The quantity for which the pro capita mortality changes by adding a new individual
d_{A_i}	Mortality of host adults
d_P	Mortality of adult parasitoids
α_i	Attack rate of adult parasitoids on host larvae
s_{iP}	Survival of juvenile parasitoids
T_{E_i}	Duration of egg host stage
T_{L_i}	Duration of larva host stage
T_{iP}	Duration of juvenile parasitoid stage

Table 3.1: *Model parameters present in the 2 host-parasitoid model. All parameters are kept constant and density-independent except the larval death rate $d_{L_i}(L_i(t)) = \mu_{L_i} + \nu_{L_i}L_i(t)$ that depends on a constant background mortality, μ_{L_i} , and on the quantity for which the pro capita mortality changes by adding a new individual, ν_{L_i} .*

Chapter 4

Invasibility conditions

This chapter summarizes the coexistence conditions of two host species of the model presented in Chapter 3. These are found by linearising the system around the equilibria with only one host species present. We show that, when no density-dependence is present, the two hosts cannot coexist but, once density dependence is introduced, we can find some conditions for hosts coexistence. In this chapter we discuss also what happens if we are in periodic conditions using numerical approximations and by giving a mathematical proof of what we have found through the approximation of the dominant eigenvalue of monodromy operator with arbitrary delay and its application to host-parasitoid models.

4.1 Single host equilibria

Coexistence conditions of the two host species for the model presented in Chapter 3 are determined by a linearisation of system (3.3) around the equilibria with only one host present. To find these equilibria (*Eq1*, the equilibrium with only host 1, and *Eq2*, with only host 2), we put all the equations of (3.3) equal to zero.

Let us find, for instance, the equilibrium when only host 1 is present. Thus, from the last equation of (3.3), by considering P constant and different from zero, we can obtain \bar{L}_1 .

$$\alpha_1 s_{1P} P L_1 - d_P P = 0$$

Once we have obtained the value for \bar{L}_1 , from the third equation, by considering

A_1 constant and different from zero, we can obtain \bar{P}_1 .

$$\rho_1 d_{A_1} A_1 e^{-d_{E_1} T_{E_1} - (\alpha_1 P + d_{L_1}(\bar{L})) T_{L_1}} - d_{A_1} A_1 = 0$$

After that, from equation two and one of (3.3), it is easy to find the values of \bar{A}_1 and \bar{E}_1 respectively.

$$\begin{aligned} \rho_1 d_{A_1} e^{-d_{E_1} T_{E_1}} (1 - e^{-(\alpha_1 \bar{P}_1 + d_{L_1}(\bar{L}_1)) T_{L_1}}) A_1 - (\alpha_1 \bar{P}_1 + d_{L_1}(\bar{L}_1)) \bar{L}_1 &= 0 \\ \rho_1 d_{A_1} \bar{A}_1 (1 - e^{-d_{E_1} T_{E_1}}) - d_{E_1} E_1 &= 0 \end{aligned}$$

The equilibrium when only host 1 is present, $Eq1$, is thus given by

$$\begin{aligned} \bar{E}_1 &= \frac{\rho_1 d_{A_1} \bar{A}_1 (1 - e^{-d_{E_1} T_{E_1}})}{d_{E_1}} \\ \bar{L}_1 &= \frac{d_P}{\alpha_1 s_{1P}} \\ \bar{A}_1 &= \frac{(\alpha_1 \bar{P}_1 + \mu_{L_1} + \nu_{L_1} \bar{L}_1) \bar{L}_1}{\rho_1 d_{A_1} e^{-d_{E_1} T_{E_1}} (1 - e^{-(\alpha_1 \bar{P}_1 + \mu_{L_1} + \nu_{L_1} \bar{L}_1) T_{L_1}})} \\ \bar{P}_1 &= \frac{\ln(\rho_1) - d_{E_1} T_{E_1} - (\mu_{L_1} + \nu_{L_1} \bar{L}_1) T_{L_1}}{\alpha_1 T_{L_1}} \end{aligned} \quad (4.1)$$

In a similar way, we can find $Eq2$, the equilibrium when only the host species 2 is present.

It is convenient to define \hat{P}_i as the value of \bar{P}_i when $\nu_{L_i} = 0$, i.e.

$$\hat{P}_i = \frac{\ln(\rho_i) - d_{E_i} T_{E_i} - \mu_{L_i} T_{L_i}}{\alpha_i T_{L_i}} \quad (4.2)$$

and similarly $\hat{L}_i = \bar{L}_i$.

In this way we obtain the equilibria without density-dependence, $\hat{Eq}1$ and $\hat{Eq}2$.

Note that $\bar{P}_i = \hat{P}_i - \frac{\nu_{L_i} \bar{L}_i}{\alpha_i}$, so that the equilibrium (Eq_i) has all its components positive if and only if

$$\hat{P}_i > \frac{\nu_{L_i} \bar{L}_i}{\alpha_i} \equiv \rho_i \exp \left\{ - \left(d_{E_i} T_{E_i} + (\mu_{L_i} + \frac{\nu_{L_i} d_P}{\alpha_i s_{iP}}) T_{L_i} \right) \right\} > 1. \quad (4.3)$$

In what follows, we will implicitly assume that (4.3) holds for $i = 1, 2$.

Proposition 4.1.1 summarizes the outcome of the linearisation of the system at the equilibria when only one host is present.

Proposition 4.1.1. *Equilibria Eq1 and Eq2 are both unstable if and only if $\hat{P}_1 < \hat{P}_2 + \frac{\nu_{L_1}}{\alpha_1} \hat{L}_1$ and $\hat{P}_2 < \hat{P}_1 + \frac{\nu_{L_2}}{\alpha_2} \hat{L}_2$.*

Proof. The outcome of the linearisation of (3.3) around equilibrium Eq1 (4.1) can be reduced to a single equation

$$\begin{aligned}
A_2'(t) &\approx \bar{M}_{L_2}(t) - d_{A_2} A_2(t) \\
&= M_{E_2}(t - T_{L_2}) e^{-\int_{t-T_{L_2}}^t (\alpha_2 \bar{P}_1 + \mu_{L_2}) dy} - d_{A_2} A_2(t) \\
&= \rho_2 d_{A_2} A_2(t - T_{E_2} - T_{L_2}) e^{-d_{E_2} T_{E_2}} e^{-\int_{t-T_{L_2}}^t (\alpha_2 \bar{P}_1 + \mu_{L_2}) dy} - d_{A_2} A_2(t) \\
&= \rho_2 d_{A_2} A_2(t - T_{E_2} - T_{L_2}) e^{-d_{E_2} T_{E_2}} e^{-\mu_{L_2} T_{L_2} - \alpha_2 T_{L_2} \bar{P}_1} - d_{A_2} A_2(t) \\
&= \rho_2 d_{A_2} A_2(t - T_{E_2} - T_{L_2}) e^{-d_{E_2} T_{E_2}} e^{-\mu_{L_2} T_{L_2} - \alpha_2 T_{L_2} \frac{\ln(\rho_1) - d_{E_1} T_{E_1} - (\mu_{L_1} + \nu_{L_1} \bar{L}_1) T_{L_1}}{\alpha_1 T_{L_1}}} \\
&\quad - d_{A_2} A_2(t)
\end{aligned} \tag{4.4}$$

Thus, by following for instance [111], A_2 increases if

$$\begin{aligned}
\rho_2 e^{-d_{E_2} T_{E_2} - \mu_{L_2} T_{L_2} - \alpha_2 T_{L_2} \frac{\ln(\rho_1) - d_{E_1} T_{E_1} - (\mu_{L_1} + \nu_{L_1} \bar{L}_1) T_{L_1}}{\alpha_1 T_{L_1}}} - 1 &> 0 \\
\frac{\ln(\rho_1) - d_{E_1} T_{E_1} - (\mu_{L_1} + \nu_{L_1} \bar{L}_1) T_{L_1}}{\alpha_1 T_{L_1}} &< \frac{\ln(\rho_2) - d_{E_2} T_{E_2} - \mu_{L_2} T_{L_2}}{\alpha_2 T_{L_2}}
\end{aligned} \tag{4.5}$$

In the same way, A_1 increases if

$$\frac{\ln(\rho_2) - d_{E_2} T_{E_2} - (\mu_{L_2} + \nu_{L_2} \bar{L}_2) T_{L_2}}{\alpha_2 T_{L_2}} < \frac{\ln(\rho_1) - d_{E_1} T_{E_1} - \mu_{L_1} T_{L_1}}{\alpha_1 T_{L_1}} \tag{4.6}$$

For the sake of simplicity, from (4.1) and by considering $\hat{E}q1$ and $\hat{E}q2$, the coexistence conditions (4.5) and (4.6) can be written as

$$\begin{aligned}
\hat{P}_1 &< \hat{P}_2 + \frac{\nu_{L_1}}{\alpha_1} \hat{L}_1 \\
\hat{P}_2 &< \hat{P}_1 + \frac{\nu_{L_2}}{\alpha_2} \hat{L}_2
\end{aligned} \tag{4.7}$$

□

This condition can be seen as a double invasibility condition that has often been considered to grant species coexistence [112].

Corollary 4.1.2. If $\nu_{L_1} = \nu_{L_2} = 0$, it is impossible to have mutual invasibility of $Eq1$ and $Eq2$.

Proof. The two equations in (4.7) are incompatible if $\nu_{L_1} = \nu_{L_2} = 0$. \square

Proposition 4.1.3 ensures the existence of an equilibrium where both the host species are present under density-dependence conditions when equilibria $Eq1$ and $Eq2$ are both unstable. Let us name this equilibrium $Eq12$.

Proposition 4.1.3. *Equilibrium $Eq12$ exists if and only if equilibria $Eq1$ and $Eq2$ are unstable.*

Proof. An equilibrium where both the host species are present is given by setting equal to zero both the equations for adult hosts and for the parasitoid in (3.3). Thus, we obtain

$$\begin{cases} \rho_1 e^{-d_{E_1} T_{E_1} - (\alpha_1 P^* + d_{L_1}(L_1^*)) T_{L_1}} = 1 \\ \rho_2 e^{-d_{E_2} T_{E_2} - (\alpha_2 P^* + d_{L_2}(L_2^*)) T_{L_2}} = 1 \\ \alpha_1 L_1^* s_{1P} + \alpha_2 L_2^* s_{2P} - d_P = 0 \end{cases} \quad (4.8)$$

By solving (4.8), keeping in mind $\hat{E}q1$ and $\hat{E}q2$, we have

$$\begin{cases} P^* = \hat{P}_1 - \frac{\nu_{L_1}}{\alpha_1} L_1^* \\ P^* = \hat{P}_2 - \frac{\nu_{L_2}}{\alpha_2} L_2^* \\ L_1^* = \hat{L}_1 - \frac{\alpha_2 s_{2P}}{\alpha_1 s_{1P}} L_2^* \end{cases} \quad (4.9)$$

Since the equilibrium value of the parasitoid with both the hosts has to be equal, we have

$$\hat{P}_1 - \frac{\nu_{L_1}}{\alpha_1} L_1^* = \hat{P}_2 - \frac{\nu_{L_2}}{\alpha_2} L_2^*$$

This equation, together with the last of (4.9) is a linear system in the unknowns L_1^* and L_2^* that can be easily solved yielding to simple algebraic calculations, and obtaining

$$\begin{aligned} L_1^* &= \alpha_1 \hat{L}_1 \left(\frac{\alpha_2 (\hat{P}_1 - \hat{P}_2) + \nu_{L_2} \hat{L}_2}{\alpha_2 \nu_{L_1} \hat{L}_1 + \alpha_1 \nu_{L_2} \hat{L}_2} \right) \\ L_2^* &= \alpha_2 \hat{L}_2 \left(\frac{\alpha_1 (\hat{P}_2 - \hat{P}_1) + \nu_{L_1} \hat{L}_1}{\alpha_1 \nu_{L_2} \hat{L}_2 + \alpha_2 \nu_{L_1} \hat{L}_1} \right) \\ P^* &= \frac{\alpha_1 \nu_{L_2} \hat{L}_2 \hat{P}_1 - \nu_{L_1} \nu_{L_2} \hat{L}_2 \hat{L}_1 + \alpha_2 \nu_{L_1} \hat{L}_1 \hat{P}_2}{\alpha_1 \nu_{L_2} \hat{L}_2 + \alpha_2 \nu_{L_1} \hat{L}_1} \end{aligned} \quad (4.10)$$

The values of L_1^* and L_2^* are both positive if and only if (4.7) holds. As for P^* , the numerator in the third of (4.10) can be rewritten as

$$\nu_{L_2} \hat{L}_2 (\alpha_1 \hat{P}_1 - \nu_{L_1} \hat{L}_1) + \alpha_2 \nu_{L_1} \hat{L}_1 \hat{P}_2$$

which is positive because of (4.3).

Using (4.7) in (4.10), we obtain

$$L_1^* < \hat{L}_1 \left(\frac{\alpha_2 \nu_{L_1} \hat{L}_1 + \alpha_1 \nu_{L_2} \hat{L}_2}{\alpha_2 \nu_{L_1} \hat{L}_1 + \alpha_1 \nu_{L_2} \hat{L}_2} \right) = \hat{L}_1.$$

Similarly

$$L_2^* < \hat{L}_2 \left(\frac{\alpha_1 \nu_{L_2} \hat{L}_2 + \alpha_2 \nu_{L_1} \hat{L}_1}{\alpha_1 \nu_{L_2} \hat{L}_2 + \alpha_2 \nu_{L_1} \hat{L}_1} \right) = \hat{L}_2.$$

In other words, the equilibrium value for each host species in presence of the other is always lower than in absence. Hence, the presence of the common parasitoid always causes an indirect competition between the two species.

As for the parasitoid density at equilibrium, using the relation between \hat{P}_i and \bar{P}_i , we can rewrite

$$P^* = \frac{\nu_{L_2} \hat{L}_2 \alpha_1 \bar{P}_1 + \alpha_2 \nu_{L_1} \hat{L}_1 \hat{P}_2}{\alpha_1 \nu_{L_2} \hat{L}_2 + \alpha_2 \nu_{L_1} \hat{L}_1}$$

showing that P^* is a weighted mean between \bar{P}_1 and \hat{P}_2 . Symmetrically, one can also write

$$P^* = \frac{\alpha_1 \nu_{L_2} \hat{L}_2 \hat{P}_1 + \nu_{L_1} \hat{L}_1 \alpha_2 \bar{P}_2}{\alpha_1 \nu_{L_2} \hat{L}_2 + \alpha_2 \nu_{L_1} \hat{L}_1}$$

showing that P^* is a weighted mean between \hat{P}_1 and \bar{P}_2 .

If, as often will be the case, $\min\{\hat{P}_1, \hat{P}_2\} \geq \max\{\bar{P}_1, \bar{P}_2\}$, it follows that equilibrium parasitoid density in presence of both hosts is higher than with either alone, but we cannot prove that this intuitive feature always holds.

In any case, the above computation show that P^* is always positive, as required. □

It is clear also from (4.10) that, when $\nu_{L_1} = \nu_{L_2} = 0$, coexistence between two hosts is not possible.

4.2 Invasibility under periodic conditions

Conditions for invasibility and host coexistence may change if periodic solutions are considered. Indeed, it has been shown [95] that (4.1) can be destabilized via Hopf bifurcation with the emergence of a stable periodic solution. In particular, Murdoch *et al.* show that this happens when the adult stage is infinitesimally short ($d_A \rightarrow \infty$). Thus, in order to see whether the double invasibility condition holds, it becomes necessary studying the stability of periodic solutions with only one host present.

The complexity of the proposed model hinders such a general achievement with analytical means. Resorting to linearisation leads to rather cumbersome characteristic equations whose analysis, in general, is unattainable (see Appendix A for further details). However, the recent literature on DDEs furnishes efficient numerical routines to tackle the several tasks required in this regard. In particular, in this section we make use of four reliable tools, namely:

- M1 the method in [113] to approximate the rightmost eigenvalue(s) of the linearisation around given equilibria;
- M2 the method in [114] to approximate the dominant multiplier(s) of the linearisation around given periodic orbits;
- M3 (an adaptation of) the method in [115] to compute periodic solutions of non-linear problems;
- M4 the Matlab built-in function `dde23` to integrate in time Cauchy problems for non-linear equations, see [116].

The four methods are often combined in a framework of parameter continuation, i.e., results for a certain parameter value are obtained starting from results previously computed for a different but close parameter value. Aside, note that an updated and complete presentation of M1 and M2 can be found in [117], with user-friendly and freely available Matlab codes.

In order to have a model with a small number of parameters, we let only parameters related to fecundity and adult mortality of the two hosts vary, i.e., ρ_1 , ρ_2 , d_{A_1} and d_{A_2} . All the other parameters are kept fixed at the values listed in Table 4.1.

The first goal is to see when 1-host periodic solutions are possible, say host 1 without loss of generality. To this aim, we fix e.g., $\rho_1 = 5$, and consider the

Parameter	Value
d_{E_i}	0.2
μ_{L_i}	0.1
ν_{L_i}	0.1
s_{iP}	1
α_i	1
T_{E_i}	1
T_{L_i}	1
T_{iP}	1
d_P	1.1

Table 4.1: *Parameter values used in the computation. We analyse the case when two hosts are identical except for the adult host mortality d_A and the fecundity ρ .*

non-trivial equilibrium of (3.3) without host 2 for varying d_{A_1} . Based on the use of M1, we found that the equilibrium is asymptotically stable as far as $d_{A_1} < d_{HB_1}$ with $d_{HB_1} \approx 0.3089$. At this value the associated rightmost complex-conjugate pair of eigenvalues crosses the imaginary axis left-to-right in a Hopf bifurcation, Figure 4.1. The equilibrium loses stability and a periodic solution arises. The latter is computed as follows. M3 is applied for d_{A_1} slightly above d_{HB_1} , with initial guess the equilibrium itself. Indeed, the method converges to a periodic solution, with rather small amplitude. To obtain a more pronounced periodic behaviour, we increase d_{A_1} incrementally, each step starting the solution from the previously computed one. This way we are able to compute a distinct periodic solution for $d_{A_1} = 0.35$ with period $\Omega \approx 18.5938$, Figure 4.1 right and Table 4.2.

Such solution, call it $(E_1^\dagger, L_1^\dagger, A_1^\dagger, P_1^\dagger)$, is confirmed by using M4: integration forward in time leaves it unchanged.

The next step is to see whether host 2 can invade under the above determined periodic conditions. So we keep $\rho_1 = 5$ and $d_{A_1} = 0.35$ fixed and linearise (3.3) around $(E_1^\dagger, L_1^\dagger, A_1^\dagger, 0, 0, 0, P_1^\dagger)$. It is not difficult to realize that the stability of host 2 can be inferred by analysing only the equation for its adults, i.e.,

$$A_2'(t) \approx \rho_2 d_{A_2} A_2(t - T_{E_2} - T_{L_2}) e^{-d_{E_2} T_{E_2}} e^{-\mu_{L_2} T_{L_2} - \alpha_2 \int_{t-T_{L_2}}^t P^\dagger(y) dy} - d_{A_2} A_2(t). \quad (4.11)$$

This is a linear non autonomous DDE with periodic coefficients, periodicity essentially due to the behaviour of the parasitoid. According to Floquet theory

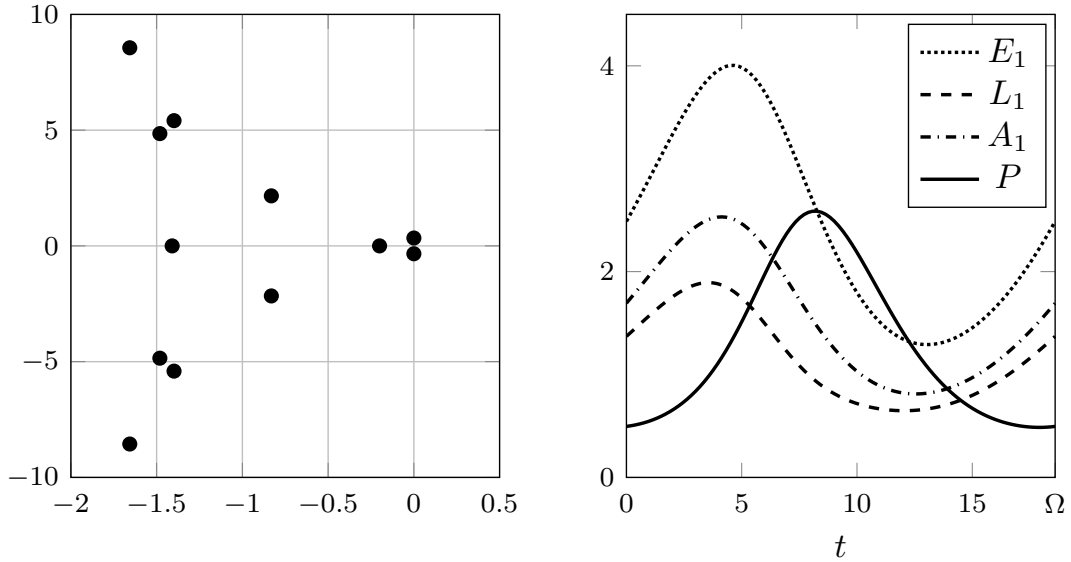


Figure 4.1: Eigenvalues at Hopf bifurcation for $d_{A_1} = d_{HB_1} \approx 0.3089$ and $\rho_1 = 5$ (left) and periodic solutions for $d_{A_1} = 0.35$ and $\rho_1 = 5$ (right) of Host 1 for the parameters values in Table 4.2.

(see, e.g., [118]), the stability of its null solution depends on whether the dominant multiplier lies inside or outside the unit circle in the complex plane. Thus we compute the modulus of this quantity by using M2 for varying ρ_2 and d_{A_2} . In this way we construct a surface $\mathbb{R}^2 \rightarrow \mathbb{R}$, whose curve of level 1 divides the (d_{A_2}, ρ_2) -plane into stable and unstable regions.

Figure 4.2 shows this boundary (thick line), obtained with Matlab contour.

A simple verification let us conclude that host 2 can invade when (d_{A_2}, ρ_2) is above this curve, otherwise coexistence is not possible. For comparison, in the same figure we add also the straight (dashed) line representing the first invasibility condition (4.7). If the equilibrium Eq_1 was stable, invasion of host 2 would be possible for ρ_2 above the line and would not depend on the value of d_{A_2} . We then see that the invasibility of the equilibrium Eq_1 and the presence of the periodic solution $(E_1^\dagger, L_1^\dagger, A_1^\dagger, 0, 0, 0, P_1^\dagger)$ makes easier the invasion of host 2 if d_{A_2} is small and harder if d_{A_2} is large.

The effect of fluctuations on host coexistence can be illustrated more specifically in Figure 4.3.

In it we study both invasibility conditions in the (d_A, ρ_2) -plane having assumed

Parameter	Value
ρ_1	5
d_{E_1}	0.2
μ_{L_1}	0.1
ν_{L_1}	0.1
d_{A_1}	0.35 (0.3089)
s_{1P}	1
α_1	1
T_{E_1}	1
T_{L_1}	1
T_{1P}	1
d_P	1.1

Table 4.2: Parameter values used to compute a distinct periodic solution for $d_{A_1} = 0.35$.

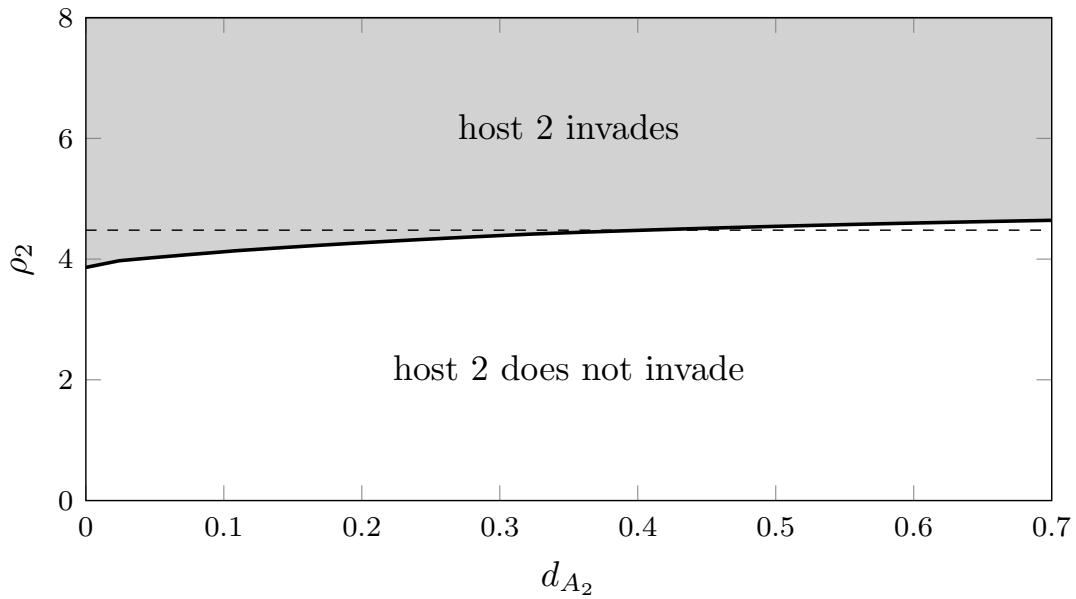


Figure 4.2: The thick line represents the boundary that divides the (d_{A_2}, ρ_2) -plane into stable and unstable regions by having fixed $\rho_1 = 5$, $d_{A_1} = 0.35$. The straight dashed line represent instead the value $\rho_1 e^{-\frac{\nu_L d_P T_L}{\alpha s_P}}$ that comes from (4.7).

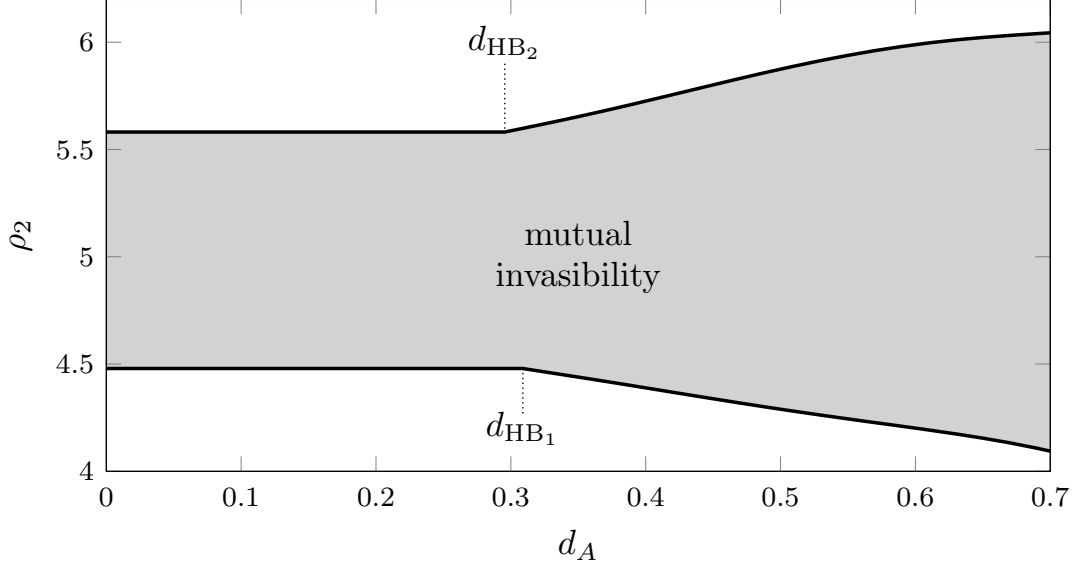


Figure 4.3: For $\rho_1 = 5$, and $d_{A_1} = d_{A_2} = \text{var}$, when $d_A > d_{HB}$, host 2 can invade for $\rho_2 > \bar{\rho}(d_A)$, a decreasing function of d_A , and host 1 can invade for $\rho_1 < \hat{\rho}(d_A)$, an increasing function of d_A .

$d_{A_1} = d_{A_2} =: d_A$ while keeping $\rho_1 = 5$ fixed. The shaded region of mutual invasibility is obtained as follows. The straight lines for lower values of d_A account for (4.7), i.e.,

$$\rho_1 e^{-\frac{\nu_L d_P T_L}{\alpha_S P}} < \rho_2 < \rho_1 e^{\frac{\nu_L d_P T_L}{\alpha_S P}}.$$

The lower straight line ends at the Hopf bifurcation value d_{HB_1} as previously determined. For greater values of d_A we repeat the same arguments above: we compute the periodic solution in absence of host 2 and we study its local stability by searching for the value of ρ_2 giving the dominant multiplier on the unit circle for (4.11). By repeating the procedure over all values of $d_A > d_{HB_1}$, we obtain the lower curve of Figure 4.3. As before, host 2 can invade when introduced in a system where host 1 coexists with the parasitoid, if the parameter values are above the curve so computed; it will be excluded if they are below.

For the increasing part of the upper bound of the shaded region, we repeat the reasoning by exchanging the roles of the two hosts. More precisely, for a fine mesh of points in that region of the (d_A, ρ_2) -plane we compute a periodic solution of (3.3) in absence of host 1.

For each point, we linearise the equation of host 1 around the computed periodic solution and determine the dominant multiplier. The curve is then

obtained by selecting those points with dominant multiplier on the unit circle. Notice that this curve joins the upper straight line at a value $d_A = d_{HB_2} < d_{HB_1}$. Indeed, this is correct since $\rho_2 > 5$ and hence the Hopf bifurcation for host 2 (in absence of host 1) occurs at a lower value of d_A than that of host 1 (in absence of host 2), which was found for $\rho_1 = 5$. Figure 4.3 shows clearly that with larger values of d_A that cause each host alone to fluctuate with the parasitoid, there is an ampler region in (ρ_1, ρ_2) where invasibility conditions are satisfied, presumably leading to coexistence.

More surprisingly, this procedure shows that, when periodic solutions arise, double invasibility (and thus presumably coexistence) is possible even without density-dependence, a case where it has been seen (Corollary 4.1.2) that double invasibility of equilibria is impossible.

In this case, it is easy to show that, if $d_{A_1} = d_{A_2}$, host 2 will invade a periodic solution with only host 1 if $\rho_1 > \rho_2$ and vice versa; double invasibility is then impossible when $d_{A_2} = d_{A_1}$. In order to explore possible coexistence, we fix therefore the values of ρ_1 and d_{A_1} and let ρ_2 and d_{A_2} vary. Precisely, we set $\rho_1 = 5$, $d_{A_1} = 0.3$ and $\nu_{L_1} = \nu_{L_2} = 0$, and repeat the procedure used for Figure 4.2 to construct the solid thick curve in Figure 4.4, below which host 1 excludes host 2 and coexistence is not possible.

The dashed thick curve represents the condition for invasibility of the host 2 periodic solution (or equilibrium). For larger values of d_{A_2} , this second curve is computed by exchanging the roles of the two hosts, i.e., by following the same procedure used to obtain the upper bound of the dashed region of Figure 4.3. For lower values of d_{A_2} , instead, there cannot be periodic solutions of (3.3) without host 1, since d_{A_2} is below the Hopf bifurcation point. To the left of this value, the dashed thick curve corresponds to the straight line obtained from (4.7). Indeed, the dotted thin curve is the bifurcation curve of the equilibrium *Eq2*: the right curve part is the locus of the Hopf bifurcations leading to periodic solutions; the bottom segment is the locus of trans critical bifurcation with the trivial equilibrium. Both segments are obtained by using M1: the former searching for the rightmost eigenvalue in zero, the second for the rightmost conjugate pair on the imaginary axis.

Double invasibility conditions hold when (ρ_2, d_{A_2}) belong to the shaded region enclosed between the two curves. We then see that, thanks to the periodicity induced by instability of the single-species equilibria, coexistence becomes possible even when both host populations are regulated by the parasitoid, in absence of density-dependence.

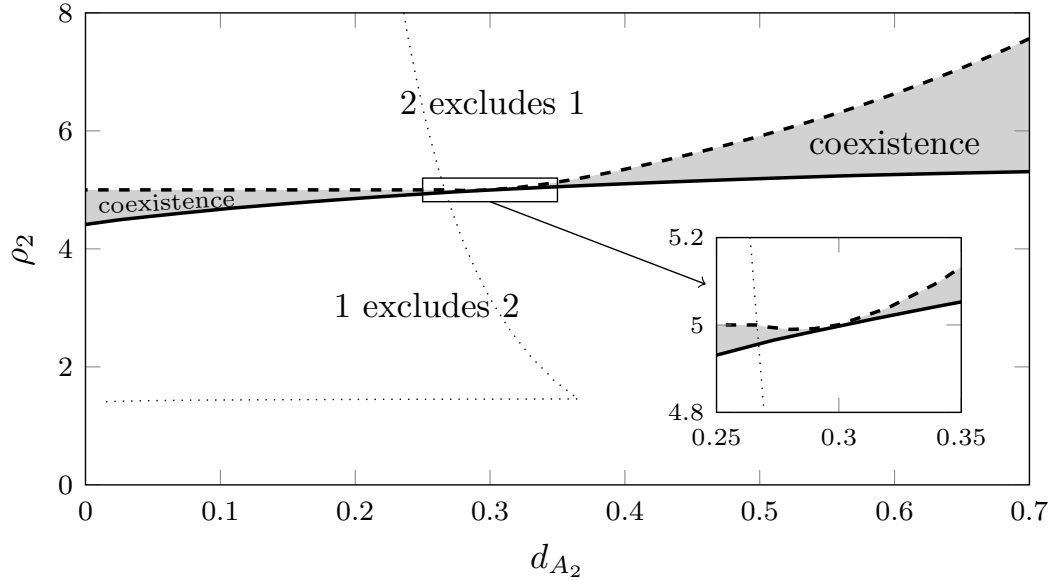


Figure 4.4: *The thick curve represents the condition for invasibility of the host 2 periodic solution with $\rho_1 = 5$, $d_{A_1} = 0.3$ and $\nu_{L_1} = \nu_{L_2} = 0$. The solid thick curve represents instead the boundary that divides the (d_{A_2}, ρ_2) -plane into stable and unstable regions, below which coexistence is not possible. The dotted thin curve is the bifurcation curve of the equilibrium Eq2: the right curve part is the locus of the Hopf bifurcations leading to periodic solutions; the bottom segment is the locus of trans critical bifurcation with the trivial equilibrium.*

In Section 4.3 and 4.4 we give a heuristic explanation of host coexistence without density-dependence, using an approximation of the threshold coefficient for a scalar linear periodic delay-differential equation [119].

4.3 Approximation of dominant eigenvalue of monodromy operator with arbitrary delay

Several authors have studied the linear delay equation with periodic coefficients (see i.e. [119]).

Let the equation be

$$x'(t) = \alpha (\beta f(t)x(t - \tau) - x(t)) \quad (4.12)$$

Chen and Wu [119] have shown that exists a $\beta^* \in (0, \infty)$ such that the zero

solution is stable if $\beta < \beta^*$ and unstable if $\beta > \beta^*$.

Here we show how to approximate β^* by assuming that f is a 1-periodic sinusoidal of small amplitude. In order to make explicit computations, assume

$$f(t) = 1 + \varepsilon \cos(2\pi t)$$

and expand in order of ε .

Hence, the problem is to find β such that

$$x'(t) = \alpha (\beta(1 + \varepsilon \cos(2\pi t))x(t - \tau) - x(t)) \quad (4.13)$$

has 1-periodic solutions.

Let

$$\begin{aligned} x(t) &= x_0(t) + \varepsilon x_1(t) + \varepsilon^2 x_2(t) + \dots \\ \beta &= \beta_0 + \varepsilon \beta_1 + \varepsilon^2 \beta_2 + \dots \end{aligned} \quad (4.14)$$

At zero order, the solution is $\beta_0 = 1$, $x_0(t) \equiv c$, that we set equal to 1.

At first order

$$x_1'(t) = \alpha (\beta_1 + \cos(2\pi t) + x_1(t - \tau) - x_1(t)) \quad (4.15)$$

Assuming that $x_1(t)$ is 1-periodic, we immediately have

$$0 = \int_0^1 x_1'(t) dt = \alpha \left(\beta_1 + \int_0^1 \cos(2\pi t) dt + \int_0^1 x_1(t - \tau) dt - \int_0^1 x_1(t) dt \right) \quad (4.16)$$

As the integral of cosine is zero and $\int_0^1 x_1(t - \tau) dt = \int_0^1 x_1(t) dt$, $\beta_1 = 0$.

Thus, equation (4.15) becomes

$$x_1'(t) = \alpha (\cos(2\pi t) + x_1(t - \tau) - x_1(t)) \quad (4.17)$$

for which we search for a periodic solution.

If we assume that

$$x_1(t) = KC_t + LS_t \quad (4.18)$$

where $C_t = \cos(2\pi t)$ and $S_t = \sin(2\pi t)$. Then (4.18) becomes

$$x_1'(t) = -2\pi KS_t + 2\pi LC_t$$

On the other hand after simple algebraic computations, by considering $A = \cos(2\pi\tau)$ and $B = \sin(2\pi\tau)$, it follows that

$$x_1(t - \tau) = KAC_t + KBS_t + LAS_t - LBC_t.$$

By equating the terms of (4.17), we obtain

$$C_t(2\pi L - \alpha - \alpha AK + \alpha BL + \alpha K) = S_t(2\pi K + \alpha BK + \alpha AL - \alpha L) \quad (4.19)$$

from which we get the system in K and L ,

$$\begin{cases} K(2\pi + \alpha B) - L\alpha(1 - A) = 0 \\ K\alpha(1 - A) + L(2\pi + \alpha B) = \alpha \end{cases} \quad (4.20)$$

From which

$$\begin{cases} K = \frac{\alpha^2(1-A)}{(2\pi+\alpha B)^2+\alpha^2(1-A)^2} \\ L = \frac{\alpha(2\pi+\alpha B)}{(2\pi+\alpha B)^2+\alpha^2(1-A)^2} \end{cases} \quad (4.21)$$

Using (4.18) with (4.21) the required periodic solution of (4.17) is easily obtained. By considering the second order, as $\beta_1 = 0$, the equation is given by

$$x_2'(t) = \alpha(\beta_2 + C_t x_1(t - \tau) + x_2(t - \tau) - x_2(t)). \quad (4.22)$$

By assuming that a periodic solution is present, and using the fact that $\int_0^1 x_2(t - \tau) dt = \int_0^1 x_2(t) dt$, it is possible to obtain

$$0 = \int_0^1 x_2'(t) dt = \alpha \left(\beta_2 + \int_0^1 C_t x_1(t - \tau) dt \right) \quad (4.23)$$

i.e.

$$\begin{aligned} \beta_2 = - \int_0^1 C_t x_1(t - \tau) dt = & -K \int_0^1 \cos(2\pi t) \cos(2\pi(t - \tau)) dt + \\ & -L \int_0^1 \cos(2\pi t) \sin(2\pi(t - \tau)) dt \end{aligned} \quad (4.24)$$

This can be written in a simpler way by considering that

$$\begin{aligned} \int_0^1 \cos(2\pi t) \cos(2\pi(t - \tau)) dt &= \frac{1}{2} \cos(2\pi\tau) = \frac{A}{2} \\ \int_0^1 \cos(2\pi t) \sin(2\pi(t - \tau)) dt &= -\frac{1}{2} \sin(2\pi\tau) = -\frac{B}{2} \end{aligned}$$

thus (4.24) becomes

$$\begin{aligned} \beta_2 &= \frac{-\alpha^2(1-A)A + \alpha(2\pi + \alpha B)B}{2((2\pi + \alpha B)^2 + \alpha^2(1-A)^2)} = \\ &= \frac{\alpha^2(1-A) + 2\pi\alpha B}{2(2\alpha^2(1-A) + 4\pi(\pi + \alpha B))} \end{aligned} \quad (4.25)$$

using that $A^2 + B^2 = 1$.

This shows that β_2 is always positive, consistently with the previous result in case $\tau = 1/2$.

Let us consider $\beta_2 = G(\alpha)$. It is immediate to see that $G(0) = 0$ and $G(\infty) = \frac{1}{4}$. Moreover

$$G'(\alpha) = \frac{(1-A)\pi^2\alpha + \pi^3B}{(\alpha^2(1-A) + 2\pi(\pi + \alpha B))^2}. \quad (4.26)$$

$G' > 0$ in $(0, \bar{\alpha})$ and $G' < 0$ on $(\bar{\alpha}, \infty)$ where $\bar{\alpha}$ is the root of a quadratic equation, that does not seem to have a simple expression.

4.4 Application to host-parasitoid model

In the case without density-dependence, assume that host 1 coexists with the parasitoid along an (attractive) T -periodic solution $(L_1^\dagger(t), A_1^\dagger(t), P_1^\dagger(t))$. The equation for adult hosts is

$$A_1^\dagger(t) = d_{A_1} \left(\rho_1 e^{-d_E T_E - d_L T_L - \alpha_1 \int_{t-T_L}^t P_1^\dagger(y) dy} A_1(t - T_E - T_L) - A_1(t) \right). \quad (4.27)$$

For the sake of simplicity, by following Section 4.2, we assume that different hosts share the values of d_E, d_L, T_E, T_L .

By considering $P_1^\dagger(t)$ as a given function, the monodromy operator corresponding to equation (4.27) has dominant eigenvalue equal to 1.

By changing the time ($\bar{t} = t/T$), P_1^\dagger becomes 1-periodic, and (4.27) is equal to

$$A_1^\dagger(t) = d_{A_1} T \left(\rho_1 e^{-d_E T_E - d_L T_L - \alpha_1 T \int_{t-T_L/T}^t P_1^\dagger(y) dy} A_1(t - \tau) - A_1(t) \right) \quad (4.28)$$

where $\tau = (T_E + T_L)/T$ and the functions have been rescaled.

Set

$$\begin{aligned} \alpha_1 &= d_{A_1} T \\ \beta_1 &= \rho_1 / K \\ f_1(t) &= K e^{-d_E T_E - d_L T_L - \alpha_1 T \int_{t-T_L/T}^t P_1^\dagger(y) dy} \end{aligned} \quad (4.29)$$

where

$$K = \frac{e^{d_E T_E + d_L T_L}}{\int_0^1 e^{-\alpha_1 T \int_{t-T_L/T}^t P_1^\dagger(y) dy} dt}.$$

so to have $\int_0^1 f_1(t) dt = 1$.

We assume that $f_1(t) \approx 1 + \varepsilon \cos(2\pi t)$, thus, by considering Section 4.3

$$\rho_1 \approx (1 + \varepsilon^2 G(\alpha_1)) K.$$

The invasion by a second host sharing all parameter values as in Section 4.2 will succeed if and only if the linearised equation

$$A_2^\dagger(t) = d_{A_2}T \left(\rho_2 e^{-d_E T_E - d_L T_L - \alpha T \int_{t-T_L/T}^t P_1^\dagger(y) dy} A_2(t - \tau) - A_2(t) \right) \quad (4.30)$$

has dominant monodromy eigenvalue greater than 1. The equation can be written as

$$A_2^\dagger(t) = \alpha_2 (\beta_2 f_1(t) A_2(t - \tau) - A_2(t)) \quad (4.31)$$

with $\alpha_2 = d_{A_2}T$ and $\beta_2 = \rho_2/K$.

The eigenvalue is larger than 1 if and only if

$$\rho_2 > (1 + \varepsilon^2 G(\alpha_2))K.$$

If α_1 is in the region where G is increasing, this will be possible for $\rho_2 < \rho_1$ if $\alpha_2 < \alpha_1$. Vice versa, in the region where G is decreasing.

This mechanism gives presumably rise to mutual invasibility. However, when the roles of host 1 and host 2 are switched, also the period will in principle change as well as f_i , so G does not remain the same.

It is easier showing that, if we assume that for $\alpha_2 < \alpha_1$, solutions are attracted to a stable equilibrium (this is certainly true if α_2 is small enough).

Then as all other parameters are the same, and the value of d_{A_i} does not matter, the invasion condition is easy to read as host 1 invades host 2 if and only if $\rho_2 > \rho_1$.

Thus mutual invasibility occurs if we find a pair (d_{A_1}, ρ_1) and (d_{A_2}, ρ_2) such that the first gives rise to periodic solutions and the second to stable equilibrium with

$$d_{A_2} < d_{A_1} \quad (4.32)$$

$$\frac{1 + \varepsilon^2 G(d_{A_2}T)}{1 + \varepsilon^2 G(d_{A_1}T)} < \frac{\rho_2}{\rho_1} < 1$$

where G and T refer to 1-parameters. Clearly this is only possible if G is increasing between $d_{A_2}T$ and $d_{A_1}T$. This result can be compared with Figure 4.4 and it can be noticed that it corresponds to what is seen in the left wedge of the Figure. Of course, this argument is purely heuristic as it is based on the unlikely assumption that $f_1(t)$ is exactly a sinusoidal function. However, we believe it gives some intuition on why coexistence may occur even without density-dependence.

Chapter 5

Discussion

This chapter summarizes and discusses the main results obtained by analysing the interactions between two different hosts and a common parasitoid. We compare our results with what was found in other studies. We discuss also the limitations of this model and introduce some possible improvements such as different stage duration, multiple parasitoids that can attack different host life stages or evolutionary dynamics.

In this part of the dissertation we have provided the first, as far as we know, analysis of a continuous-time model for a system consisting of a parasitoid species attacking two different host species.

The model is built on the framework proposed by [95] assuming that developmental time in all stages is fixed, while other authors [97] have allowed for distributed lengths of developmental stages, and have shown that such an assumption is crucial for the possibility of equilibrium coexistence of several parasitoid species on a single host species.

The other assumption used is that the two host species do not compete directly but are regulated by independent resources, acting through a density-dependent mortality in the larval stage. Under this assumption, it is possible to find an explicit condition for the existence of an equilibrium where both host species coexist with the parasitoid. This condition is equivalent, as it often occurs in population model, to the double invasibility condition, i.e. that both equilibria with a single host species are unstable relatively to the invasion of the other host species. Although the two host species do not compete directly, they are subject to apparent competition (see i.e. [120, 121]) through the shared parasitoid.

In the special case without density-dependence in the hosts, the condition for

coexistence is never satisfied, so that necessarily one host species will exclude the other. When host regulation occurs only because of the parasitoid, the species more strongly regulated by the parasitoid will get extinct, because the parasitoid will be able to reach even higher densities at which the host species with a weaker regulation gets under control.

However, it is well known that host-parasitoid system can exhibit cycles, as usual in systems of predator-prey type, but more easily because of the delays built in the stage structure. The previous analysis holds if each system with a single-host tends to an equilibrium, but becomes irrelevant when a single host-parasitoid system converges to a periodic solution. In this case, in order to assess the double invasibility condition [112], it is necessary to analyse the stability of the periodic solution in the complete system.

While finding explicit conditions for the stability of periodic solutions in systems of delay-differential equations is probably hopeless (it is generally impossible already in systems of two ordinary differential equations), recent advancements in the methods for the approximation of multipliers of the monodromy operator of linear delay-differential equations with periodic coefficients provide a fundamental tool for being able to numerically study the stability of a periodic solution. These methods have been coupled to a method to approximate periodic solutions of such systems, and to a continuation algorithm that allows for efficiently tracking the periodic solutions as a parameter is varied, and applied to the 2 host-1 parasitoid system in some cases that appear biologically significant.

A discussion of the results that have been obtained is that conditions for invasibility and host coexistence can be favoured by considering periodic solutions, where periodicity is due to the behaviour of the parasitoid and is not forced from the outside. In fact, periodicity favours host coexistence, up to the extreme case without density-dependence: even then, if at least one of the single host-parasitoid system converges to a periodic solution, coexistence of the two hosts is possible, albeit under rather stringent conditions on the parameters. Li and Smith [122] found that coexistence of multiple host species and multiple parasitoid species needs existence of a periodic solution, while Murdoch *et al.* [95] discussed instead this possibility for an infinitesimally short invulnerable adult stage and constant fecundity.

It has been known for several decades, since the seminal work by De Mottoni and Schiaffino [123] and by Cushing [124] that coexistence of competitors is easier if the environment fluctuates periodically (see also [125]). This system is different, in that periodicity is not forced from outside but is generated intrinsically by host-parasitoid interactions. While the result may not be surprising, it is worthwhile

noticing that the effect is the same; it can be said that fluctuations in one host-parasitoid system improve the chances of a second host species to coexist.

Host-parasitoid systems can be considered just as predator-prey system in which the predator has a specialized life cycle. It can be noted that in predator-prey systems without density-dependence (i.e. the classical Volterra system with neutral cycles) a simple computation shows that it is impossible to satisfy the double invasibility. In this sense, host-parasitoid systems based on delay-differential equations are more stable than predator-prey systems and may be more suitable for examining general ecological principles.

In the presented model, it is assumed that there is no dependence of attack rate on parasitoid density but it is well known [126–128] that if density-dependence is included, results on coexistence and the effect on host abundance can be altered. Moreover, consumer species adaptively adjust their consumption behaviour when they are in presence of more host species [129–133]. In [134], Abrams and Kawecki studied parasitoid trade-off in its ability to exploit two different hosts. In particular, they modelled the dynamics of two independent host populations that share a common parasitoid and examined different types of adaptation in parasitoid attack rate. They found that adaptive behaviour and evolution frequently destabilize population dynamics and increase the difference between host densities. Thus, it would be a great improvement to see what happens if we apply adaptive dynamics to our model. By considering [110], we can see that the parasitoids taken into account have a preference for *D. melanogaster* but, using what was found in [134], we could maybe say something more on their preference for different host species from a mathematical point of view.

Another point that can be improved is to consider different parasitoid species that can attack different host stages. In fact, according to [110], different species of parasitoids can attack different species of hosts at different life stages. Stacconi *et al.* found that *D. suzukii* can be attacked and parasitized by several indigenous parasitoids of *D. melanogaster*, in particular a larval koinobiont and solitary endoparasitoid, *L. heterotoma*, and a generalist pupal ectoparasitoid, *P. vindemiae*. These parasitoids can be somewhat included in this model by considering that we merged these two life stages into the larval stage present in (3.3) but we can also extend the presented model by considering [97], where an one host-two parasitoid model is studied. In this way, we could not only see coexistence conditions of different host species when a parasitoid is present but also study what happens when a new parasitoid is introduced into this system.

Despite these limitations, our analysis provides evidence of different conditions of host coexistence and model like the one presented in this dissertation may be

relevant for modelling control strategies for *D. suzukii* based on native parasitoids of indigenous fruit flies.

Appendix A

Characteristic equation for dynamics of host-parasitoid interactions and coexistence of different hosts

Let us find the characteristic equation for the dynamics of host-parasitoid interactions to find stability conditions. To investigate local stability, imagine that the system has remained at steady state for all $t \leq 0$ and is perturbed from this steady state at some time $t > 0$. We consider small perturbations from equilibrium, linearise both the balance equations and the vital-rate definitions about the steady state, and derive a 'characteristic equation', whose roots must have negative real parts for local stability.

We define

$$\begin{aligned}e(t) &= E(t) - E^* \\l(t) &= L(t) - L^* \\a(t) &= A(t) - A^* \\p(t) &= P(t) - P^*\end{aligned}\tag{A.1}$$

Denote with

$$\gamma_L = \mu_L + \alpha P^* + \nu_L L^*$$

The first thing that we want to do is a simplification of both M_E and M_L .

Since

$$\begin{aligned} M_E &= \rho d_A A(t - T_E) e^{-d_E T_E} \\ M_L &= M_E(t - T_L) e^{-\int_{t-T_L}^t (\alpha P(y) + \nu_L L(y) + \mu_L) dy} \end{aligned} \quad (\text{A.2})$$

and, by considering the perturbations (A.1), we can easily obtain

$$\begin{aligned} M_E(t) &= \rho d_A (A^* + a(t - T_E)) e^{-d_E T_E} \\ M_L(t) &= \rho d_A (A^* + a(t - T_E - T_L)) e^{-d_E T_E} e^{-\gamma_L T_L - \int_{t-T_L}^t \alpha p(y) + \nu_L l(y) dy} \end{aligned} \quad (\text{A.3})$$

Consider now the Taylor expansion. We can find the final form of the linearisation of M_L

$$\begin{aligned} M_L &= \rho d_A A^* e^{-d_E T_E - \gamma_L T_L} + \rho d_A a(t - T_E - T_L) e^{-d_E T_E - \gamma_L T_L} + \\ &\quad - \rho d_A A^* e^{-d_E T_E - \gamma_L T_L} \int_{t-T_L}^t \alpha p(y) + \nu_L l(y) dy \end{aligned} \quad (\text{A.4})$$

Finally, after some algebra, we can obtain

$$\begin{aligned} \dot{e}(t) &= \rho d_A a(t) - \rho d_A a(t - T_E) e^{-d_E T_E} - d_E e(t) \\ \dot{l}(t) &= \rho d_A a(t - T_E) e^{-d_E T_E} - \rho d_A a(t - T_E - T_L) e^{-d_E T_E - \gamma_L T_L} + \rho d_A A^* e^{-d_E T_E - \gamma_L T_L} \\ &\quad \int_{t-T_L}^t \alpha p(y) + \nu_L l(y) dy - \alpha P^* l(t) - \alpha p(t) L^* - (d_L + 2\nu_L L^*) l(t) \\ \dot{a}(t) &= \rho d_A a(t - T_E - T_L) e^{-d_E T_E - \gamma_L T_L} + \\ &\quad - \rho d_A A^* e^{-d_E T_E - \gamma_L T_L} \int_{t-T_L}^t \alpha p(y) + \nu_L l(y) dy - d_A a(t) \\ \dot{p}(t) &= \alpha P^* l(t - T_P) s_P + \alpha L^* p(t - T_P) s_P - d_P p(t) \end{aligned} \quad (\text{A.5})$$

We are looking for a solution of the form $x(t) = x e^{\lambda t}$ where the x on the rhs is a constant.

Let define, for simplicity of notation

$$\begin{aligned}
\Pi_E^1 &= e^{-d_E T_E} \\
\Pi_E^2 &= e^{-(\lambda+d_E)T_E} \\
\Pi_E^1 &= e^{-\gamma_L T_L} \\
\Pi_E^2 &= e^{-(\lambda+\gamma_L)T_L}
\end{aligned} \tag{A.6}$$

From (A.5) using (A.6), we obtain

$$\begin{aligned}
\lambda e &= \rho d_A a (1 - \Pi_E^2) - d_E e \\
\lambda l &= \rho d_A \left[a (1 - \Pi_L^2) \Pi_E^2 + (\alpha p + \nu l) A^* \Pi_E^1 \frac{\Pi_L^1 - \Pi_L^2}{\lambda} \right] + \\
&\quad - \alpha (P^* l + p L^*) - (d_L + 2\nu L^*) l \\
\lambda a &= \rho d_A \left[a \Pi_E^2 \Pi_L^2 - (\alpha p + \nu l) A^* \Pi_E^1 \frac{\Pi_L^1 - \Pi_L^2}{\lambda} \right] - d_A a \\
\lambda p &= \alpha s_P e^{-\lambda T_P} (P^* l + p L^*) - d_P p
\end{aligned} \tag{A.7}$$

From the last equation we can express p in terms of l writing $p = P(\lambda)l$ where

$$P(\lambda) = \frac{\alpha s_P P^* e^{-\lambda T_P}}{\lambda + d_P - \alpha s_P e^{-\lambda T_P} L^*} \tag{A.8}$$

Using this form into the second equation we have that also l can be expressed in terms of a as $l = L(\lambda)a$, where

$$L(\lambda) = \frac{\rho d_A (1 - \Pi_L^2) \Pi_E^2}{\lambda + d_L + 2\nu L^* + \alpha (P^* + L^* P(\lambda)) - \rho d_A A^* \Pi_E^1 (\alpha P(\lambda) + \nu) \frac{\Pi_L^1 - \Pi_L^2}{\lambda}} \tag{A.9}$$

If we substitute them into the third equation we obtain the characteristic equation in the form $G(\lambda) = 1$

$$G(\lambda) = \frac{\rho d_A}{\lambda + d_A} \left[\Pi_E^2 \Pi_L^2 - (\alpha P(\lambda) L(\lambda) + \nu L(\lambda)) A^* \Pi_E^1 \frac{\Pi_L^1 - \Pi_L^2}{\lambda} \right] \tag{A.10}$$

A.1 Density-dependence two hosts present

In this case the only things that will change are the equations for p , l and a but they will do it in an easy way.

$$\begin{aligned}
\lambda e_i &= \rho_i d_{A_i} a_i (1 - \Pi_{E_i}^2) - d_{E_i} e_i \\
\lambda l_i &= \rho_i d_{A_i} \left[a_i (1 - \Pi_{L_i}^2) \Pi_{E_i}^2 + (\alpha_i p + \nu_i l_i) A_i^* \Pi_{E_i}^1 \frac{\Pi_{L_i}^1 - \Pi_{L_i}^2}{\lambda} \right] \\
&\quad - \alpha_i (P^* l_i + p L_i^*) - (d_{L_i} + 2\nu_i L_i^*) l_i \\
\lambda a_i &= \rho_i d_{A_i} \left[a_i \Pi_{E_i}^2 \Pi_{L_i}^2 - (\alpha_i p + \nu_i l_i) A_i^* \Pi_{E_i}^1 \frac{\Pi_{L_i}^1 - \Pi_{L_i}^2}{\lambda} \right] - d_{A_i} a_i \\
\lambda p &= \sum_{i=1}^2 \alpha_i s_{iP} e^{-\lambda T_P} (P^* l_i + p L_i^*) - d_P p
\end{aligned} \tag{A.11}$$

We can express a_i in terms of l_i and p writing $a_i = A_i(\lambda)(\alpha_i p + \nu_i l_i)$ where

$$A_i(\lambda) = \frac{-X_i \frac{\Pi_{L_i}^1 - \Pi_{L_i}^2}{\lambda}}{\lambda + d_{A_i} - \rho_i d_{A_i} \Pi_{E_i}^2 \Pi_{L_i}^2} \tag{A.12}$$

Using this form into the previous equations we have that l can be expressed in terms of p as $l_i = L_i(\lambda)p$, where

$$L_i(\lambda) = \frac{\alpha_i \rho_i d_{A_i} \Pi_{E_i}^2 (1 - \Pi_{L_i}^2) A_i(\lambda) + X_i \alpha_i \frac{\Pi_{L_i}^1 - \Pi_{L_i}^2}{\lambda} - \alpha_i L_i^*}{\lambda + \alpha_i P^* + d_{L_i} + 2\nu_i L_i^* - \rho_i d_{A_i} \Pi_{E_i}^2 (1 - \Pi_{L_i}^2) A_i(\lambda) \nu - X_i \nu \frac{\Pi_{L_i}^1 - \Pi_{L_i}^2}{\lambda}} \tag{A.13}$$

If we substitute them into the third equation we obtain the characteristic equation in the form $G(\lambda) = 1$

$$G(\lambda) = \frac{\sum_{i=1}^2 \alpha_i s_{iP} e^{-\lambda T_P} (P^* L_i(\lambda) + L_i^*)}{\lambda + d_P} \tag{A.14}$$

Part III

Simulations of biological control through parasitoids of *Drosophila suzukii*

Chapter 1

Introduction

This chapter gives a brief biological introduction on *D. suzukii* and the parasitoids that can attack it. Then are presented the experiments conducted by Tochen *et al.* and Stacconi *et al.* that can be considered useful to apply the model presented in Part II to raw data. We have to keep in mind that, since experiments were conducted late in the season, obtained results are not reliable.

1.1 Biological background

Drosophila suzukii, the spotted-wing drosophila (described by [83]) is a recently introduced pest fruit fly coming from South-east Asia. It was detected the first time in European and North American fruit production regions [84–89] during 2008 and has been recently discovered also in South America [135].

The main characteristic that differentiate this species from most other species of *Drosophilidae* is its ability to lay eggs in healthy, ripening fruits [136] that may become unmarketable causing significant economic losses [90–94].

To reduce *D. suzukii* populations several approaches have been attempted: chemical control, trap control or natural enemies control. The main tool that is currently used by growers are insecticides, even if they can be inefficient [137,138]. Also mass trapping techniques result useful to reduce populations of *D. suzukii* [89] but the method that is taken into account in this paper is the use of natural enemies as possible biocontrol agents against *D. suzukii* [139–141].

These natural enemies are generally parasitoids that induce a high rate of mortality in their host populations due to high natural average rate of parasitism [142].

By following the preliminary surveys of [139] and [143], it emerges that *D. suzukii* can be attacked mostly by a larval koinobiont and solitary endoparasitoid, *Leptopilina heterotoma* (associated both with *D. suzukii* and *D. melanogaster*), and by a generalist pupal ectoparasitoid, *Pachycrepoideus vindemiae*.

The fact that these parasitoids can be associated with both *D. suzukii* and *D. melanogaster* lead us to develop a model that describes this situation. It has to be taken into account that, from a general point of view, a lot of different host and parasitoid species are present and that there can be a preference and an adaptation between the species as in [134] but this is the simplest setting from which to start.

In host-parasitoid models, many host species can be attacked by different parasitoids. Murdoch *et al.* [95] considered a model of populations with discrete generations with a single host and a single parasitoid. They assumed that there are two developmental stages, immature and mature, in both the host and the parasitoid, and then investigated the effects that overlapping generations and invulnerable stages produce on the stability of the system to find that an invulnerable age class, a shorted adult parasitoid life span and lower host fecundity tend to stabilize a model with overlapping generations. Briggs *et al.* [82, 97] generalized their model by adding another parasitoid species and by developing a general model in which different parasitoid species attack the same host at different developmental stages. They showed that coexistence of two parasitoids is not guaranteed by their preference for different host developmental stages and even that, with a fixed host stage duration, coexistence between parasitoids is not possible.

A background on the experiments conducted by Tochen *et al.* [144] and Stacconi *et al.* [110] is presented in Section 1.2. In Chapter 2 we describe the models studied (two hosts-two parasitoid model and one host-one parasitoid model) and present the data extrapolated from the studies of Tochen *et al.* and Stacconi *et al.*. In Chapter 3 we show preliminary results of the application of the one host-one parasitoid model to raw data. We test the impact of different choices for the attack rate and increased death rates to reduce parasitoid effective fecundity respect to laboratory conditions. Moreover we show what happens if parasitoids are introduced into the system before the hosts have reached the equilibrium. It turns out that even if the attack rate is small, parasitoids have a significant impact on host population even if, under this condition, it takes a lot of time. Finally, in Chapter 4 we discuss the obtained results.

1.2 Experiments

To apply the model presented in Part II we need data both for the hosts and the parasitoids. For this reason we take into account the studies of Tochen *et al.* [144] and Stacconi *et al.* [110] that performed experiments both under laboratory conditions and field conditions.

Tochen *et al.* studied in fact *D. suzukii* under different temperature conditions to analyse its developmental period, survival and fecundity. [144] shows that temperature has a significant influence on the fruit fly since, as it increases, developmental periods decrease. However they noticed also that at 30°C, the highest temperature tested, development periods of *D. suzukii* increased. This demonstrates that above this temperature the developmental extremes for the species were approached. In their studies, fruit was exposed to *D. suzukii* females for 30 minutes at a temperature around 22°C. Fruit was then removed and examined to see how many eggs there were laid in. Results show that the highest reproductive rate for *D. suzukii* was recorded at 22°C. This made us able to compare extrapolated data from this paper with results obtained by Stacconi *et al.*

Stacconi *et al.* performed a series of experiments both under laboratory and field conditions to evaluate the presence and the efficacy of natural enemies that can be associated with *D. suzukii*. Their studies involved one larval parasitoid (*Leptopilina heterotoma*) and two pupal parasitoids (*Pachycrepoideus vindemiae* and *Trichopria drosophilae*). To analyse parasitoids behaviour and their effect on *D. suzukii*, they used three indices: the degree of infestation (DI, proportion of host larvae or pupae successfully parasitized), the success rate of parasitism (SP, probability that a host larva or pupa yields an adult parasitoid) and the total encapsulation rate (TER). Their results show that *P. vindemiae* and *L. heterotoma* are able to attack and develop on *D. suzukii* even if they are indigenous parasitoids of *D. melanogaster* where both the degree of infestation and the success rate of parasitism were higher.

In addition, they studied parasitoids preference for medium and *Drosophila*'s life stages and their fecundity and life duration, parameters that we were not able to find in literature. They found that *P. vindemiae* can produce and lay eggs throughout life until a sharp decline before death, while *Trichopria*'s fecundity is higher in the first part of its life and then decrease rapidly and *L. heterotoma* is an unknown factor since their experiments were conducted late in the season and thus host larvae could have been too small or too big for this parasitoid.

By considering life duration of these parasitoids, it results that *P. vindemiae*

has a longer life if it is in presence of parasitization, while for *Trichopria* it is longer without it. Last, the case of *L. heterotoma* is different because it seems that its life duration is independent from parasitization.

The second kind of experiments that Stacconi *et al.* performed is field and semi field experiments.

Results from field experiments assure that a population of *Trichopriidae* has established after its introduction while it has never been collected where it was not previously introduced. In semi field experiments, they noticed a decrement in host population when parasitoids were introduced. However, since these experiments, were performed late in the season, these results are not reliable. For this reason, we analyse only the data extrapolated from [110,144].

Chapter 2

Methods

The aim of this chapter is to introduce an extended version of the model presented in Chapter 3 in which we add a new class in host life stages and a different parasitoid. In this way, we obtain a model that can describe more realistically what happens in the fields of the province of Trento, Italy. Thus we start with a two hosts-two parasitoids model and then we concentrate on a one host-one parasitoid model to use it as a starting point to analyse data extrapolated from [110, 144].

2.1 Two hosts-two parasitoids model

Since Stacconi *et al.* performed experiments on two different *Drosophilidae* species and on different indigenous parasitoid species, we extend the model presented in Chapter 3 including two different parasitoids and a new host stage, the pupae. The choice to consider only two parasitoid species is due to the fact that in [110] was found that *Trichopria drosophilae* females produced only males in Italy and thus no further replications have been performed.

Under this assumptions, host species life cycle is now divided into four developmental stages: eggs, E , larvae, L , pupae, P and adults, A . We assume that host larvae are attacked by adult parasitoid of species 1, Q , while pupae by adult parasitoid of species 2, R . All the assumptions of this model are the same as in Chapter 3. Thus we assume that hosts can not survive to parasitoids attack and death and birth rates (except for the larval stage) and stage durations are constant and density-independent.

Thus, the two hosts-two parasitoid model is given by

$$\begin{aligned}
E'_i(t) &= \rho_i d_{A_i} A_i(t) - M_{E_i}(t) - d_{E_i} E_i(t) \\
L'_i(t) &= M_{E_i}(t) - M_{L_i}(t) - \alpha_{Q_i} Q(t) L_i(t) - d_{L_i}(L_i(t)) L_i(t) \\
P'_i(t) &= M_{L_i}(t) - M_{P_i}(t) - \alpha_{R_i} R(t) P_i(t) - d_{P_i} P_i(t) \\
A'_i(t) &= M_{P_i}(t) - d_{A_i} A_i(t) \\
Q'(t) &= \sum_{i=1}^2 \alpha_{Q_i} Q(t - T_{iQ}) L_i(t - T_{iQ}) s_{iQ} - d_Q Q(t) \\
R'(t) &= \sum_{i=1}^2 \alpha_{R_i} R(t - T_{iR}) P_i(t - T_{iR}) s_{iR} - d_R R(t)
\end{aligned} \tag{2.1}$$

where

$$\begin{aligned}
\beta_i &= \rho_i d_{A_i} \\
d_{L_i}(L_i(t)) &= \mu_{L_i} + \nu_{L_i} L_i(t) \\
M_{E_i}(t) &= \rho_i d_{A_i} A_i(t - T_{E_i}) e^{-d_{E_i} T_{E_i}} \\
M_{L_i}(t) &= M_{E_i}(t - T_{L_i}) e^{-\int_{t-T_{L_i}}^t (\alpha_{Q_i} Q(y) + d_{L_i}(L_i(t))) dy} \\
M_{P_i}(t) &= M_{L_i}(t - T_{P_i}) e^{-\int_{t-T_{P_i}}^t (\alpha_{R_i} R(y) + d_{P_i}) dy}
\end{aligned} \tag{2.2}$$

All model parameters are described in Table 2.1.

2.1.1 Equilibria Coexistence

Coexistence conditions for (2.1) are determined as in Chapter 3 by a linearisation of the system around the equilibrium.

The equilibrium when only host 1 (H_1) and Q are present is

$$\begin{aligned}
\hat{E}_{1Q} &= \frac{\rho_1 d_{A_1} \hat{A}_{1Q} (1 - e^{-d_{E_1} T_{E_1}})}{d_{E_1}} \\
\hat{L}_{1Q} &= \frac{d_Q}{\alpha_{Q_1} s_{1Q}} \\
\hat{P}_{1Q} &= \frac{\rho_1 d_{A_1} e^{-(\alpha_{Q_1} \hat{Q}_1 T_{L_1} + d_{L_1}(\hat{L}_{1Q}) T_{L_1} + d_{E_1} T_{E_1})} (1 - e^{-d_{P_1} T_{P_1}}) \hat{A}_{1Q}}{d_{P_1}} \\
\hat{A}_{1Q} &= \frac{(\alpha_{Q_1} \hat{Q}_1 + d_{L_1}(\hat{L}_{1Q})) \hat{L}_{1Q}}{\rho_1 d_{A_1} e^{-d_{E_1} T_{E_1}} (1 - e^{-(\alpha_{Q_1} \hat{Q}_1 + d_{L_1}(\hat{L}_{1Q})) T_{L_1}})} \\
\hat{Q}_1 &= \frac{\ln(\rho_1) - d_{E_1} T_{E_1} - d_{P_1} T_{P_1} - d_{L_1}(\hat{L}_{1Q}) T_{L_1}}{\alpha_{Q_1} T_{L_1}}
\end{aligned} \tag{2.3}$$

Parameter	Description
β	Host birth rate
d_E	Host egg death rate
$d_L(L)$	Host i larva death rate
d_P	Host i pupa death rate
d_A	Host adult death rate
d_Q	Adult parasitoid death rate of parasitoid Q
d_R	Adult parasitoid death rate of parasitoid R
α_Q	Attack rate of adult parasitoids on host larvae
α_R	Attack rate of adult parasitoids on host pupae
s_Q	Survival rate of juvenile parasitoids Q
s_R	Survival rate of juvenile parasitoids R
T_E	Duration of egg host stage
T_L	Duration of larva host stage
T_P	Duration of pupa host stage
T_Q	Duration of adult parasitoid Q stage
T_R	Duration of adult parasitoid R stage

Table 2.1: Model parameters present in the two hosts-two parasitoids model. All parameters are kept constant and density-independent except of the larval death rate that depends on larvae density.

Instead the equilibrium when only R is present with host 1 is

$$\begin{aligned}
\hat{E}_{1R} &= \frac{\rho_1 d_{A_1} \hat{A}_{1R} (1 - e^{-d_{E_1} T_{E_1}})}{d_{E_1}} \\
0 &= \rho_1 d_{A_1} \hat{A}_{1R} e^{-d_{E_1} T_{E_1}} (1 - e^{-d_{L_1} (\hat{L}_{1R})}) - d_{L_1} (\hat{L}_{1R}) \hat{L}_{1R} \\
\hat{P}_{1R} &= \frac{d_{R_1}}{\alpha_{R_1} s_{1R}} \\
\hat{A}_{1R} &= \frac{(\alpha_{R_1} \hat{R}_1 + d_{P_1}) \hat{P}_{1R}}{\rho_1 d_{A_1} e^{-(d_{E_1} T_{E_1} + d_{L_1} (\hat{L}_{1R}) T_{L_1})} (1 - e^{-(\alpha_{R_1} \hat{R}_1 + d_{P_1}) T_{P_1}})} \\
\hat{R}_1 &= \frac{\ln(\rho_1) - d_{E_1} T_{E_1} - d_{L_1} (\hat{L}_{1R}) T_{L_1} - d_{P_1} T_{P_1}}{\alpha_{R_1} T_{P_1}}
\end{aligned} \tag{2.4}$$

By considering [97], we can see that, when only one host is present, Q can invade when

$$\hat{L}_{1R} > \frac{d_Q}{\alpha_{Q1}s_{1Q}}$$

and R can invade when

$$\hat{P}_{1Q} > \frac{d_R}{\alpha_{R1}s_{1R}}.$$

However, since data on both hosts and both parasitoids are not reliable because of experiments performed late in the season, we decide to start with a simpler model with only one host and one parasitoid.

2.2 One host-one parasitoid model

Since raw data on *L. heteroma* were scattered, we decided to apply the model with one host (*D. suzukii*) and one pupal parasitoid (*P. vindemia*). Thus we assume that the life cycle of the host can be divided into four developmental stages: eggs, E , larvae, L , pupae, P and adults, A . We assume that an interspecific competition is present at the larval stage so that, in absence of parasitoids, the host population reach a carrying capacity.

By following the stage preference of *P. vindemiae*, we assume that adult parasitoids, R , can attack only the pupal stage of the host and that they can lay a single egg inside the host. As a starting point, we assume that hosts can not survive to parasitoids attack by encapsulating them and that attack and death rates (except for the larval stage) are constant and density-independent. Since data on the percentage of female offspring, π_H , are available, we assume here that host birthrate is

$$\beta = \pi_H \rho d_A = \frac{\pi_H \rho}{T_A}, \quad (2.5)$$

and juvenile parasitoid survival rate is

$$s_R = \exp(-d_{JR}T_{JR}). \quad (2.6)$$

Thus, the one host-one parasitoid model is given by

$$\begin{aligned}
E'(t) &= \beta A(t) - M_E(t) - d_E E(t) \\
L'(t) &= M_E(t) - M_L(t) - d_L(L(t))L(t) \\
P'(t) &= M_L(t) - M_P(t) - \alpha_R R(t)P(t) - d_P P(t) \\
A'(t) &= M_P(t) - d_A A(t) \\
R'(t) &= \alpha_R R(t - T_R)P(t - T_R) - d_R R(t)
\end{aligned} \tag{2.7}$$

where

$$\begin{aligned}
M_E(t) &= \beta A(t - T_E)e^{-d_E T_E} \\
M_L(t) &= M_E(t - T_L)e^{-\int_{t-T_L}^t d_L(L(y))dy} \\
M_P(t) &= M_L(t - T_P)e^{-\int_{t-T_P}^t (\alpha_R R(y) + d_P)dy}
\end{aligned} \tag{2.8}$$

All model parameters are described in Table 2.2.

2.2.1 Equilibrium with no parasitoids

To analyse extrapolated data, we start by considering that the host population is at an equilibrium without parasitoids and then we add a percentage of parasitoids to see their impact on the host population. This means that initial host values must satisfy

$$\begin{aligned}
\hat{E} &= \frac{\beta \hat{A}(1 - e^{-d_E T_E})}{d_E} \\
\hat{L} &= \frac{\ln(\rho \pi_H) - d_E T_E - d_L T_L - d_P T_P}{T_L \nu_L} \\
\hat{P} &= \frac{\beta e^{-(d_L \hat{L})T_L + d_E T_E}(1 - e^{-d_P T_P}) \hat{A}}{d_P} \\
\hat{A} &= \frac{d_L(\hat{L})\hat{L}}{\beta e^{-d_E T_E}(1 - e^{-d_L(\hat{L})T_L})}
\end{aligned} \tag{2.9}$$

2.3 Parameters extrapolation

To obtain parameter values to use in our simulations, we can look at [110,144]. Tochen *et al.* studied in fact *D. suzukii* developmental period, survival, and fecundity under different temperature conditions. In Table 1 of [144], they found that, under optimal temperature conditions (22 – 26°C), a *Drosophila's* egg has

Parameter	Description
β	Host birth rate
d_E	Host egg death rate
$d_L(L)$	Host larva death rate
d_P	Host pupa death rate
d_A	Host adult death rate
d_R	Adult parasitoid death rate
α	Attack rate of adult parasitoids on host pupae
s_{JR}	Survival rate of juvenile parasitoids
T_E	Duration of egg host stage
T_L	Duration of larva host stage
T_P	Duration of pupa host stage
T_R	Duration of adult parasitoid stage
π_H	Percentage of female offspring in hosts
π_R	Percentage of female offspring in parasitoid

Table 2.2: *Model parameters present in the one host-one parasitoid model. All parameters are kept constant and density-independent except of the larval death rate that depends on larvae density.*

the 70% of probabilities to survive and to become an adult, and that the time spent to become an adult is around 14 days (3 as eggs, 5 as larvae and 6 as pupae). Since we do not know anything about the survivor ship in intermediate states, we assume that

$$d_E = \mu_L = d_P = -\frac{\ln 0.7}{14} = 0.025.$$

By considering (2.2), Tables 1 and 3 of [144], where host fecundity rate at 22°C is equal to 62 and adult host stage duration is of 10.5 days, and [145] where host female offspring results equal to 0.5, we obtain that

$$\beta = \frac{\rho\pi_H}{T_A} = \frac{62 \times 0.5}{10.5} = 2.95.$$

From this we can also obtain $d_A = \frac{1}{T_A} = 0.095$.

In the same way, by following [110], we have that at $23^\circ C$ females of *P. vindemiae* produce a similar number of offspring throughout their life, until a sharp decline before their death. They survive for more or less 21.5 days and parasitized a mean lifetime total of 78.4 pupae with 68.4 offspring successfully emerging as adults, of which 80% were female. Since sex ratio decreased with maternal age, we fix it prudently to 75%. From these data we obtain that the 86.8% of juvenile parasitoids survives until adulthood. Thus, as we have done for the host, juvenile death rate is given by

$$d_{JR} = -\frac{\ln 0.87}{T_{JR}} = 0.0067.$$

where $T_{JR} = 21$ (value extrapolated from Figure 4 of [110]), and adult death rate is equal to 0.047.

Table 2.3 summarizes data extrapolated from [110, 144].

It is easy to notice that, in Table 2.3, two parameters are missing: the attack rate, α_R , and ν_L , the quantity for which the pro capita mortality changes by adding a new individual.

Actually, these two parameters can be considered as one parameter since we can use an arbitrary scaling to measure host density. Thus, we decide to fix the density-dependence as to have for instance 100 pupae at equilibrium. By considering (2.9) and Table 2.3, via simple algebraic calculations, we obtain

$$\nu_L = 0.00092.$$

Since we have obtained ν_L , we can put the attack rate at its maximum value as to have that, at that value, parasitoids can lay all the eggs that they can lay under laboratory conditions, 78.4.

Under these conditions, the attack rate is given by

$$\alpha_R = \frac{78.4}{100 \times 21.5} = 0.036.$$

Parameter	Description	Value
β	Host birth rate	2.95
d_E	Host egg death rate	0.025
μ_L	Host larva death rate	0.025
d_P	Host pupa death rate	0.025
d_A	Host adult death rate	0.095
d_{JR}	Juvenile parasitoid death rate	0.0067
d_R	Adult parasitoid death rate	0.047
s_{JR}	Survival rate of juvenile parasitoids	0.87
T_E	Duration of egg host stage	3
T_L	Duration of larva host stage	5
T_P	Duration of pupa host stage	6
T_{JR}	Duration of juvenile parasitoid stage	21
T_R	Duration of adult parasitoid stage	21.5
π_H	Probability of female host	0.5
π_P	Probability of female parasitoid	0.75

Table 2.3: *Parameter extrapolated from [110, 144] used to see parasitoids impact on a host population at equilibrium.*

Chapter 3

Preliminary results

The aim of this chapter is to show preliminary results of the application of the presented model to raw data. We run simulations using parameters extrapolated from [110, 144] and by considering the one host-one parasitoid model (2.7) presented in the previous Chapter. We decide to test the impact of different choices for the attack rate and increased death rates because it reduces parasitoid effective fecundity respect to laboratory values.

3.1 Simulations

3.1.1 Laboratory conditions

Hosts at equilibrium

We start by considering that the host population has reached an equilibrium without parasitoid. By considering (2.9), values extrapolated from [110, 144] and the obtained value of ν , it is possible to find that at equilibrium we have 1399 eggs, 671 larvae, 101 pupae and 164 adults. From this we decide to introduce different parasitoid percentages of adult hosts (1%, 5%, 10%, 50%) to analyse their impact on host population.

We run simulations for 500 days even if it is not a realistic time choice since, in this preliminary model, we do not take into account temperatures and seasonality but it is mathematically interesting.

To start we fix four different values for the attack rate ($\frac{1}{10}\alpha_R$, $\frac{1}{4}\alpha_R$, $\frac{1}{2}\alpha_R$ and α)

since probably attack rates in the field will be such that fecundity is quite lower than what found in the laboratory experiments. We want now to compare the times at which host pupae are halved when we introduce the different percentages of parasitoids.

Table 3.1 summarizes the times needed by parasitoids to halve host pupae under different combinations of attack rates and percentage of introduced parasitoids.

	$\frac{1}{10}\alpha_R$	$\frac{1}{4}\alpha_R$	$\frac{1}{2}\alpha_R$	α_R
1%	130.4	67.28	46.9	25.35
5%	94.68	47.88	25.15	22.6
10%	79.78	29.07	23.78	1.64
50%	47.22	1.05	0.46	0.27

Table 3.1: *Time needed by parasitoids to halve host pupae under different combinations of attack rate and percentage of introduced parasitoids.*

It is easy to see in Table 3.1 that, by increasing the attack rate, the time needed to halve host pupae decrease rapidly. Since the introduction of 50% of parasitoids is presumably not achievable in nature without collateral effects for the environment or too high cost for farmers, we decide to exclude it from the choice of the best percentage value and we tested it only for a modelling curiosity. It can be noticed that, excluding the last case, the best case is obtained when a 10% of parasitoid is introduced since it is the only case where host pupae are halved in less than 20 days at maximum attack rate. Thus, it seems that the control would be effective only with an high percentage of introduced parasitoids or a sufficiently high attack rate. In fact, if the right attack rate is for instance $\frac{\alpha}{10}$, we would never be able to control the host population in a short time.

Figure 3.1 shows different attack rates under the best choice of parasitoids introduction according to Table 3.1.

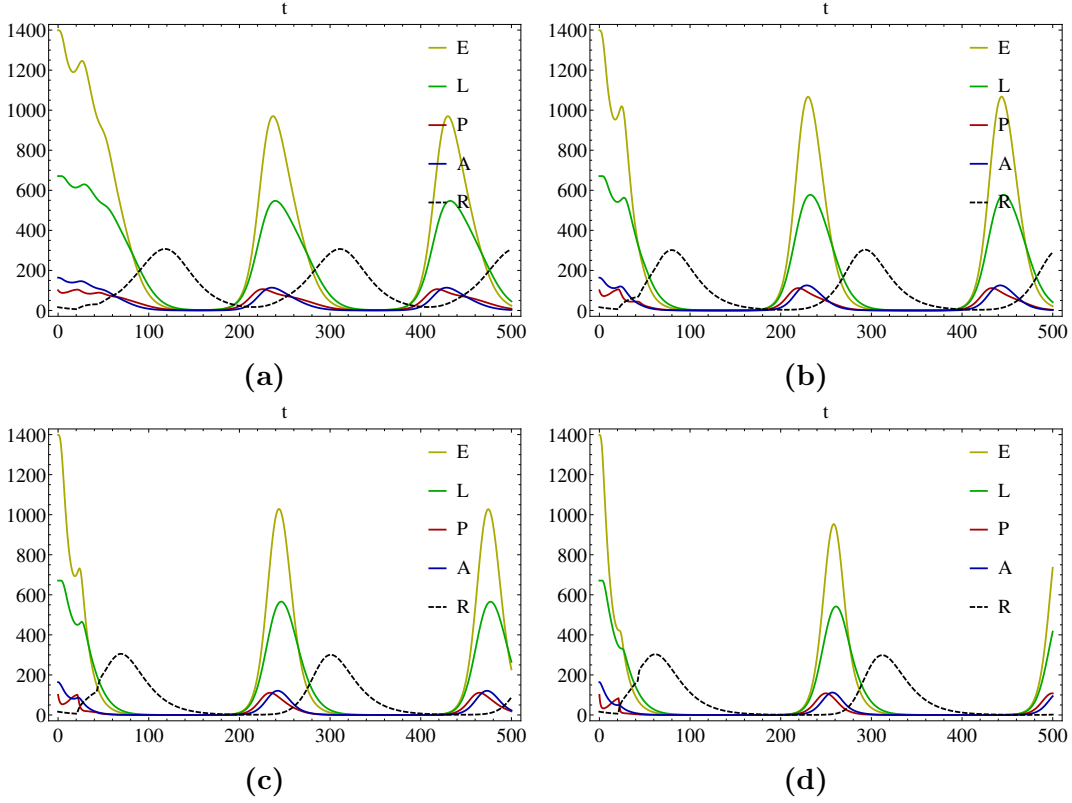


Figure 3.1: Under laboratory conditions simulations. Panel (a), (b), (c) and (d) represent the case with an initial adult parasitoid value equal to 10% of adult hosts, in 500 days with attack rates $\frac{\alpha}{10}$, $\frac{\alpha}{4}$, $\frac{\alpha}{2}$, α respectively.

It can be seen that, even if initially parasitoids have a strong effect on host population, they then shift it to an oscillatory regime.

By considering the choice made on introduction parasitoid percentage, an interesting question to ask is what could happen if parasitoids introduction occurs before the equilibrium is reached.

Hosts not at equilibrium

Since at the beginning of the season only a small number of adult hosts is present, we decide to test what happens if we introduce parasitoids under these conditions.

Since we know that, at equilibrium we have 164 adults, we decide to start from an initial situation with 5 adults, and no hosts at any other stage.

Figure 3.2 shows that, when no parasitoids are present, host population reaches values close to equilibrium at time x around 65 days.

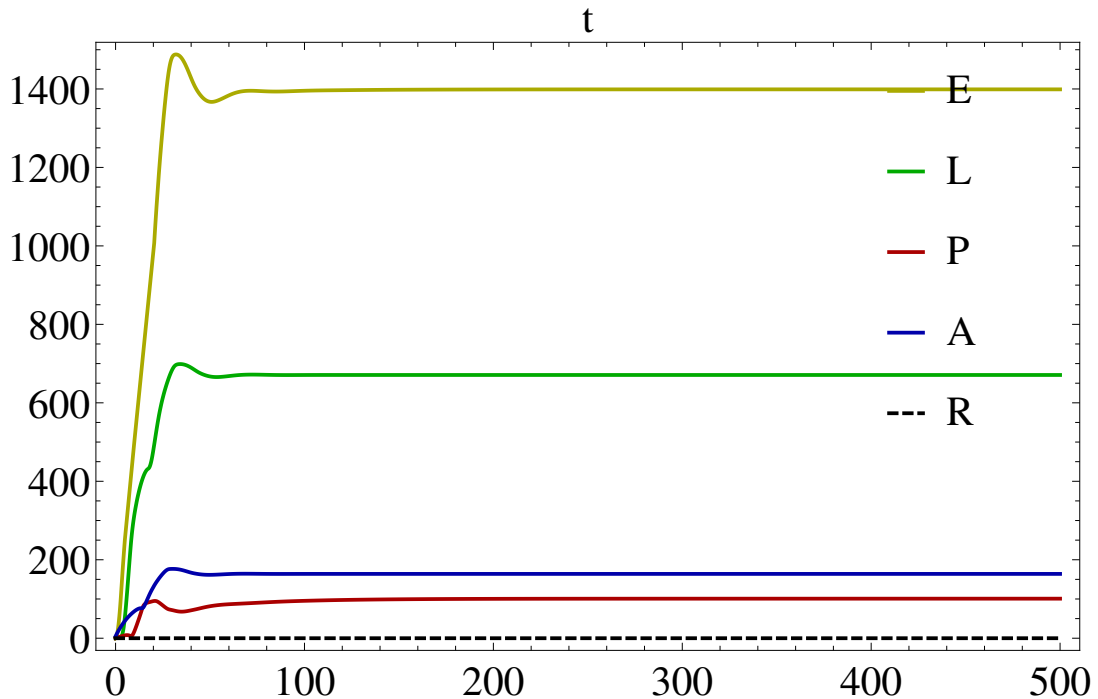


Figure 3.2: Under laboratory conditions simulations when no parasitoids are introduced and we start with only five adult hosts.

Different percentages of introduced parasitoids

According to what was found previously, we know what happens if we introduce a certain amount of parasitoids after time x . We now want to know what could happen if we introduce always the same percentage of parasitoids at times smaller than x . We chose to take into consideration $x = 0, 12, 20$, and 65. The choice of $x = 0$ is due to the fact that it is possible to know how many hosts there are at the beginning of the season. Values $x = 12$ and $x = 20$ are instead chosen to see if the impact of the parasitoids is different if we take an initial value respectively below or above 50 pupae (half of the pupae at equilibrium). Figure 3.3 shows what happens when the host population is not at equilibrium

when no parasitoids are present, and parasitoids with attack rate $\frac{\alpha}{10}$ are introduced at time $x = 20$.

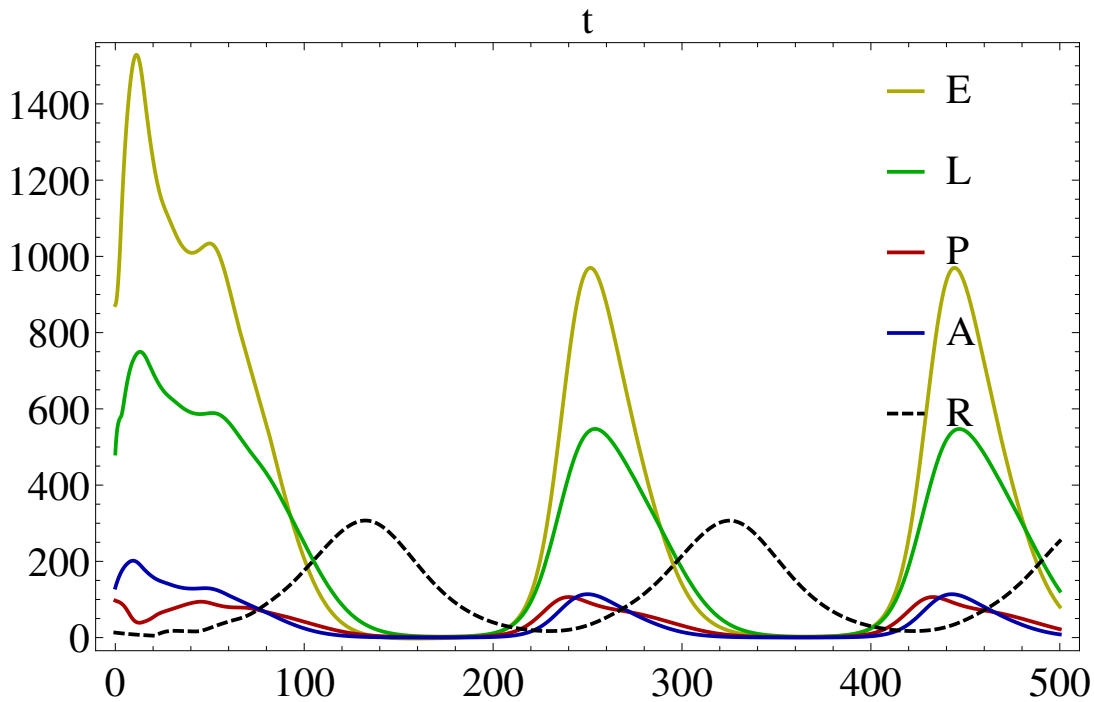


Figure 3.3: Under laboratory conditions simulations with an initial adult parasitoid value equal to 10% of adult hosts introduced at time $x = 20$, in 500 days with attack rates $\frac{\alpha}{10}$.

It can be seen that hosts decrease rapidly even when the attack rate is at $\frac{1}{10}$ of its maximum value. Thus, parasitoids can be possibly released when host population is low.

A different way to introduce parasitoids that could be useful for farmers is to introduce always the same quantity of parasitoids.

Constant quantity of introduced parasitoids

We decide to introduce always 0.5 parasitoids that is the 10% of initial adult host at time 0, since it is possible to know how many hosts there can be at the beginning of the season. Then, as we have done before, we want to know what

could happen if we introduce parasitoids at different times.

For instance, let us see what happens in the worst case when there is a huge difference in the value of introduced parasitoids and the host population values. Figure 3.4 shows thus what happens when the host population is at equilibrium when no parasitoids are present, and a constant amount of parasitoids (equal to 0.5 parasitoids) is then introduced.

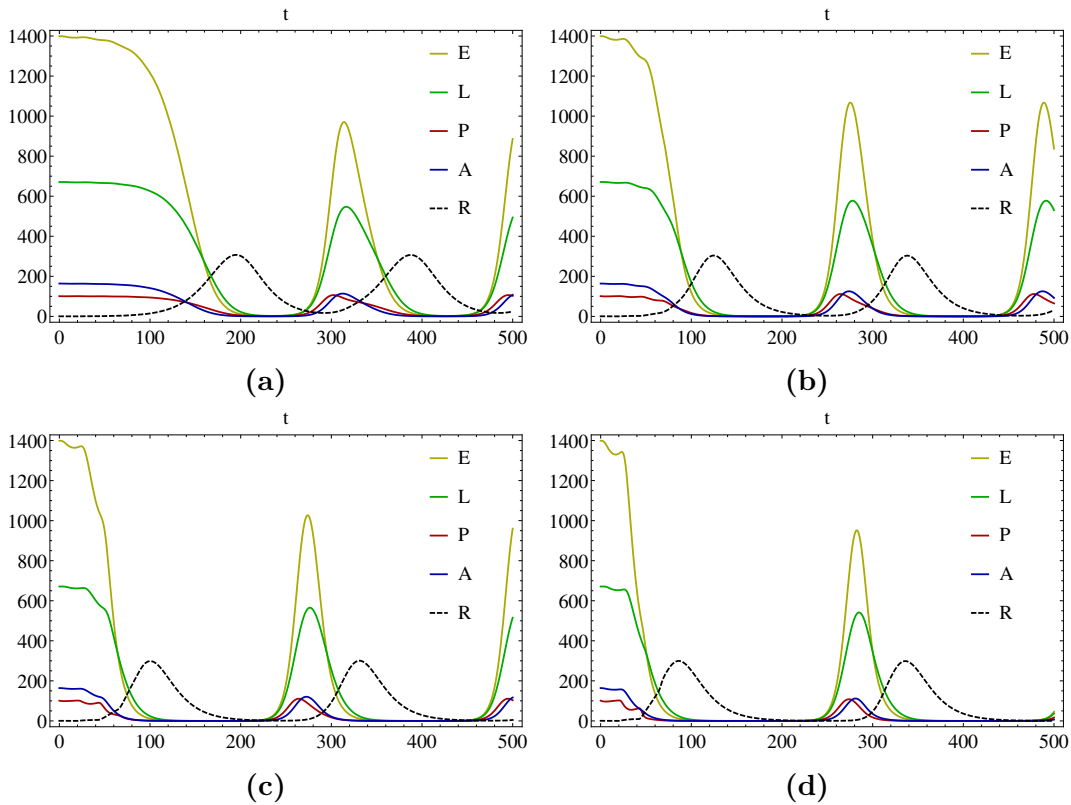


Figure 3.4: Under laboratory conditions simulations. Panel (a), (b), (c) and (d) represent the case with an initial adult parasitoid constant value equal to 0.5, in 500 days introduced when host population is at equilibrium with attack rates $\frac{\alpha}{10}$, $\frac{\alpha}{4}$, $\frac{\alpha}{2}$, α respectively.

In this figure can be seen that, even with attack rate at $\frac{1}{10}$ of its maximum value, parasitoids would have a strong effect on host population, even if the initial quantity of introduced parasitoids is very low compared to the host population. However, under these conditions, an effect would require more than 100 days.

3.1.2 Increased death rates

The last case that we take into account is a case in which we decide to keep the attack rate constant and equal to 0.036 and we vary the mortality rates both of hosts and parasitoids to reduce parasitoid effective fecundity respect to laboratory values. Since we do not have notions on how much the mortality of hosts and parasitoids increases outside laboratory conditions, we decide that the new death rates are obtained by doubling previous adult host and parasitoid death rates and by adding a 0.001 to the death rate of juvenile parasitoids.

Table 3.2 shows the new death rate values.

Parameter	Value
d_A	0.19
d_{JR}	0.0077
d_R	0.095

Table 3.2: *Parameters obtained by considering that probably in nature death rates both of hosts and of parasitoids can be higher than the rates obtained under laboratory conditions.*

As we have done under laboratory conditions, Table 3.3 summarizes the times needed by parasitoids to obtain 50 host pupae under different combinations of percentages of parasitoids and times of parasitoid introduction.

Also in this case we decide not to consider the 50% of parasitoid introduction and thus the best percentage choice seems to be 10% as before. By comparing the last column of Table 3.3 and the last column of Table 3.1, it can be notice that parasitoids need a bit more time to obtain 50 host pupae even if the values are really closed.

Thus, we want to see if an increased death rate both in hosts and parasitoids does not matter or if it improves the control even if the time needed to halve the pupae is similar to the one with laboratory death rates.

Figure 3.5 compares the cases when the host population is at equilibrium and 10% of parasitoids with maximum attack rate α are introduced under laboratory conditions on death rates and with increased death rates.

It can be noticed that, even if the times to halve host pupae are similar under both conditions (a bit larger with increased death rates), when we increase both

	0	12	20	65
1%	82.67	7.88	43.35	27
5%	70.2	44.42	24.03	23
10%	60.9	25.31	22.54	1.76
50%	49.01	22.27	0.24	0.34

Table 3.3: Time needed by parasitoids to obtain 50 host pupae under different combinations of attack rate and percentage of introduced parasitoids when the attack rate is at its maximum value 0.036.

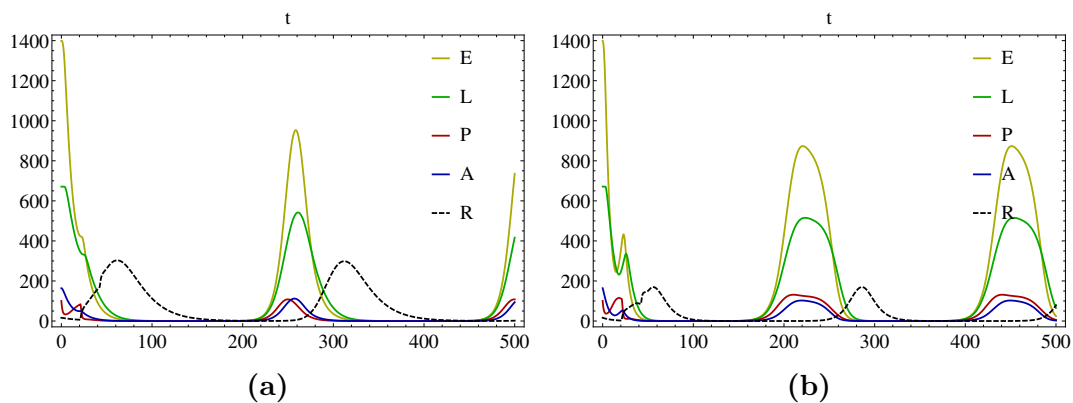


Figure 3.5: Increased death rates. Panel (a) and (b) represent the case with fixed $\alpha = 0.036$ and an initial adult parasitoid value equal to 10%, in 500 days introduced when host population is at equilibrium. Laboratory death rates in panel a), and increased death rates in panel b)

the death rates of hosts and parasitoids, the total host population decreases more rapidly than in the other case. Thus, it can be seen that presumably in nature, if the parasitoids are introduced at the equilibrium, they can have a more significant impact on host population than in laboratory.

Chapter 4

Discussion

This chapter summarizes and discusses the main results obtained by analysing the interactions between one host and one parasitoid under different attack rate conditions, percentages of parasitoid introduction and times of parasitoid introduction.

In this part of the dissertation, we start from the studies of [110, 144] from which we extrapolated data useful to apply a changed version of the model presented in Part II to raw data. We decide to change our model since, by considering [110], we noticed that *D. suzukii* can be attacked by parasitoids with different host stage preferences. We introduced a two hosts-two parasitoids model with an additional host life stage, the pupae. However, since its analysis was too complicated and needed a lot of unknown parameters, we decided to use a simplified version of it. Thus, by analysing the studies of Tochen *et al.* and Stacconi *et al.*, we chose to consider *D. suzukii* as the host and *P. vindemiae* as the parasitoid. This choice was due to the fact that data on *L. heterotoma* were scattered and that *Tricophria*'s females produced only males and thus no further replications have been performed.

Once data on these species were extrapolated, we analysed different conditions on the attack rate and parasitoids presence to see the impact of parasitoid introduction on host populations. We found that, using different values of the attack rate until it reaches its maximum value, the control would be effective only with an high percentage of introduced parasitoids or a sufficiently high attack rate. In fact, if the attack rate is at $\frac{1}{10}$ of its maximum value, we would never be able to control the host population in sufficiently short time. From these results it can also be noticed that, even if under these conditions the parasitoids

can initially have a strong impact on host population, they then shift it to an oscillatory regime.

We found also that, if we want to simulate what happens at the beginning of the season by adding a fixed percentage of parasitoids, under high introduction of parasitoids (10% of initial adult host population), their effect on the host population is fast even if the attack rate is at $\frac{1}{10}$ of its maximum value. From these simulations, we can conclude that growers can possibly release parasitoids when host population is low and see a significant impact on it.

In the third case that we have taken into account, we have decided to keep constant the amount of parasitoids introduced in the system. This choice is interesting because at the beginning of the season it is easy to obtain values of the total amount of hosts present by considering what can be found into traps or in particular places. In this case, we found that, if we introduce the 0.5 parasitoids at all times (the 10% of adult hosts at time $x = 0$) even when hosts are at equilibrium and the attack rate is at $\frac{1}{10}$ of its maximum value, parasitoids would have a strong effect on host population. However, from a practical point of view, this effect would not be satisfactory since it would require more than 100 days.

Finally, we considered that maybe in nature mortality rates could be higher than those obtained in laboratory. Thus, we decided to keep the attack rate at the maximum obtained value and we increased the mortality rates both of hosts and parasitoids. Since we do not know how much these rates increase outside laboratory conditions, our choices are arbitrary and can be also totally or partially wrong. We found that, the time needed by parasitoid to halve host pupae increases a bit respect to the values found under laboratory conditions but the total host population decreases more rapidly in this case. Thus, presumably in nature, if parasitoids with a maximum attack rate are introduced when the host population is at equilibrium, they can have a more significant impact on host population than under laboratory conditions.

Thus, even if these are only preliminary results, our analysis provides evidence of a great impact of parasitoid introduction on host population and assures that parasitoids can be effective biocontrol agents.

Bibliography

- [1] **Camacho A, et al.** Explaining rapid reinfections in multiple-wave influenza outbreaks: Tristan da Cunha 1971 epidemic as a case study. *P R Soc Ser B* 2011; **278**: 3635-3643.
- [2] **Calatayud L, et al.** Pandemic (H1N1) 2009 virus outbreak in a school in London, April-May 2009: an observational study. *Epidemiol Infect* 2010; **138**: 183-191.
- [3] **Guinard A, et al.** Outbreak of influenza A(H1N1)v without travel history in a school in the Toulouse district, France, June 2009. *Eurosurveillance* 2009; **14**: 2335-2346.
- [4] **Health Protection Agency West Midlands H1N1v Investigation Team.** Preliminary descriptive epidemiology of a large school outbreak of influenza A(H1N1)v in the West Midlands, United Kingdom, May 2009. *Eurosurveillance* 2009; **14**: pii=19264.
- [5] **Kar-Purkayastha I, et al.** The importance of school and social activities in the transmission of influenza A(H1N1)v: England, April-June 2009. *Eurosurveillance* 2009; **14**: pii=19311.
- [6] **Lessler J, et al.** Outbreak of 2009 pandemic influenza A(H1N1) at a New York City school. *N Engl J Med* 2009; **361**: 2628-2636.
- [7] **Smith A, et al.** An outbreak of influenza A(H1N1)v in a boarding school in South East England, May-June 2009. *Eurosurveillance* 2009; **14**: pii=19263.
- [8] **Gurav YK, et al.** Pandemic influenza A(H1N1) 2009 outbreak in a residential school in Panchgani, Maharashtra, India. *Indian J Med Res* 2010; **132**: 67-71.

- [9] **Marchbanks TL, et al.** An outbreak of 2009 pandemic influenza A (H1N1) virus infection in an elementary school in Pennsylvania. *Clin Infect Dis* 2011; **52**: S154-S160.
- [10] **Centers for Disease Control and Prevention (CDC).** Performance of rapid influenza diagnostic tests during two school outbreaks of 2009 pandemic influenza A (H1N1) virus infection - Connecticut, 2009. *MMWR* 2009; **58**: 1029-1932.
- [11] **Zhao H, Joseph C, Phin N.** Outbreaks of influenza influenza-like illness in schools in England and Wales, 2005/06. *Eurosurveillance* 2007; **12**: E3-4.
- [12] **Centers for Disease Control and Prevention.** Swine-Origin influenza A (H1N1) virus infections in a school-New York City, April 2009. *MMWR* 2009; **58**: 470-472.
- [13] **Baguelin M, et al.** Assessing Optimal Target Populations for Influenza Vaccination Programmes: An Evidence Synthesis and Modelling Study. *PLoS Med* 2013; **10**: e1001527.
- [14] **Mossong J, et al.** Social Contacts and Mixing Patterns Relevant to the Spread of Infectious Diseases. *PLoS Med* 2008; **5**: e74.
- [15] **Fumanelli L, et al.** Inferring the Structure of Social Contacts from Demographic Data in the Analysis of Infectious Diseases Spread. *PLoS Comp Biol* 2012; **8**: e1002673.
- [16] **Cauchemez S, et al.** Role of social networks in shaping disease transmission during a community outbreak of 2009 H1N1 pandemic influenza. *P Natl Acad Sci USA* 2011; **7**: 2825-2830.
- [17] **O'Neill PD, et al.** Analyses of infectious disease data from household outbreaks by Markov chain Monte Carlo methods. *J R Stat Soc Ser C* 2000; **49**: 517-542.
- [18] **O'Neill PD, Roberts GO.** Bayesian inference for partially observed stochastic epidemics. *J R Stat Soc Ser A* 1999; **162**: 121-129.
- [19] **Anderson R, May R.** *Infectious Diseases in Humans*. Oxford University Press, Oxford, 1992.

- [20] **Dieckmann O, Heesterbeek J.** *Mathematical Epidemiology of Infectious Diseases*. Wiley, Chichester, New York, 2000.
- [21] **Fraser C, et al.** Factors that make an infectious disease outbreak controllable. *PNAS* 2004; **101**: 6146-6151.
- [22] **Hamer WH.** Epidemic disease in England. *Lancet* 1906; **1**: 733-739.
- [23] **Ross R.** An application of the theory of probabilities to the study of a priori pathometry. Part i. *P Roy Soc Lond A Mat* 1916; **92**: 204-230.
- [24] **Ross R, Hudson H.** An application of the theory of probabilities to the study of a priori pathometry. Part ii. *P Roy Soc Lond A Mat* 1917a; **93**: 212-225.
- [25] **Ross R, Hudson H.** An application of the theory of probabilities to the study of a priori pathometry. Part i. *P Roy Soc Lond A Mat* 1917b; **93**: 225-240.
- [26] **Kermack WO, McKendrick AG.** A contribution to the mathematical theory of epidemics. *P Roy Soc A* 1927; **115**: 700-721.
- [27] **Kermack WO, McKendrick AG.** Contributions to the mathematical theory of epidemics-II. The problem of endemicity. *P Roy Soc A* 1932; **138**: 55-83
- [28] **Kermack WO, McKendrick AG.** Contributions to the mathematical theory of epidemics-III. Further studies of the problem of endemicity. *P Roy Soc A* 1933; **141**: 94-122.
- [29] **Chowell G, et al.** SARS outbreaks in Ontario, Hong Kong and Singapore: the role of diagnosis and isolation as a control mechanism. *J Theor Biol* 2003; **224**: 1-8.
- [30] **Wang W, Ruan S.** Simulating the sars outbreak in Beijing with limited data. *J Theor Biol* 2004; **227**: 369-379.
- [31] **Nishiura H, et al.** Pros and cons of estimating the reproduction number from early epidemic growth rate of influenza A (H1N1) 2009. *Theor Biol Med Model* 2010; **7**: 1.
- [32] **Lipsitch M, et al.** Transmission dynamics and control of severe acute respiratory syndrome. *Science* 2003; **300**: 1966-1970.

- [33] **Austin D, Kakehashi M, Anderson R.** The transmission dynamics of antibiotic-resistant bacteria: the relationship between resistance in commensal organisms and antibiotic consumption. *P Roy Soc Lond B Bio* 1997; **246**: 1629-1638.
- [34] **Gupta S, et al.** Parasite virulence and disease patterns in plasmodium falciparum malaria. *P Natl Acad Sci USA* 1994; **91**: 3715-3719.
- [35] **Gupta S, Ferguson N, Anderson R.** Chaos, persistence, and evolution of strain structures in antigenically diverse infectious agents. *Science* 1998; **280**: 912.
- [36] **Ferguson N, Donnelly CA, Anderson RM.** Transmission dynamics and epidemiology of dengue: insights from age-stratified sero-prevalence surveys. *Philos T Roy Soc B* 1999; **354**: 757-768.
- [37] **Minayev P, Ferguson N.** Improving the realism of deterministic multi-strain models: implications for modelling influenza A. *J R Soc Interface* 2009; **6**: 509-518.
- [38] **Rosenblueth, Wiener N.** The Role of Models in Science. *Philos Sci* 1945; **12**: 316-321.
- [39] **Naylor TJ, et al.** *Computer Simulation techniques*. Wiley, New York, 1966.
- [40] **Abbey H.** An examination of the Reed-Frost theory of epidemics. *Hum Biol* 1952; **24**: 201.
- [41] **Greenwood M.** On the statistical measure of infectiousness. *J Hyg Camb* 1931; **31**: 336.
- [42] **O'Neill PD.** A tutorial introduction to Bayesian inference for stochastic epidemic models using Markov chain Monte Carlo methods. *Math Biosci* 2002; **180**: 103-114.
- [43] **Zeng D, et al.** *Infectious Disease Informatics and Biosurveillance*. Springer Science & Business Media, 2010.
- [44] **Metropolis N, et al.** Equation of state calculations by fast computing machines. *J Chem Phys* 1953; **21**: 1087-1092.
- [45] **Hastings, W. Keith.** Monte Carlo sampling methods using Markov chains and their applications. *Biometrika* 1970; **57**: 97-109.

- [46] **Geman S, Geman D.** Stochastic relaxation, Gibbs distribution and the Bayesian restoration of images. *IEEE T Pattern Anal* 1984; **6**: 721-741.
- [47] **Gelfand AE, Smith AFM.** Sampling-based approaches to calculating marginal densities. *J Am Stat Assoc* 1990; **85**: 398-409.
- [48] **Gelman A, Rubin DB.** A single series from the Gibbs sampler provides a false sense of security. *B-Statistics* 1992; **4**: 625-631.
- [49] **Gelman A, Rubin DB.** Inference from iterative simulation using multiple sequences. *Stat Sci* 1992; **7**: 457-472.
- [50] **Green PJ.** Reversible jump Markov chain Monte Carlo computation and Bayesian model determination. *Biometrika* 1995; **82**: 711-732.
- [51] **Roberts GO, Gelman A, Gilks WR.** Weak convergence and optimal scaling of random walk Metropolis Algorithms. *Ann Appl Probabb* 1997; **7**: 110-120.
- [52] **Gamerman D, Lopes HF.** *Markov chain Monte Carlo: stochastic simulation for Bayesian inference.* CRC Press, 2006.
- [53] **Park S, et al.** Outbreak of 2009 pandemic influenza A (H1N1) at a school - Hawaii, May 2009. *MMWR* 2009; **58**: 1440-1444.
- [54] **Ghani AC, et al.** The Early Transmission Dynamics of H1N1pdm Influenza in the United Kingdom. *PLoS Curr* 2009; **1**: RRN1 130.
- [55] **Suess T, et al.** Shedding and Transmission of Novel Influenza Virus A/H1N1 Infection in Households-Germany, 2009. *Am J Epidemiol* 2010; **171**: 1157-1164.
- [56] **Gilks WR, Richardoson S, Spiegelhalter DJ.** *Markov Chain Monte Carlo in practice.* Chapman & Hall/CRC, London, 1996.
- [57] **Wallinga J and Lipsitch M.** How generation intervals shape the relationship between growth rates and reproductive numbers. *P R Soc Lond B* 2007; **274**: 599-604.
- [58] **King AA, et al.** Avoidable errors in the modelling of outbreaks of emerging pathogens, with special reference to Ebola. *Proc R Soc London B Biol Sci* 2015; **282**: 20150347.

- [59] **Smith DL, et al.** Revisiting the Basic Reproductive Number for Malaria and Its Implications for Malaria Control. *PLoS Biol* 2007; **5**: e42.
- [60] **Yang Y, et al.** The transmissibility and control of pandemic influenza A(H1N1) virus. *Science* 2009; **326**: 729-733.
- [61] **Fraser C, et al.** Pandemic potential of a strain of influenza A (H1N1): early findings. *Science* 2009; **324**: 1557-1561.
- [62] **Pourbohloul B, et al.** Initial human transmission dynamics of the pandemic (H1N1) 2009 virus in North America. *Influenza Other Respir Viruses* 2009; **3**: 215-222.
- [63] **Italian Institute of Health.** Influnet. (<http://www.iss.it/iflu/>).
- [64] **Spiegelhalter DJ, et al.** Bayesian measures of model complexity and fit (with discussion). *J R Stat Soc Ser B* 2002; **64**: 583-639.
- [65] **Van der Linde A.** DIC in variable selection. *Stat Neerl* 2005; **59**: 45-56.
- [66] **Gemmetto V, Barrat A, Cattuto C.** Mitigation of infectious disease at school: targeted class closure vs school closure. *BMC Infect Dis* 2014; **14**: 695.
- [67] **Stehle J, et al.** High-resolution measurements of face-to-face contact patterns in a primary school. *PloS ONE* 2011; **271**: 166-180.
- [68] **Fumanelli L, et al.** Model-based Comprehensive Analysis of School Closure Policies for Mitigating Influenza Epidemics and Pandemics. *PLoS Comp Biol* 2016; **12**: e1004681.
- [69] **Cauchemez S, et al.** School closures during the 2009 influenza pandemic: national and local experiences. *BMC Infect Dis* 2014; **14**: 207.
- [70] **Cauchemez S, et al.** A Bayesian MCMC approach to study transmission of influenza: application to household longitudinal data. *Stat Med* 2004; **23**: 3469-3487.
- [71] **Jong MCM, Diekmann O, Heesterbeek H.** *How does transmission of infection depend on population size.* Epidemic models: their structure and relation to data. Cambridge University Press, Cambridge, United Kingdom, 1995, 84-94.

- [72] **Ajelli M, et al.** Model predictions and evaluation of possible control strategies for the 2009 A/H1N1v influenza pandemic in Italy. *Epidemiol Infect* 2011; **139**: 68-79.
- [73] **Boëlle PY, et al.** Transmission parameters of the A/H1N1 (2009) influenza virus pandemic: a review. *Influenza Other Respir Viruses* 2011; **5**: 306-316.
- [74] **White LF, et al.** Estimation of the reproductive number and the serial interval in early phase of the 2009 influenza A/H1N1 pandemic in the USA. *Influenza Other Respir Viruses* 2009; **3**: 267-276.
- [75] **Ajelli M, et al.** The role of different social contexts in shaping influenza transmission during the 2009 pandemic. *Sci Rep* 2014; **4**: 7218.
- [76] **Cauchemez S, et al.** Estimating the impact of school closure on influenza transmission from Sentinel data. *Nature* 2008; **452**: 750-754.
- [77] **Merler S, et al.** Pandemic Influenza A/H1N1pdm in Italy: Age, Risk and Population Susceptibility. *PLoS ONE* 2013; **8**: e74785.
- [78] **Getz WM, Mills NJ.** Host-parasitoid coexistence and egg-limited encounter rates. *Amer Nat* 1996; 333-347.
- [79] **Godfray HCJ.** *Parasitoids: behavioral and evolutionary ecology*. Princeton University Press, 1994.
- [80] **Gause GF.** *The struggle for existence*. Courier Corporation, 2003.
- [81] **Chesson PL, Case TJ.** *Overview: nonequilibrium community theories: chance, variability, and history*. Community ecology. Edited by J. Diamond and TJ Case. Harper and Row Publishers, Inc., New York, 1986, 229-239.
- [82] **Briggs CJ.** Competition among parasitoid species on a stage-structured host and its effect on host suppression. *Amer Nat* 1993; 372-397.
- [83] **Matsumura S.** *6000 illustrated insects of Japan-Empire*. 1931.
- [84] **Calabria G, et al.** First records of the potential pest species *Drosophila suzukii* (Diptera: Drosophilidae) in Europe. *J Appl Entomol* 2012; **136**: 139-147.

- [85] **Cini A, Ioriatti C, Anfora G.** A review of the invasion of *Drosophila suzukii* in Europe and a draft research agenda for integrated pest management. *Bull Insectol* 2012; **65**: 149-160.
- [86] **Cini A, et al.** Tracking the invasion of the alien fruit pest *Drosophila suzukii* in Europe. *J Pest Sci* 2014; **87**: 559-566.
- [87] **Grassi ALBERTO, et al.** *Drosophila* (Sophophora) *suzukii* (Matsumura), new pest of soft fruits in Trentino (North-Italy) and in Europe. *IOBC/WPRS Bull* 2011; **70**: 121-128.
- [88] **Hauser M.** A historic account of the invasion of *Drosophila suzukii* (Matsumura) (Diptera: Drosophilidae) in the continental United States, with remarks on their identification. *Pest Manag Sci* 2011; **67**: 1352-1357.
- [89] **Walsh DB, et al.** *Drosophila suzukii* (Diptera: Drosophilidae): Invasive pest of ripening soft fruit expanding its geographic range and damage potential. *J Integr Pest Manag* 2011; **1**: 1-7.
- [90] **Bolda MP, Goodhue RE, Zalom FG.** Spotted wing drosophila: potential economic impact of a newly established pest. *Agric Resour Econ Update* 2010; **13**: 5-8.
- [91] **De Ros G, et al.** The potential economic impact of *Drosophila suzukii* on small fruits production in Trentino (Italy). *IOBC/WPRS Bull* 2013; **91**: 317-321.
- [92] **Gerdeman BS, et al.** Biology and management of spotted wing drosophila, *Drosophila suzukii* (Matsumura) in small fruits in the Pacific Northwest. *IOBC/WPRS Bull* 2011; **70**: 129-136.
- [93] **Goodhue RE, et al.** Spotted wing drosophila infestation of California strawberries and raspberries: economic analysis of potential revenue losses and control costs. *Pest Manag Sci* 2011; **67**: 1396-1402.
- [94] **Rota-Stabelli O, Blaxter M, Anfora G.** *Drosophila suzukii*. *Curr Biol* 2013; **23**: R8-R9.
- [95] **Murdoch WW, et al.** An Invulnerable Age Class and Stability in Delay-Differential Parasitoid-Host Models. *Amer Nat* 1987; **129**: 263-282.

- [96] **Nisbet RM, Gurney WSC.** *Stage-Structure Models of Uniform Larval Competition.* Mathematical Ecology. Springer Berlin Heidelberg, 1984, 97-113.
- [97] **Briggs CJ, Nisbet RM, Murdoch WW.** Coexistence of Competing Parasitoid Species on a Host with a Variable Life Cycle. *Theor Pop Biol* 1993; **44**: 341-373.
- [98] **Volterra V.** Fluctuations in the abundance of a species considered mathematically. *Nature* 1926; **118**: 558-560.
- [99] **Loots I, Lotka AJ.** On the true rate of natural increase: As exemplified by the population of the United States, 1920. *Amer Statist Assoc* 1925; **20**: 305-339.
- [100] **Rosezweig ML, MacArthur RH.** Graphical representation and stability conditions of predator-prey interactions. *Am Nat* 1963; **97**: 209-223.
- [101] **Volterra V.** *Variazioni e fluttuazioni del numero d'individui in specie animali conviventi.* C. Ferrari, 1927.
- [102] **McKendrick AG, Pai MK.** The rate of multiplication of micro-organisms: A mathematical study. *Proc Roy Soc Edinburgh* 1910; **31**: 649-655.
- [103] **Ricklefs RE.** *Ecology.* Chiron Press, Newton, 1973.
- [104] **Slobodkin LB.** *Growth and regulation of animal populations.* Holt, Rinehart and Winston, New York, 1961.
- [105] **Gurtin ME, MacCamy RC.** Non-linear age-dependent population dynamics. *Arch Rat Mech Anal* 1974; **3**: 281-300.
- [106] **Gurtin ME, MacCamy RC.** *Population dynamics with age dependence.* Nonlinear Analysis and Mechanics: Heriot-Watt Symposium. Vol. 3. Pitman New York, 1979.
- [107] **Hoppensteadt F.** *Mathematical theories of populations: Demographics, genetics and epidemics.* Reg. Conf. Series in Appl Math, SIAM, Philadelphia, 1975.
- [108] **Oster G.** The dynamics of non-linear models with age structure. Studies in mathematical biology. Part II: Population and communities. *MAA Studies in Mathematics* 1978; **16**: 411-438.

- [109] **Oster G, Guckenheimer J.** *Bifurcation phenomena in population models.* In: *The Hopf Bifurcation and its Applications.* Springer New York, 1976, 327-353.
- [110] **Rossi Stacconi MV, et al.** Host stage preference, efficacy and fecundity of parasitoids attacking *Drosophila suzukii* in newly invaded areas. *Biol Control* 2015; **84**: 28-35.
- [111] **Smith H.** *An introduction to delay differential equations with applications to the life sciences. Vol. 57.* Springer Science & Business Media, 2010.
- [112] **Metz JAJ, Nisbet RM, Geritz SAH.** How should we define 'fitness' for general ecological scenarios? *TREE* 1992; **7**: 173-209.
- [113] **Breda D, Maset S, Vermiglio R.** Pseudospectral differencing methods for characteristic roots of delay differential equations. *SISC* 2005; **27**: 482-495.
- [114] **Breda D, Maset S, Vermiglio R.** Approximation of eigenvalues of evolution operators for linear retarded functional differential equations. *SISC* 2012; **50**: 1456-1483.
- [115] **Engelborghs K, et al.** Collocation Methods for the Computation of Periodic Solutions of Delay Differential Equations. *SISC* 2001; **22**: 1593-1609.
- [116] **Shampine LF, Thompson S.** Solving DDEs in MATLAB. *Appl Numer Math* 2001; **37**: 441-458.
- [117] **Breda D, Maset S, Vermiglio R.** *Stability of linear delay differential equations - A numerical approach with MATLAB.* SpringerBriefs in Control, Automation and Robotics, T. Basar, A. Bicchi and M. Krstic eds., Springer, New York, 2015.
- [118] **Hale JK, Verduyn Lunel SM.** *Introduction to functional differential equations, 2nd edn.* No. 99 in AMS series. Springer, New York, 1993.
- [119] **Chen Y, Wu J.** *Threshold dynamics of scalar linear periodic delay-differential equations.* Infinite Dimensional Dynamical Systems, Springer, New York, 2012, 269-278.
- [120] **Holt RD.** Predation, apparent competition, and the structure of prey communities. *Theor Popul Biol* 1977; **12**: 197-229.

- [121] **Holt RD, Lawton JH.** Apparent competition and enemy-free space in insect host-parasitoid communities. *Amer Nat* 1993; 623-645.
- [122] **Li B, Smith HL.** Periodic coexistence of four species competing for three essential resources. *Math Biosci* 2003; **184**: 115-135.
- [123] **De Mottoni P, Schiaffino A.** Competition systems with periodic coefficients: a geometric approach. *J Math Biol* 1981; **11**: 319-335.
- [124] **Cushing JM.** Periodic solutions of two species interaction models with lags. *Math Biosci* 1976; **31**: 143-156.
- [125] **Smith HL, Waltman P.** *The theory of the chemostat: dynamics of microbial competition. Vol. 13.* Cambridge university press, 1995.
- [126] **Godfray HC, Waage JK.** Predictive modelling in biological control: The mango mealy bug (*Rastrococcus invadens*) and its parasitoids. *J Appl Ecol* 1991; **28**: 434-453.
- [127] **May RM, Hassel MP.** The dynamics of multiparasitoid-host interactions. *Am Nat* 1981; **117**: 234-261.
- [128] **Kakehashi M, Suzuki Y, Iwasa Y.** Niche overlap of parasitoid in host-parasitoid systems its consequences to single versus multiple introduction controversy in biological control. *J Appl Ecol* 1984; **21**: 115-131.
- [129] **Murdoch WW.** Switching in general predators: Experiments on predator specificity and stability of prey populations. *Ecol Monogr* 1969; **39**: 335-354.
- [130] **Murdoch WW, Oaten A.** Predation and population stability. *Adv Ecol Res* 1975; **9**: 1-131.
- [131] **May RM.** Predators that switch. *Nature* 1977; **269**: 103-104.
- [132] **Abrams PA** The functional responses of adaptive consumers of two resources. *Theor Popul Biol* 1987; **32**: 262-288.
- [133] **Tregenza TC, Thompson DJ, Parker GA.** Interference and the ideal free distribution: Oviposition in a parasitoid wasp. *Behav Ecol* 1996; **7**: 387-394.
- [134] **Abrams A, Kawecki TJ.** Adaptive Host Preference and the Dynamics of Host-Parasitoid Interactions. *Theor Pop Biol* 1998; **56**: 307-324.

- [135] **Depra M, et al.** The first records of the invasive pest *Drosophila suzukii* in the South American continent. *J Pest Sci* 2014; doi:10.1007/s10340-014-0591-5
- [136] **Lee JC, et al.** In focus: spotted wing drosophila, *Drosophila suzukii*, across perspectives. *Pest Manag Sci* 2011; **67**: 1349-1351.
- [137] **Yee WL, Alston DG.** Behavioral responses, rate of mortality, and oviposition of western cherry fruit fly exposed to malathion, zeta-cypermethrin, and spinetoram. *J Pest Sci* 2012; **85**: 141-151.
- [138] **Van Timmeren S, Isaacs R.** Control of spotted wing drosophila, *Drosophila suzukii*, by specific insecticides and by conventional and organic crop protection programs. *Crop Prot* 2013; **54**: 126-133.
- [139] **Brown PH, et al.** The discovery and rearing of a parasitoid (Hymenoptera: Pteromalidae) associated with spotted wing drosophila, *Drosophila suzukii* in Oregon and British Columbia. *ESA Ann Meet*, 2011.
- [140] **Chabert S, et al.** Ability of European parasitoids (Hymenoptera) to control a new invasive Asiatic pest, *Drosophila suzukii*. *Biol Control* 2012; **63**: 40-47.
- [141] **Gabarra R, et al.** Prospects for the biological control of *Drosophila suzukii*. *Biocontrol* 2015; **60**: 331-339.
- [142] **Fleury F, et al.** Ecological and genetic interactions in *Drosophila*-parasitoids communities: a case study with *D. melanogaster*, *D. simulans* and their common *Leptopilina* parasitoids in south-eastern France. *Genetica* 2004; **120**: 181-194.
- [143] **Rossi Stacconi MV, et al.** First field records of *Pachycrepoideus vindemiae* as a parasitoid of *Drosophila suzukii* in European and Oregon smallfruit production areas. *Entomologia* 2013; **1**: 11-16.
- [144] **Tochen S, et al.** Temperature-related development and population parameters for *Drosophila suzukii* (Diptera: Drosophilidae) on cherry and blueberry. *Environ Entomol* 2014; **43**: 501-510.
- [145] **Emiljanowicz LM, et al.** Development, reproductive output and population growth of the fruit fly pest *Drosophila suzukii* (Diptera: Drosophilidae) on artificial diet. *J Ec Entomol* 2014; **107**: 1392-1398.

Declaration

I, Valentina Clamer, hereby declare that this Ph.D. thesis was carried out by me for the degree of Doctor of Philosophy in Mathematics under the guidance and supervision of Prof. Andrea Pugliese, Department of Mathematics, University of Trento, Italy.

I certify that this thesis has not been accepted for the award of any other degree or diploma in my name, in any university or other tertiary institution and, to the best of my knowledge and belief, contains no material previously published or written by another person, except where due reference has been made in the text. In addition, I certify that no part of this work will, in the future, be used in a submission in my name, for any other degree or diploma in any university or other tertiary institution without the prior approval of the University of Trento and where applicable, any partner institution responsible for the joint-award of this degree.

This work is the intellectual property of the author. You may copy up to 5% of this work for private study, or personal, non-commercial research. Any re-use of the information contained within this document should be fully referenced, quoting the author, title, university, degree level and pagination. Queries or requests for any other use, or if a more substantial copy is required, should be directed in the owner(s) of the Intellectual Property Rights.

I give consent to this copy of my thesis, when deposited in the University Library, being made available for loan and photocopying, subject to the provisions of the Copyright Act 1968. I also give permission for the digital version of my thesis to be made available on the web, via the University's digital research repository, the Library Search and also through web search engines, unless permission has been granted by the University to restrict access for a period of time.